TRANSFORMING GROWTH FACTOR BETA 1 MODULATES ELECTROPHYSIOLOGICAL PARAMETERS OF VAS DEFERENS EPITHELIAL CELLS

by

SHENG YI

M.S., Kansas State University, 2009

AN ABSTRACT OF A DISSERTATION

submitted in partial fulfillment of the requirements for the degree

DOCTOR OF PHILOSOPHY

Department of Anatomy and Physiology
College of Veterinary Medicine

KANSAS STATE UNIVERSITY
Manhattan, Kansas

2013

Abstract

Transforming growth factor β1 (TGF-β1) is a cytokine that reportedly affects the severity of cystic fibrosis lung disease. The goal of this project was to define the effect of TGF-β1 on vas deferens, an organ that is universally affected in male cystic fibrosis patients.

In the first study, experiments were conducted using freshly isolated porcine vas deferens epithelial cells. Primary porcine vas deferens epithelial cells exposed to TGF-β1 exhibited a significantly reduced basal transepithelial electrical resistance (R_{te}). TGF-β1-induced reduction in R_{te} was prevented by SB431542, a TGF-β receptor I inhibitor, indicating that the effect of TGF-β1 requires the activation of TGF-β receptor I. Western blot and immunohistochemistry results showed the expression of TGF-β receptor I in native vas deferens epithelia, indicating that the impaired barrier function and anion secretion that were observed in cultured vas deferens cells can likely be observed in the native context. Immunohistochemical outcomes showed that TGF-β1 exposure led to loss of organization of tight junction proteins occludin and claudin-7. These outcomes suggest that TGF-β1 impairs the barrier integrity of epithelial cells lining the vas deferens.

In a parallel study that employed PVD9902 cells that are derived from porcine vas deferens, TGF-β1 exposure significantly reduced anion secretion stimulated by forskolin, forskolin/IBMX, and 8-pCPT-cAMP, suggesting that TGF-β1 affects downstream targets of the cAMP signaling pathway. Real-time RT-PCR and western blot analysis showed that TGF-β1 exposure reduced both the mRNA and the protein abundance of cystic fibrosis transmembrane conductance regulator (CFTR). Pharmacological studies showed that the inhibitory effect of TGF-β1 on forskolin-stimulated anion secretion was abrogated by SB431542 and attenuated by SB203580, a p38 mitogen-activated protein kinase (MAPK) inhibitor. These outcomes suggest that TGF-β1, *via* the activation of TGF-β receptor I and p38 MAPK signaling, reduces CFTR expression, and thus impairs CFTR-mediated anion secretion.

Outcomes from these studies suggest that, in epithelial cells lining the vas deferens, TGF-β1 exposure leads to an impaired physical barrier and/or reduced anion secretion, which is expected

to modify the composition and the maintenance of the luminal environment and thus, is expected to reduce male fertility.

TRANSFORMING GROWTH FACTOR BETA 1 MODULATES ELECTROPHYSIOLOGICAL PARAMETERS OF VAS DEFERENS EPITHELIAL CELLS

by

SHENG YI

M.S., Kansas State University, 2009

A DISSERTATION

submitted in partial fulfillment of the requirements for the degree

DOCTOR OF PHILOSOPHY

Department of Anatomy and Physiology
College of Veterinary Medicine

KANSAS STATE UNIVERSITY
Manhattan, Kansas

2013

Approved by:

Major Professor
Dr. Bruce Schultz

Copyright

Abstract

Transforming growth factor β1 (TGF-β1) is a cytokine that reportedly affects the severity of cystic fibrosis lung disease. The goal of this project was to define the effect of TGF-β1 on vas deferens, an organ that is universally affected in male cystic fibrosis patients.

In the first study, experiments were conducted using freshly isolated porcine vas deferens epithelial cells. Primary porcine vas deferens epithelial cells exposed to TGF-β1 exhibited a significantly reduced basal transepithelial electrical resistance (R_{te}). TGF-β1-induced reduction in R_{te} was prevented by SB431542, a TGF-β receptor I inhibitor, indicating that the effect of TGF-β1 requires the activation of TGF-β receptor I. Western blot and immunohistochemistry results showed the expression of TGF-β receptor I in native vas deferens epithelia, indicating that the impaired barrier function and anion secretion that were observed in cultured vas deferens cells can likely be observed in the native context. Immunohistochemical outcomes showed that TGF-β1 exposure led to loss of organization of tight junction proteins occludin and claudin-7. These outcomes suggest that TGF-β1 impairs the barrier integrity of epithelial cells lining the vas deferens.

In a parallel study that employed PVD9902 cells that are derived from porcine vas deferens, TGF-β1 exposure significantly reduced anion secretion stimulated by forskolin, forskolin/IBMX, and 8-pCPT-cAMP, suggesting that TGF-β1 affects downstream targets of the cAMP signaling pathway. Real-time RT-PCR and western blot analysis showed that TGF-β1 exposure reduced both the mRNA and the protein abundance of cystic fibrosis transmembrane conductance regulator (CFTR). Pharmacological studies showed that the inhibitory effect of TGF-β1 on forskolin-stimulated anion secretion was abrogated by SB431542 and attenuated by SB203580, a p38 mitogen-activated protein kinase (MAPK) inhibitor. These outcomes suggest that TGF-β1, *via* the activation of TGF-β receptor I and p38 MAPK signaling, reduces CFTR expression, and thus impairs CFTR-mediated anion secretion.

Outcomes from these studies suggest that, in epithelial cells lining the vas deferens, TGF-β1 exposure leads to an impaired physical barrier and/or reduced anion secretion, which is expected

to modify the composition and the maintenance of the luminal environment and thus, is expected to reduce male fertility.

Table of Contents

List of Figures

List of Tables

Acknowledgements

First and foremost, I want to express my sincere thanks to my major advisor, Dr. Bruce Schultz, for supporting me academically and emotionally through my master and doctoral study.

Thanks to my committee members, Dr. Fernando Pierucci-Alves, Dr. Peying Fong, Dr. Philine Wangemann, Dr. Sherry Fleming, for providing insightful suggestions.

I am particularly thankful to Dr. Fernando Pierucci-Alves for introducing me this project and for providing me scientific advice.

Thanks to my outside chairperson, Dr. Rollie J. Clem.

Thanks to our Department Head, Dr. Michael J. Kenney.

Thanks to my former Master's research advisor, Dr. John Tomich.

Thanks to my labmates Dr. Vladimir Akoyev, Florence Wang, Pradeep Malreddy, Qian Wang, and all other past and current members of the Schultz lab for their assistance. Thanks to Joel Sanemman, Don Harbidge for their kind help. It is a pleasure to work with you and to learn from you.

And finally, thanks to my parents Tianxiang Yi and Qin Yuan, and thanks to my friends for your encouragement, support, and love.

Chapter 1 - Introduction

Overview

Cystic fibrosis is a recessive genetic disorder caused by mutations of the gene encoding the cystic fibrosis transmembrane conductance regulator (CFTR), a multifunctional membrane protein that regulates anion permeation. CFTR plays a role in the normal function of many biological systems and mutant CFTR forms are associated with pathology in many systems, including the respiratory, gastrointestinal, digestive, and reproductive systems. Cystic fibrosis affects the architecture of the vas deferens and thus induces male infertility. The severity of cystic fibrosis, especially cystic fibrosis lung disease, is not only mediated by the *CFTR* genotype, but also is affected by other factors such as transforming growth factor β1 (TGF-β1), a cytokine that is expressed in many organs and is present at a relatively high concentration in the male reproductive tract.

The aim of this dissertation is to describe effects of TGF-β1 on cultured porcine vas deferens epithelial cells. Electrophysiological parameters, including transepithelial electrical resistance (R_{te}) and short circuit current (I_{sc}), were measured to determine whether TGF-β1 would affect the barrier integrity of and/or ion transport across vas deferens epithelium. TGF-β1-induced electrophysiological changes in vas deferens potentially indicate whether TGF-β1 could affect male fertility and whether TGF-β1 would likely aggravate cystic fibrosis-related pathology.

This chapter will start with an introduction of TGF-β1: production and activation; signaling pathways; and its physiological and pathological roles. The impact of TGF-β1 on fibrotic diseases, especially on cystic fibrosis, will be described specifically. The following component of this chapter will present the causes and the effects of cystic fibrosis, including the effect of cystic fibrosis on male fertility. The subsequent component will introduce the male reproductive tract, especially the vas deferens. Porcine vas deferens epithelial cells, including both cultures of freshly-isolated vas deferens epithelial cells and PVD9902 cells, will be presented. The tight junction integrity of the vas deferens epithelia, as well as the ion transport across this epithelium will also be discussed.

Transforming Growth Factor Beta 1

Introduction

The TGF-β superfamily consists of structurally related cytokines that are involved in a wide range of cellular processes such as cell growth, cell migration, differentiation, proliferation, apoptosis, wound healing, and immune function. The large, and still growing, TGF-β superfamily consists of bone morphogenetic proteins, growth and differentiation factors, anti-Muellerian hormone, activin, inhibin, nodal, and the TGF-β subfamily (53).

Five members of the TGF-β subfamily have been identified: TGF-β1, TGF-β2 and TGF-β3 in mammals, TGF-β4 in birds, and TGF-β5 in amphibians. Among these isoforms, TGF-β1 is the most abundant. TGF-β1 was first reported in 1978 (24) following its discovery in the medium of murine sarcoma virus-transformed mouse fibroblast cells. The fibroblast-conditioned medium was concentrated by lyophilization and the dissolved concentrate induced colony formation of normal rat kidney fibroblasts in soft agar (24). Isolation of these factors using gel filtration chromatography identified two polypeptides that are responsible for the "transforming" activity, separately named TGF-α and TGF-β (2, 24). Later, TGF-α was characterized as a member of the epidermal growth factor family while TGF-β, the factor that had the property of inducing kidney fibroblast colony formation in soft agar, was identified as a growth factor that is not exclusively derived from tumors, but expressed at variable levels in numerous normal tissues, such as liver, heart, and kidney (80, 81).

TGF-β1 Production

TGF-β1 is translated as a precursor protein called pre-pro-TGF-β1 (Figure 1.1). Pre-pro-TGF-β1, in most mammals such as humans, mice, rats, pigs, and dogs, is a monomer that contains 390 amino acids with an N-terminal pre-region (signal peptide; amino acids 1-29), a pro-region (latency associated peptide, LAP; amino acids 30-278), and the "mature" peptide (mature-TGF-β1; amino acids 279-390) at the C-terminus. The signal peptide directs the translocation of pre-pro-TGF-β1 and is cleaved off in the endoplasmic reticulum. After cleavage of the signal peptide, two monomers are linked by disulfide bonds in both the LAP and the "mature" peptide

portions of pre-pro-TGF-β1 to form a homodimer called pro-TGF-β1. The pro-TGF-β1 later is processed proteolytically in the Golgi by furin, a pro-protein convertase, yielding a dimer of LAP and a dimer of mature-TGF-β1. Although the peptides are cleaved by furin, the LAP dimer and the mature-TGF-β1 dimer remain associated non-covalently to form a latent complex called the small latent complex (SLC) with a molecular mass of ~100 kDa. Within the Golgi, the LAP dimer of SLC covalently binds to the latent TGF-β-binding protein (LTBP) and forms the large latent complex (LLC) with a molecular mass of ~220 kDa (62). LTBP belongs to the superfamily of fibrillin-like extracellular matrix (ECM) proteins, interacts with other ECM proteins such as fibrillin and fibronectin, and thus targets LLC to the ECM for the storage of TGF-β1 (68).

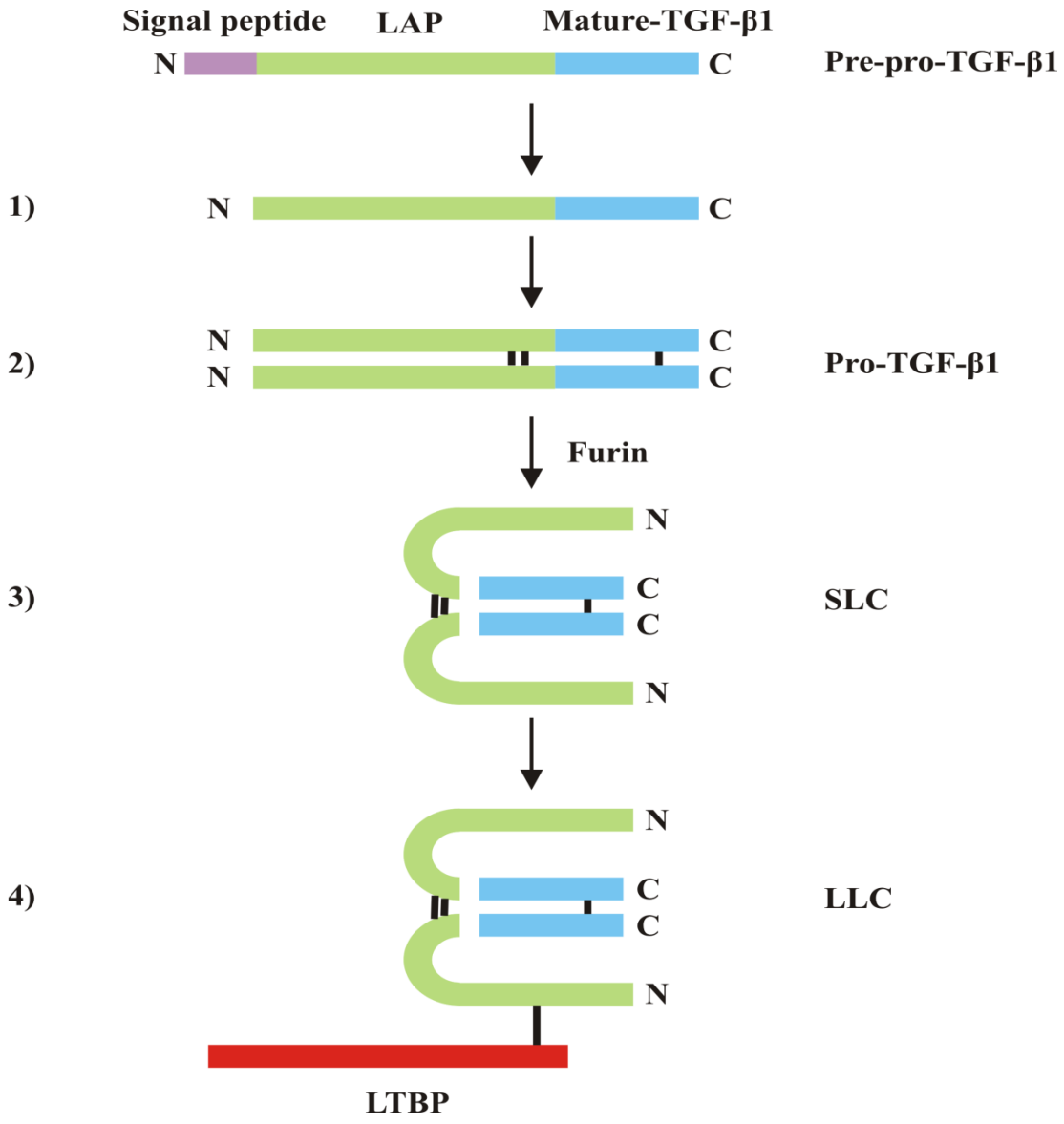

Figure 1.1 Schematic representation of the structure of TGF-β1 and the formation of latent TGF-β1 complexes.

TGF-β1 is synthesized as pre-pro-TGF-β1 and undergoes several processing steps prior to its secretion, as indicated: 1) the signal peptide is cleaved off; 2) two monomers dimerize through disulfide bonds to form pro-TGF-β1; 3) pro-TGF-β1 is cleaved by furin and forms small latent complex (SLC), a non-covalent association of "mature" TGF-β1 dimer and latency associated peptide (LAP) dimer; 4) SLC binds to the latent TGF-β-binding protein (LTBP) and forms large latent complex (LLC).

Activation of TGF-β1

Activation of latent TGF-β1 releases biologically active TGF-β1, which binds to TGF-β1 receptors and elicits multifunctional activities. The activation process involves 2 steps: first, LTBP is cleaved, releasing the LLC from the ECM; second, the LAP dimer goes through a conformational change or proteolysis, disrupting the non-covalent interaction between the LAP dimer and the "mature" TGF-β1 dimer. The disruption of the non-covalent association releases a 25 kDa dimer of "mature" TGF-β1, which is the active form of TGF-β1.

Latent TGF-β1 can be activated by the cellular microenvironment, including pH, temperature, or chaotropic agents. Acidification, alkalinisation, heating, and treatment with chaotropic agents, such as urea, denature LAP and release active TGF-β1. Lawrence *et al* (46) showed that activation of latent TGF-β1 in chicken embryo fibroblast cell-conditioned medium can be achieved by exposure to urea. Brown *et al* (10) reported that human recombinant latent TGF-β1 can be activated by acidification using a pH between 4.1 and 3.1, by alkalinisation using a pH between 11.0 and 11.9, and by heating to >65°C. Lyons *et al* (51) demonstrated that extreme acid or base treatment at pH 1.5 or 12 can activate latent TGF-β1, while mild acid treatment at pH 4.5 can also activate latent TGF-β1, although its activating effect is much weaker than the treatment at pH 1.5.

Latent TGF-β1 can be activated also by plasmin, a serine protease involved in the degradation of the ECM. Plasmin is released as an inactive enzyme precursor, plasminogen, from the liver into circulation. Plasminogen can be converted into active plasmin by tissue plasminogen activator, kallikrein and factor XII (Hageman factor). Plasmin promotes the proteolytic cleavage of LTBP from ECM as well as the degradation of LAP and, thus, the release of active TGF-β1. Treatment of rat kidney fibroblastic cell-conditioned medium with plasmin resulted in the activation of latent TGF-β1 to an extent similar to that of mild acid (pH 4.5) (51). Plasmin inhibitors, such as aprotinin, ε-amino-n-caproic acid, and α2 plasmin inhibitor, blocked the inhibitory effect of active TGF-β1 on cell movement (83). These outcomes identify the critical role of plasmin in the activation of latent TGF-β1.

The activation of latent TGF-β1 is also mediated by thrombospondin-1 (TSP-1), a matricellular glycoprotein. TSP-1 interacts with both LAP and the "mature" TGF-β1 to form a trimolecular complex, which leads to a conformational change of LAP followed by a release of active TGF-β1 (18). Similar to TGF-β1 null mice, TSP-1 null mice showed vascular muscle hyperplasia, alveolar hemorrhage, bronchial epithelial hyperplasia, and pancreatic islet cell hyperplasia. These pathological abnormalities in TSP-1 null mice were normalized with TSP-1-derived peptide (18). Additionally, treatment with blocking peptide that interferes with the activation process of TGF-β1 by TSP-1 reduced the abundance of active TGF-β1 and decreased glomerular ECM accumulation and decreased proteinuria in a mouse model of proliferative glomerulonephritis (21). All these outcomes suggest that TSP-1 regulates the activation of TGF-β1.

Integrins, transmembrane receptors that mediate the attachment between cells and ECM, are TGF-β1 activators as well. $\alpha_v\beta_6$ was the first integrin identified as a TGF-β1 activator (57). $\alpha_v\beta_6$ binds to LAP, pulls LAP from the "mature" TGF-β1, and releases active TGF-β1 by cell movement (41). $\alpha_v\beta_6$-expressing cells induced increased TGF-β1 activity, and the increased TGF-β1 activity can be blocked by antibodies raised against either active TGF-β1 or $\alpha_v\beta_6$ (57). Similar to TGF-β1-null mice, $\alpha_v\beta_6$-null mice (33) and mice with a mutation of the integrin-binding site (106) developed inflammation of many organs, suggesting that integrin $\alpha_v\beta_6$ activates latent TGF-β1.

Expression of TGF-β1

TGF-β1 is ubiquitously expressed. Immunohistochemical labeling demonstrated high abundance of TGF-β1 in adrenal gland, bone marrow, kidney, ovary, and placenta as well as the widespread expression of TGF-β1 in other tissues such as cartilage, heart, pancreas, skin, and uterus in adult mice (95). Outcomes from northern blots showed that TGF-β1 mRNA is expressed in every tissue examined (95).

TGF-β1 is also present at measurable levels in body fluids and secretions, suggesting that it may have an endocrine or lumicrine function (Table 1.1). A fact worthy of attention is the relatively high abundance of TGF-β1 in seminal plasma, which is more than 17 fold of its concentration in

normal human plasma (60, 70). The concentrations of many cytokines in seminal plasma of fertile men, including interleukin-1, -2, -5, -6, -7, -10, -12, -13, and -17, tumor necrosis factor-α, interferon-α, interferon-γ, TGF-β1, granulocyte colony-stimulating factor, and granulocyte-macrophage colony-stimulating factor, have been quantitated. Among these cytokines, TGF-β1 is present in the highest concentration and it is present in all samples (70). The high concentration of TGF-β1 in seminal plasma suggests that it likely plays an important role in reproductive success and that there maybe effects in the male reproductive tract. We speculate that dysregulation of TGF-β1 activity in the male reproductive tract could have clinical importance. The effects of TGF-β1 on vas deferens epithelial cells are reported in Chapter 2 and Chapter 3.

Table 1.1 TGF-β1 concentrations reported in normal human fluids

Human fluid	TGF-β1 concentration
Plasma	5 ng/ml
Urine	300 pg/mg creatinine
Synovial effusion	< 1 ng/ml
Cerebrospinal fluid	20.5 pg/ml
Bronchoalveolar lavage fluid	5.5 pg/ml
Seminal plasma	85-238 ng/ml

Table modified from (60, 62, 70).

TGF-β1 Signaling

TGF-β1 regulates multiple cellular processes through a general mechanism in which active TGF-β1 binds to and activates transmembrane receptors, initiates the canonical Smad signaling pathway and/or non-canonical signaling pathways, and thus mediates biological effects (14, 108).

TGF-β Receptor Activation

TGF-β receptors, including receptor I and receptor II, are required for TGF-β signal transduction (Figure 1.2). Both TGF-β receptor I and TGF-β receptor II contain a small cysteine-rich extracellular region, a single transmembrane region, and an intracellular region that contains a serine/threonine protein kinase domain. TGF-β receptor I also contains an intracellular region, named the GS domain, that is rich in glycines and serines (53).

In the absence of TGF-β1, both receptor I and receptor II exist as homodimers in the cell surface. TGF-β1 binds to the pre-formed dimer of TGF-β receptor II to initiate TGF-β1 signaling. The binding of TGF-β1 to TGF-β receptor II dimer allows subsequent recruitment of TGF-β receptor I dimer and results in the formation of a stable tetrameric receptor complex. TGF-β receptor II is a constitutively active kinase. Upon formation of the ligand-induced receptor complex, TGF-β receptor II transactivates receptor I by phosphorylation at serine and threonine residues in their GS domains. Activated TGF-β receptor I activates the canonical signaling pathway and/or non-canonical signaling pathways (89).

The Canonical Smad Signaling Pathway

Smad proteins were the first identified effectors for TGF-β receptors (54). They are the vertebrate homologues of the *Drosophila* protein MAD (mothers against decapentaplegic) and the *Caenorhabditis elegans* protein SMA (small body size). Smad proteins are divided into 3 groups based on their functions: the receptor-activated Smads (R-Smads, Smad1, 2, 3, 5, and 8), the common mediator Smad (Co-Smad, Smad4), and the inhibitory Smads (I-Smads, Smad6 and 7). Smad2 and Smad3 mediate signals from TGF-β1 and affect the transcription of target genes, while Smad7 regulates TGF-β1 responses by a negative feedback mechanism (Figure 1.2).

After TGF-β1 binding and the consequent phosphorylation of TGF-β receptor I, Smad2/3 are recruited to the receptor complex with the assistance of Smad anchor for receptor activation (SARA), a protein that interacts with both the receptor complex and Smad2/3. Upon the binding to the TGF-β1 receptor complex, Smad2/3 are phosphorylated directly by TGF-β receptor I. The phosphorylation-activated Smad2/3 dissociate from both the receptor complex and SARA. With the aid of scaffolding proteins such as TGF-β receptor I associated protein-1 (TRAP-1), Smad4 is bound to phosphorylated Smad2/3 to form an R-Smad/Co-Smad complex. The R-Smad/Co-

Smad complex translocates into the nucleus, recognizes and binds to Smad binding elements (SBE) in the promoter sequences of target genes, interacts with additional transcription co-regulators, regulates the expression of target genes, and thus affects various cell functions. The transcription co-regulators include factors such as activator protein-1 (AP-1) and forkhead box protein H1 (FOXH1 or FAST-1) and co-activators such as CBP/p300.

The Smad signaling pathway is negatively controlled by I-Smads. Smad7 competes with Smad2/3 for the binding site on the activated TGF-β receptor complex, prevents Smad2/3 from being phosphorylated, and blocks downstream activation of the Smad signaling pathway (14, 53).

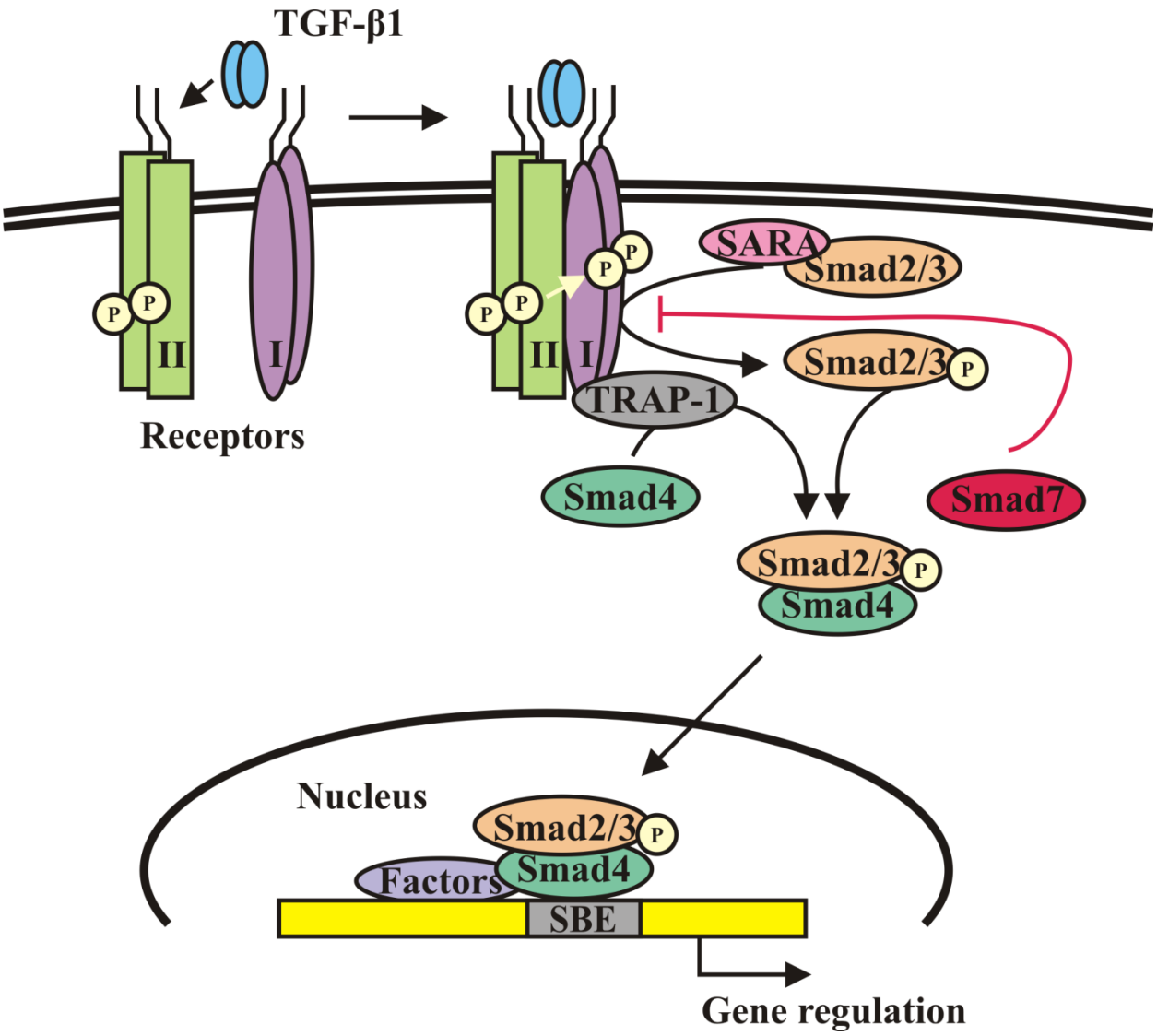

Figure 1.2 Schematic representation of the canonical Smad signaling pathway.

Upon the binding of TGF-β1 to TGF-β receptor II and the subsequent formation of the activated TGF-β receptor II and receptor I complex, Smad2/3 are recruited and phosphorylated. Phosphorylated Smad2/3 initiate the canonical Smad signaling pathway. Phospho-Smad2/3 are then released from the TGF-β receptor complex and form a complex with Smad4. The formed Smad complex relocates to the nucleus, interacts with Smad binding elements (SBE), and regulates cell-specific target gene(s). The canonical Smad pathway is inhibited by Smad7. SARA, Smad anchor for receptor activation; TRAP-1, TGF-β receptor I associated protein-1.

In addition to directly regulating gene expression in the canonical signaling pathway, Smad proteins also regulate other pathways, *e.g.* the protein kinase A (PKA) signaling pathway (104, 105, 107). PKA is activated typically by the elevation of intracellular cAMP concentration. Independently of cAMP, TGF-β1-induced Smad3/Smad4 complex binds to the regulatory subunits of PKA, releases the PKA catalytic subunits, and activates the PKA signaling pathway. This mechanism reportedly contributes to the growth inhibition and epithelial-mesenchymal transition (EMT) (105, 107).

The Non-Canonical Signaling Pathways

Emerging evidence suggests that the Smad signaling pathway does not explain all TGF-β1-associated effects. In addition to the canonical Smad signaling pathway (Figure 1.2), TGF-β1 also is able to induce signals through the activation of non-canonical signaling pathways, including the c-Jun N-terminal kinase (JNK), the p38 mitogen-activated protein kinase (p38 MAPK), the extracellular signal-regulated kinase (Erk), the Ras homolog (Rho)-like GTPase, and the phosphoinositide 3-kinase (PI3K) signaling pathways.

p38 MAPK- and JNK-activated cascades are the most-studied pathways among the non-canonical signaling pathways (Figure 1.3). When TGF-β receptor I is in its non-phosphorylated basal state, it interacts with TGF-β-activated kinase 1 (TAK1), a serine/threonine kinase in the mitogen-activated protein kinase kinase kinase (MAPKKK) family, TAK1-binding protein-2 (TAB2), and tumor necrosis factor (TNF) receptor-associated factor 6 (TRAF6), a ubiquitin ligase that catalyzes the ubiquitylation of itself and other molecules upon ligand binding (45). Upon the binding of TGF-β receptor II and the subsequent phosphorylation of TGF-β receptor I, TRAF6 undergoes auto-ubiquitination and induces the ubiquitination and dissociation of TAK1 from the TGF-β receptor complex. Released TAK1 binds to TAK1-binding protein-1 (TAB1), which triggers the autophosphorylation and activation of TAK1. Activated TAK1 phosphorylates MAP kinase kinase 3/6 (MKK3/6) and/or MAP kinase kinase 4 (MKK4), which phosphorylate and activate p38 MAPK and JNK, respectively (45). Activated p38 MAPK and/or JNK target transcription factors, such as activating transcription factor 2 (ATF2) and c-Jun, activate or repress target genes, and regulate cellular responses such as apoptosis and EMT (16, 108).

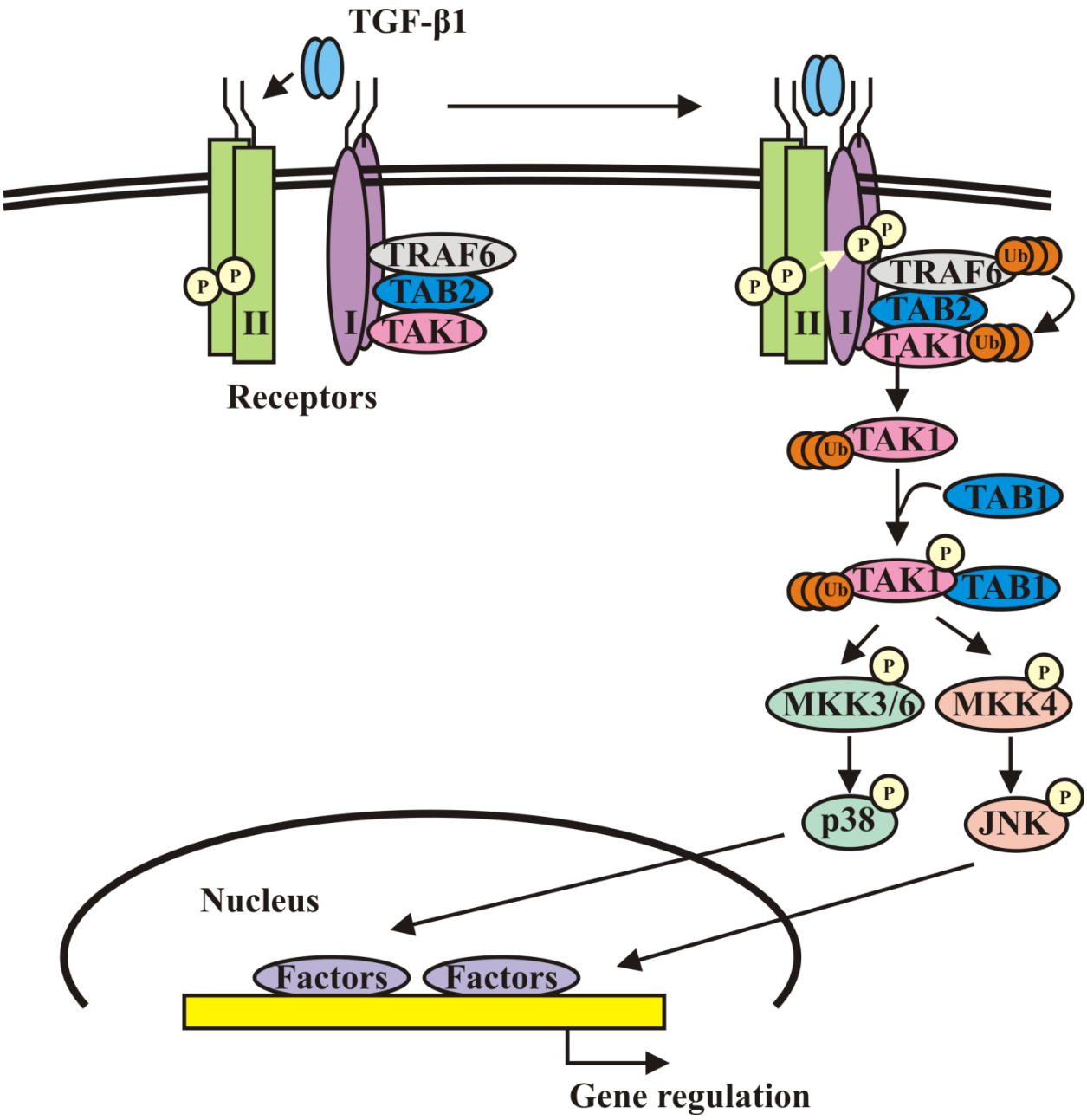

Figure 1.3 Schematic representation of the JNK/p38 MAPK signaling pathway.

Upon the activation of TGF-β receptor complex, auto-ubiquitination of tumor necrosis factor (TNF) receptor-associated factor 6 (TRAF6) induces the ubiquitination and release of TGF-β-activated kinase 1 (TAK1). TAK1 interacts with TAK1-binding protein-1 (TAB1) and is then auto-phosphorylated. Phosphorylated TAK1 transmits TGF-β1 signals to the p38 MAPK and the JNK signaling pathway to regulate target genes. Ub, ubiquitin.

In addition to the p38 MAPK and the JNK pathway, TGF-β also activates the Erk signaling pathway. Activated TGF-β receptor complex recruits growth factor receptor binding protein 2 (GRB2) and Son of Sevenless (SOS). SOS catalyzes the Ras exchange of GDP for GTP and thus activates Ras, Raf, and their downstream target Erk. Activated Erk affects transcription factors such as Snail, a repressor of E-cadherin transcription, and thus mediates EMT (108).

Members of the Rho-like GTPase family also are involved in TGF-β1 signaling in polarized epithelial cells. Upon the binding of TGF-β1, Par6, a scaffold protein that colocalizes with TGF-β receptor I at tight junctions, is phosphorylated by the receptor complex. Phosphorylated Par6 recruits Smurf1 and mediates the ubiquitination and degradation of RhoA, which enables the dissolution of tight junctions during EMT (63).

Another kinase that is activated by TGF-β1 is PI3K. Activated TGF-β receptor complex, possibly through a physical interaction, activates PI3K, and phosphorylates its downstream effector Akt. Activated Akt further phosphorylates glycogen synthase kinase 3β (GSK3β) and inhibits its activity (39). GSK3β inhibition is associated with elevated Snail transcription, and thus mediates EMT (4).

In conclusion, the full spectrum of biological responses to TGF-β1 depends on multiple signaling pathways that involve the canonical Smad signaling pathway as well as various non-canonical signaling pathways.

Physiological and Pathological roles of TGF-β1

TGF-β1 plays critical roles in many physiological functions such as the immune response, cell proliferation, apoptosis, differentiation, production of ECM, and EMT (62). Malfunctions of the TGF-β1 signaling pathway are implicated in a variety of pathological processes including autoimmune diseases, cancer, and fibrotic disorders.

TGF-β1 and Autoimmune Diseases

TGF-β1 regulates the proliferation, differentiation, and survival of lymphocytes and thus controls the immune system. For T lymphocytes, TGF-β1 inhibits the proliferation of T cells, blocks the

differentiation of T helper cells and cytotoxic T lymphocytes, induces the generation of regulatory T cells, and promotes the survival of T cells during T cell expansion and differentiation (49). For B lymphocytes, TGF-β1 inhibits the proliferation and activation of B cells, induces apoptosis in immature B cells and resting B cells, and regulates the production of immunoglobulin (48, 49). Besides its diverse roles in lymphocytes, TGF-β1 inhibits the functions of other immune cells such as natural killer cells, dendritic cells, and macrophages (49).

The protective role of TGF-β1 in many autoimmune diseases has been well documented. TGF-β1 knockout mice developed hallmarks of autoimmune diseases such as a progressive lymphocyte infiltration into multiple organs that led to death at about 3 weeks after birth due to compromised organ function (48). Intraperitoneal injection of TGF-β1 to mice inhibited collagen-induced arthritis and experimental allergic encephalomyelitis (44). Similarly, the administration of antibody to TGF-β1 exacerbated the severity of experimental allergic encephalomyelitis (55, 75). Consistent with the immunosuppressing role of TGF-β1, decreased production of TGF-β1 was found in patients with autoimmune diseases such as systemic lupus erythematosus (61) and multiple sclerosis (56). On the other hand, in later stages of autoimmune diseases, the infiltration of inflammatory cells stimulates the local production of TGF-β1, which contributes to dysregulated tissue repair and remodeling, and eventually leads to tissue fibrosis and organ damage (84). In autoimmune-prone (NZB/W F1) mice, although the expression of TGF-β1 in the lymphoid tissue was reduced compared with its expression in non-autoimmune mice, elevated levels of TGF-β1 in the kidney correlated with chronic renal lesions (involving mesangial matrix deposition, glomerular scars, tubular atrophy and interstitial fibrosis), suggesting that TGF-β1 plays dual roles in the pathogenesis of organ damage in autoimmune diseases (84).

TGF-β1 and Cancer

TGF-β1 regulates the cell cycle and thus controls cellular proliferation. In epithelial cells, TGF-β1 arrests the cell cycle at the G1 stage, inhibits cell proliferation, and promotes cell apoptosis. In cancer cells that have mutations in one or more components of the TGF-β1 signaling pathway, TGF-β1 fails to arrest cell growth or proliferation (8). TGF-β1 also can induce EMT, a biological

process characterized by reduced expression of cell junction proteins and the upregulation of mesenchymal proteins. During EMT, epithelial cancer cells lose their epithelial polarity, acquire more migratory mesenchymal cell-like properties, and gain enhanced mobility and invasiveness (38).

The different effect of TGF-β1 on normal cells *versus* cancer cells contributes to the dual role of TGF-β1 in carcinogenesis. At early stages of tumor development, TGF-β1 acts as a growth inhibitor and tumor suppressor. Mice heterozygous for the deletion of the TGF-β1 gene, that express only 10-30% of wild-type TGF-β1 protein, exhibited enhanced tumorigenesis compared to their wild-type littermates in response to chemical carcinogens (93). The tumor-prone syndromes in transgenic mice suggest that TGF-β1 has a protective effect. At later stages of tumor development, tumor cells become resistant to the growth inhibition role of TGF-β1. TGF-β1, *via* its effects on migration and invasion, acts as a tumor promoter. Elevated plasma levels of TGF-β1 have been identified in cancer patients, such as patients with hepatocellular carcinoma (36), breast cancer (37), and colorectal cancer (96). Additionally, a strong correlation between elevated serum levels of TGF-β1 and cancer invasion has been demonstrated (50, 103). Mice with TGF-β1 overexpressed in keratinocytes have been exposed to long-term carcinogens. These transgenic mice showed a suppressed benign tumor outgrowth 10-25 weeks post carcinogen initiation, but an enhanced malignant conversion rate after 26 weeks, suggesting the dual action of TGF-β1 in cancer (19).

TGF-β1 and Fibrotic Diseases

TGF-β1 stimulates ECM production, and thus accelerates wound healing and repair (9, 47). Excessive or sustained secretion of TGF-β1 induces a pathological excess of tissue repair and thus leads to fibrotic diseases of many organs (42, 102). Patients with fibrotic disease, including liver cirrhosis, idiopathic pulmonary fibrosis, chronic obstructive pulmonary disease, and skin fibrosis exhibit increased mRNA levels of TGF-β1 (6, 9, 23, 92).

A strong correlation between cystic fibrosis and TGF-β1 also has been identified (9). An *in vitro* study showed that cystic fibrosis epithelial cells produce increased levels of TGF-β1 when compared with non-cystic fibrosis controls (66). Genetic polymorphisms in the TGF-β1 gene

associate with the severity of cystic fibrosis lung disease (17). Notably, genetic variations affect the production of TGF-β1. For the single nucleotide polymorphism at position +869 (C or T) in codon 10, the TGF-β1 polymorphism T/T is associated with high TGF-β1 production and thereby has been designated as the TGF-β1 'high producer' genotype. It follows that other polymorphisms (T/C or C/C) in codon 10 are called TGF-β1 'low producer' genotypes. Clinical information from 171 patients suggested that cystic fibrosis patients having the TGF-β1 high producer genotype experienced a more rapid deterioration in lung function and developed a more severe lung disease (3). Direct measurement of TGF-β1 also suggested that the concentration of TGF-β1 affects the severity of cystic fibrosis. TGF-β1 levels in bronchoalveolar lavage fluid of pediatric cystic fibrosis patients is higher than that of non-cystic fibrosis children undergoing bronchoscopy for the evaluation of chronic/recurrent wheeze or recurrent pneumonia. Additionally, in cystic fibrosis children, an increased TGF-β1 level is associated with reduced forced expiratory volume in one second (FEV_1), suggesting a correlation between TGF-β1 levels and lung function (31). In pediatric cystic fibrosis patients, plasma TGF-β1 levels also correlate with the severity of lung disease. After antibiotic treatment for a pulmonary exacerbation, plasma TGF-β1 level decreased and FEV_1 improved (30). Additionally, TGF-β1 exposure attenuates the efficacy of correctors of ΔF508, the most common *CFTR* mutation, indicating that TGF-β1 may interfere with the cystic fibrosis clinical therapy aimed to rescue the functional defect of ΔF508 (88). All these observations suggest that higher TGF-β1 expression aggravates or increases the clinical severity of cystic fibrosis.

Cystic Fibrosis

Cystic fibrosis is a life-shortening disease first described by Dr. Dorothy Andersen in 1938 (1). It is the most common life shortening autosomal recessive diseases in Caucasians. According to data from the Cystic Fibrosis Foundation, it affects ~30,000 children and adults in the United States and ~70,000 worldwide while more than 1000 new cases are diagnosed annually (58). Cystic fibrosis is caused by defects in the gene that encodes CFTR, an anion channel that contributes to fluid and electrolyte transport across epithelia.

CFTR Gene and Protein

CFTR was localized to chromosome 7 in 1985 and was subsequently identified in 1989 (79, 100). The gene spans ~250,000 base pairs and consists of 27 exons (Figure 1.4). These 27 exons were previously numbered 1-24 with subdivisions of exon 6 (6a and 6b), exon 14 (14a and 14b) and exon 17 (17a and 17b) (110).

CFTR codes for a 1480 amino acid glycoprotein with a mature molecular mass of ~170,000 Da. Mature CFTR, in most cases, is located in the apical membrane of epithelial cells, where it provides a pathway for anion secretion. The protein contains five functional domains: two membrane-spanning domains (MSD1 and MSD2), each of which is composed of six transmembrane segments, two cytoplasmic nucleotide-binding domains (NBD1 and NBD2), and a regulatory domain (R; Figure 1.4). The transmembrane domains contribute to the formation of the CFTR pore, which allows for the movement of chloride and/or bicarbonate across the membrane down their respective electrochemical gradients (22). Gating of the CFTR pore is regulated by the R domain, which contains several consensus sites for phosphorylation. Phosphorylation of the R domain, together with the presence of ATP, drives the opening of CFTR channel (35). CFTR is phosphorylated and activated by PKA. Therefore, factors that increase the generation of cAMP, such as the binding of agonists to receptors signaling through cAMP/PKA pathways, the activation of the adenylyl cyclase, and the inhibition of phosphodiesterase, activate anion permeation through CFTR channels (85, 86). CFTR can also be activated by protein kinase C (PKC), although to a lesser extent (5, 91).

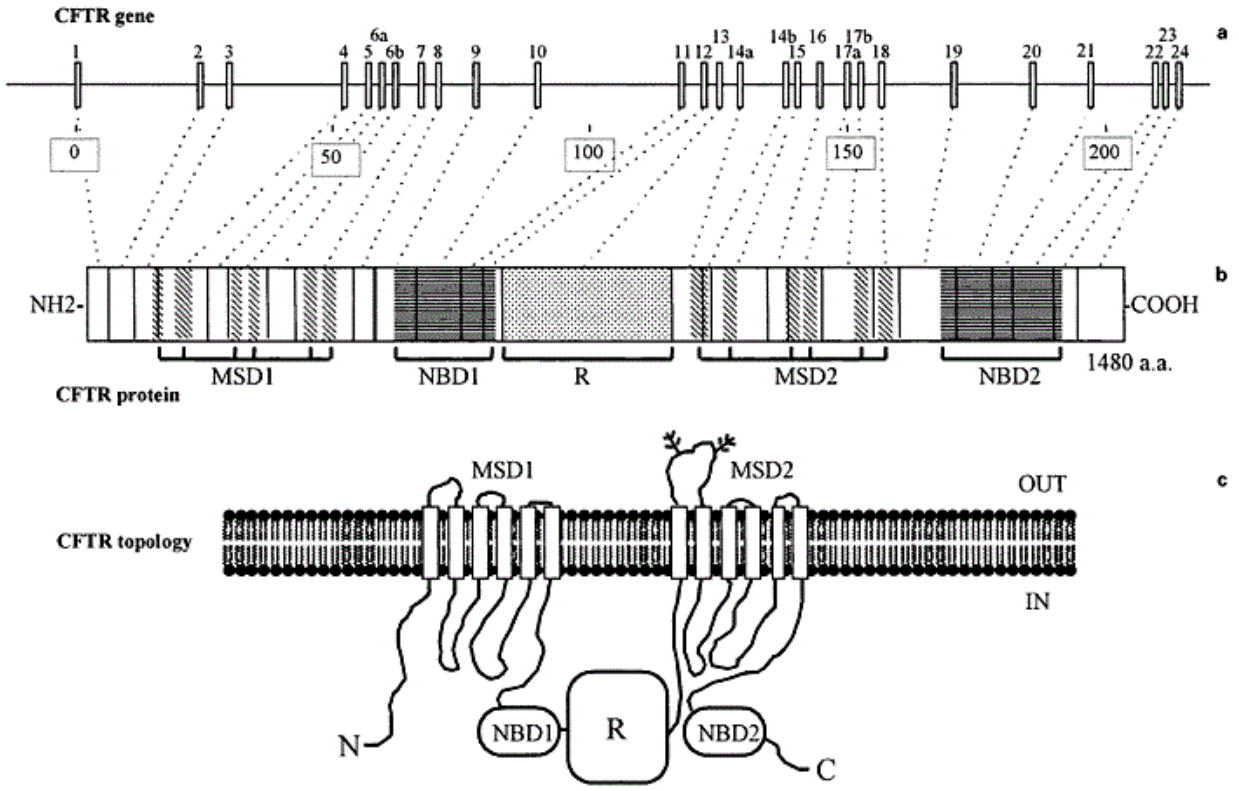

Figure 1.4 Schematic representation of the human CFTR gene and protein.

The diagram shows (a) the structure of *CFTR* with 27 exons; (b) the predicted structure of the resulting CFTR protein with five functional domains: membrane-spanning domain (MSD1), nucleotide-binding domain (NBD1), regulatory domain (R), MSD2, and NBD2; (c) the topological model of CFTR protein in the apical cell surface.

Figure modified from (109).

Since 1983, it has been demonstrated that cystic fibrosis leads to chloride impermeability in sweat glands, which suggests that CFTR is a chloride channel (72). Evidence also suggests that CFTR transports bicarbonate (34, 71). Under normal conditions, the CFTR protein functions as an anion channel that mediates the secretion of chloride and bicarbonate, which drives the movement of fluid into the luminal compartment across epithelial cells. Mutated *CFTR* codes for defective amounts and/or function of CFTR proteins. Defective CFTR protein causes impaired electrolyte and fluid secretion and dehydration of luminal contents in affected organs such as pancreas and airways throughout the respiratory system. Meanwhile, defective bicarbonate

secretion leads to a less alkaline luminal fluid in hollow organs or glands. These changes in the luminal components could induce organ damage and cause cystic fibrosis pathology in many organs.

CFTR Mutations

More than 1900 different mutations in *CFTR* have been identified to date (CFTR mutation database; http://www.genet.sickkids.on.ca/cftr). A large portion of these mutations represent the change in a single nucleotide or insertions or deletions of a number of nucleotides. Although many mutations have been documented, most of them are quite rare. Fewer than 20 mutations occur at a frequency higher than 0.1% while only 5 mutations (ΔF508, G542X, G551D, W1282X, and N1303K) occur at a frequency higher than 1% in cystic fibrosis patients.

Various mutations of the *CFTR* gene affect function in different ways. *CFTR* mutations have been categorized into five functional classes (Figure 1.5). Class 1 ('no synthesis') mutations cause a premature signal to terminate RNA translation (stop codon), resulting in little protein production and few or no functional CFTR channels. G542X and W1282X belong to this class. Class 2 ('block in processing') mutations disrupt CFTR protein folding and adversely affect protein maturation. CFTR proteins are synthesized, but are not trafficked to the apical surface to perform their ion transport function. N1303K, as well as ΔF508, the most common mutant form of *CFTR*, belong to this class. Class 3 ('block in regulation') mutations affect CFTR channel gating. Therefore, there is little or no ion movement through CFTR channels even though CFTR is synthesized and trafficked to the apical cell surface. G551D belongs to this class. Class 4 ('altered conductance') mutations cause defective anion transport through CFTR channels. R117H, a mutant form commonly associated with male infertility, but with lesser effects on pulmonary and digestive function, is an example of a class 4 mutation. Class 5 ('reduced synthesis') mutations cause reduced production of functional CFTR and thus a smaller amount of synthesized CFTR may reach the apical cell surface. A455E is a mutant form that belongs to class 5.

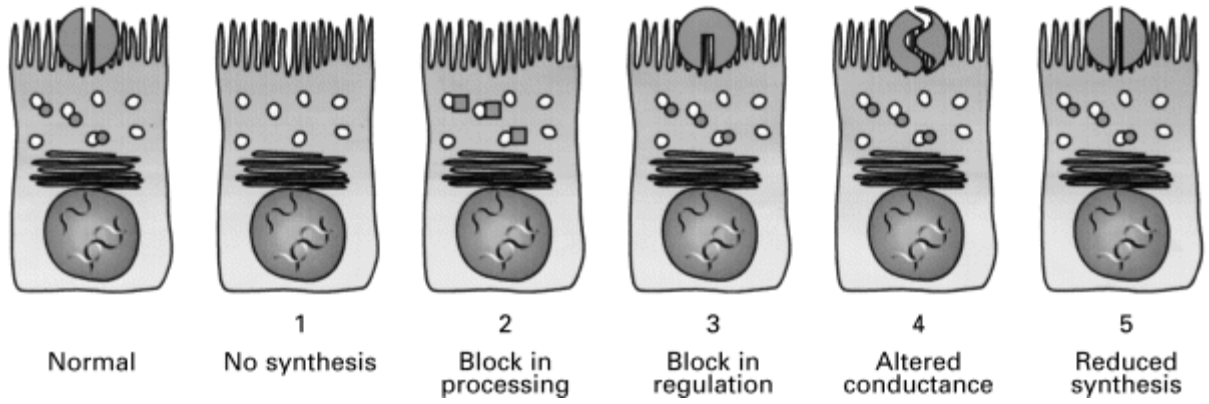

Figure 1.5 Normal *CFTR* and five functional classes of *CFTR* mutations.
CFTR codes for CFTR channels while *CFTR* mutations lead to abolished or impaired functional CFTR channels. For normal *CFTR*, CFTR protein is synthesized, trafficked to the apical cell surface, and functions as a nucleotide-gated anion channel upon its activation by cAMP dependent phosphorylation. For *CFTR* mutations, little (class 1 to 3) or less (class 4 and 5) functional CFTR is present in the apical cell surface.
Figure adapted from (90).

The severity of cystic fibrosis is associated with different types of *CFTR* mutations and the amount of functional CFTR (Table 1.2). Individuals inherit one copy of *CFTR* from each parent. Those with two 'normal' *CFTR* have 100% normal CFTR function. People with one 'normal' and one mutant *CFTR* have 50-100% of normal CFTR function depending on the severity of the mutation. They are cystic fibrosis carriers who do not have apparent cystic fibrosis symptomology. About 1 in 25 Caucasians are cystic fibrosis carriers. Individuals harboring two mutant *CFTR* alleles are cystic fibrosis patients and suffer from cystic fibrosis-associated pathologies. The more severe mutations are associated with less CFTR function, leading to more severe disease manifestations (109). Classes 1 to 3 *CFTR* mutations (Figure 1.5) are typically 'severe' *CFTR* mutations that express little or no functional CFTR at the apical cell surface while classes 4 and 5 are 'mild' or atypical *CFTR* mutations that include some residual CFTR function. For patients with two 'severe' *CFTR* mutations, the absence of functional CFTR leads to classic cystic fibrosis phenotype including meconium ileus, failure to thrive, distal intestinal obstruction, pancreatic insufficiency, recurrent bronchial infections and progressive pulmonary disease, salty sweat, obstructive biliary disease, and congenital bilateral absence of the vas deferens (CBAVD).

For patients with one 'severe' *CFTR* mutation and one 'mild' *CFTR* mutation and for patients with two 'mild' *CFTR* mutations, the expressed CFTR protein retains some function and these patients exhibit less severe clinical manifestations. These patients generally will retain some pancreatic function and exhibit reduced pulmonary involvement, but will have CBAVD. Heterozygosity for R117H and ΔF508 or homozygosity for R117H leads to CBAVD, suggesting that the male reproductive tract is more sensitive to any alterations in CFTR expression or activity (111).

Table 1.2 CFTR channel function and CFTR-associated cystic fibrosis phenotype.

Percentage of normal CFTR function	Manifestations of CFTR
< 1%	Pancreatic insufficiency Plus manifestations listed below
< 4.5%	Progressive pulmonary disease Plus manifestations listed below
< 5%	Clinically demonstrable sweat abnormality
< 10%	Congenital bilateral absence of the vas deferens (male infertility)
10-30%	Some abnormalities
31-49%	No known abnormality
50-100%	No known abnormality (carriers)

The relationships between the amount of normal CFTR function and clinical cystic fibrosis manifestation are listed.
Table modified from "Cystic Fibrosis Medicine" (http://www.cysticfibrosismedicine.com).

Effects of Cystic Fibrosis

Cystic fibrosis affects many organs including sweat glands, airway, pancreas, gastrointestinal tract, liver, gallbladder, and the reproductive system.

The sweat gland secretory coil secretes an isotonic fluid into the lumen and then salt is reabsorbed in the sweat duct before secretion, releasing hypotonic sweat (73). In cystic fibrosis patients, due to the lack of functional CFTR, the chloride conductance in the sweat gland is abolished. The conductance of epithelial sodium channel (ENaC) is also reduced in CF sweat duct (78). Impaired sodium and chloride reabsorption leads to a high salt concentration in the sweat of cystic fibrosis patients (74). Therefore, the sweat test, which measures the concentration of chloride in solution on the skin surface, has been used to screen for cystic fibrosis. People with a chloride level of greater than or equal to 60 mEq/L are likely to be diagnosed as cystic fibrosis patients.

Abnormal CFTR protein causes defective anion conductance on the apical cell surface of airway epithelial cells and leads to airway surface liquid depletion, mucus dehydration or lack of hydration, and mucus plugging of the airways. The thick mucus impairs ciliary movement, decreases mucociliary clearance, and prevents foreign particles and bacteria from being cleared effectively (99). Trapped foreign particles and bacteria lead to the infection, typically dominated by *Staphylococcus aureus* and *Pseudomonas aeruginosa* (27). Persistent and recurrent infections incite neutrophilic inflammatory responses (82), progress to chronic sinusitis and chronic lung disease, and result in the decline of lung function (77).

CFTR dysfunction in the pancreas leads to a reduced secretion of bicarbonate into the pancreatic juice resulting in a reduced fluid pH that is not optimal for digestive enzymes (40, 64). Additionally, CFTR dysfunction reduces ductal fluid secretion, causing the obstruction of pancreatic ducts by protein precipitation. Blockage of the pancreatic ducts prevents the movement of digestive enzymes into the duodenum and thus causes malabsorption of nutrients. The accumulated digestive enzymes are thought to cause destruction of the pancreas due to autodigestion and eventually lead to pancreatic fibrosis or scarring (43). Ultimately, >85% of cystic fibrosis patients are pancreatic insufficient and require enzyme supplementation.

In the gastrointestinal tract of cystic fibrosis patients, defective CFTR reduces the secretion of chloride and bicarbonate. Decreased electrolytes and water content result in the production of thick mucus (28). Accumulated intestinal mucus may lead to mucus obstruction, resulting in meconium ileus, an intestinal blockage that occurs in ~10% of newborns with cystic fibrosis

(74). Later in life, distal intestinal obstruction syndrome and constipation are frequently seen in cystic fibrosis patients (97).

Dysfunction of CFTR expressed in the epithelial cells lining the biliary tract reduces electrolyte and fluid secretion and results in increased bile viscosity. Viscous bile can obstruct bile ducts, which leads to liver damage such as focal biliary cirrhosis (32). The thick and dehydrated bile stored in the gallbladder contributes to the formation of gallstones. Altered bile composition, together with pancreatic dysfunction, also impairs fat absorption and leads to steatorrhea (101).

In the reproductive system of male cystic fibrosis patients, dysfunction of CFTR changes the anatomical structures of the epididymis, vas deferens and seminal vesicles, impairs the production and maturation of sperm, and leads to male infertility (76).

Effects of Cystic Fibrosis on Male Fertility

Reproductive duct abnormalities in male cystic fibrosis patients were first described in 1968 (25). Most male cystic fibrosis patients are infertile. Male with cystic fibrosis exhibit testes that are normal or diminished in size, epididymides that are markedly reduced in size or partially absent, scrotum that is enlarged, seminal vesicles that are atrophic and dysfunctional, and vasa deferentia that are absent (90). About 98% of male cystic fibrosis patients are affected by CBAVD, which blocks the movement of sperm from the caput epididymis to the ejaculatory ducts and results in azoospermia (20, 94). Besides the changes in the anatomical structures of the male reproductive system, the semen of male cystic fibrosis patients show abnormalities including azoospermia, reduced volume, and reduced pH (25).

Genetic screening in men with CBAVD suggested that a large portion of these individuals have mutations in their *CFTR* genes, although many do not exhibit classical clinical symptoms of cystic fibrosis (52). Cystic fibrosis carriers also exhibit a higher frequency of infertility than individuals with two normal *CFTR* alleles. Infertile men with normal vas deferens but reduced sperm quality exhibit a frequency of *CFTR* mutation that is significantly higher than the frequency of CF carriers in a general population (98).

The high frequency of male infertility in cystic fibrosis patients either with ‘mild’ or ‘severe’ mutations and in cystic fibrosis carriers suggests the importance of functional CFTR in the male reproductive system, especially in the vas deferens.

Vas Deferens

Vasa deferentia are critical structures in the male reproductive tract (Figure 1.6). Sperm are produced in seminiferous tubules in the testis, but when leaving testis are not capable of achieving fertilization. These sperm mature and acquire motility during their passage through the epididymis. During ejaculation, the smooth muscle in the vas deferens wall contracts and propels sperm to pass through the vas deferens to the ejaculatory ducts, and finally through the urethra to the outside of the body. Vasa deferentia store sperm cells and conduct sperm forward. Moreover, ion transport across the epithelial cells lining the vas deferens can rapidly alkalinize the luminal environment to which sperm are exposed, thereby contributing to sperm activation.

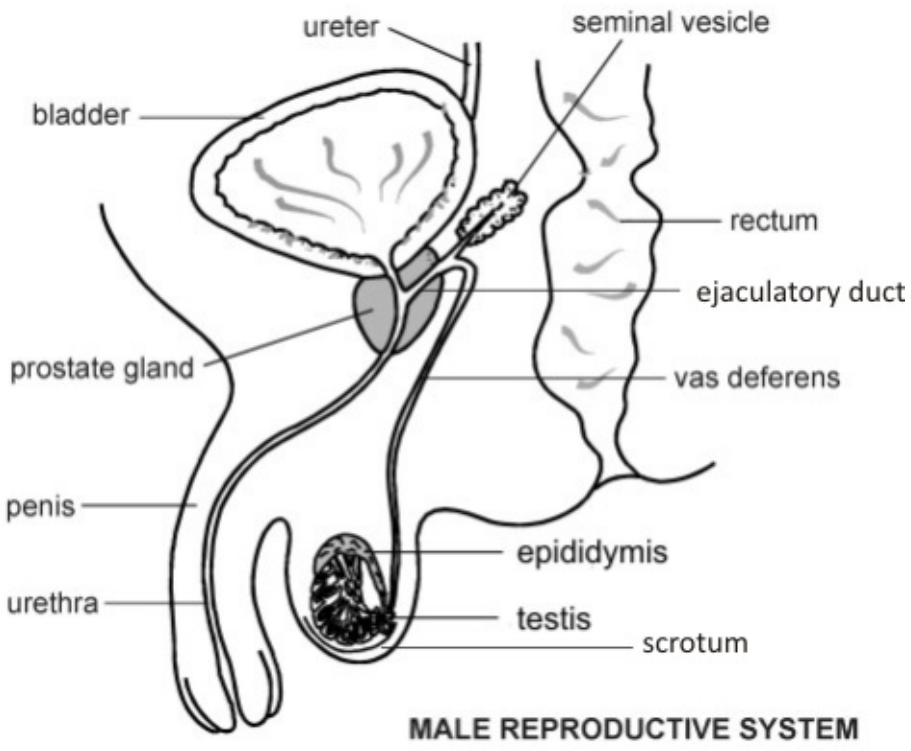

Figure 1.6 Anatomical diagram of the human male reproductive system.

The human male reproductive system contains a number of organs including scrotum, testes, epididymides, vasa deferentia, seminal vesicles, prostate gland, ejaculatory ducts, urethra, and penis.

Figure modified from http://www.patient.co.uk/diagram/Male-Reproductive-system.htm.

Obstruction or absence of the vas deferens leads to male infertility. This is seen commonly in cystic fibrosis patients and there is a higher incidence in *CFTR* mutation carriers as discussed in the previous section. In the following section, the morphology and the function of the vas deferens, ion transport across the vas deferens epithelia, and description of a cultured vas deferens epithelial cell line, PVD9902, will be introduced.

Anatomical Structure of the Vas Deferens

The vas deferens, also called sperm duct or spermatic deferens, is a thick-walled tube that begins at the caudal end of the epididymis in the scrotum, extends into the pelvic cavity to the back of the prostate, and joins with the seminal vesicles. There are two identical vasa deferentia

emerging from the two epididymides. Each is ~30 cm in length in adult humans and connects the left and right epididymides to the ejaculatory ducts.

The morphology of the vas deferens is identified by a narrow lumen in adults and surrounding thick muscular coat (Figure 1.7). The tissue lining the lumen is a layer of the mucous membrane. The mucous membrane is a pseudostratified columnar epithelium. Surrounding the mucous membrane are lamina propria and 3 layers of smooth muscle: an inner longitudinal layer, a middle circular layer, and an outer longitudinal layer that is attached to adventitia (59). As the vas deferens ascends towards the bladder, it is surrounded by arteries, veins, and nerves to form structure surrounded by connective tissue that is called the spermatic cord. At the fundus of the bladder, the vas deferens enlarges to form the ampulla, which connects to the ejaculatory duct.

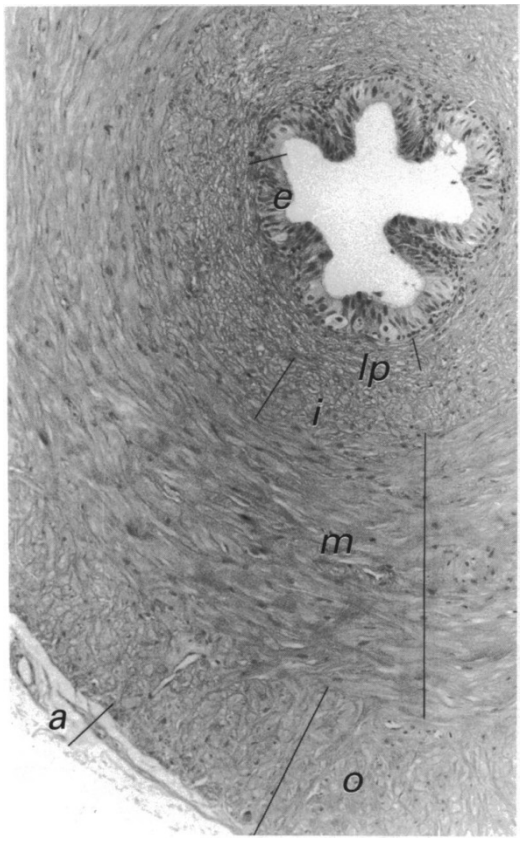

Figure 1.7 Cross-section of the vas deferens.

The vas deferens comprises 4 layers: the mucosa epithelium (e), the lamina propria (lp), the muscular coat, and adventitia (a). The muscular coat contains three layers of smooth muscle: the inner longitudinal layer (i), the middle circular layer (m), and the outer longitudinal layer (o). Figure adapted from (59).

Primary Porcine Vas Deferens Cells and PVD9902 Cells

Porcine vas deferens epithelial cells have been isolated and cultured in our laboratory to study their basic biology and especially ion transport. Primary cultures of cell derived from vas deferens express biochemical markers of epithelial cells, ZO-1 and cytokeratin, display a high R_{te} of ~3,900 Ω cm^2, and respond to numerous neuro-hormonal agents such as norepinephrine, vasopressin, ATP, adenosine, and histamine (87). Freshly isolated and cultured vas deferens epithelial cells provide a powerful tool to study the epithelial function and the ion transport mechanism in vas deferens epithelial cells.

Primary porcine vas deferens cells provide valuable data. However, one of the major concerns is reliable access to tissues and potential variability due to donors and isolation protocols. To better characterize vas deferens epithelial cells, an immortalized porcine vas deferens epithelial cell line, PVD9902, was established and characterized (13).

PVD9902 cells were derived from the isolation and culture of primary porcine vas deferens epithelial cells. After the initial isolation, the epithelial cells were passed continuously for more than 200 subcultures and cells spontaneously immortalized to form an epithelial cell line designated PVD9902. After numerous passages, cells retain their ability to proliferate in culture and their ability to form tight monolayers. The male porcine origin of PVD9902 cells has been demonstrated by chromosome characterization and its epithelial characteristic has been demonstrated by immunocytochemistry. In Ussing chamber experiments, cultured PVD9902 cells exhibit a high basal R_{te} (>6,000 Ω cm^2) and a response to forskolin that requires chloride, bicarbonate, and sodium in the bathing medium. RT-PCR results demonstrate the presence of mRNA coding for numerous membrane transport proteins in the cultured PVD9902 cells, including CFTR, SLC26A3, SLC26A6, and SLC4A4 (13). All the observations suggest that PVD9902 cells recapitulate most characteristics of primary porcine vas deferens epithelial cell cultures. Therefore, besides freshly isolated vas deferens epithelial cells, this porcine vas deferens epithelial cell line, PVD9902, provides another readily available cell model that can be used to characterize male reproductive function.

Vas Deferens Epithelial Tight Junctions

In epithelial cells lining the vas deferens, tight junction proteins are located near the apical cell surface of adjacent epithelial cells to form a physical barrier that restricts the permeability to fluid and solutes. The high basal R_{te} in cultured porcine vas deferens epithelial cells suggests that vas deferens epithelial cells form a very tight monolayer that effectively separates the luminal from the abluminal compartments. Additionally, immunohistochemical results suggest the presence of tight junction proteins in vas deferens epithelia (13, 87).

Tight junctions contain three major types of transmembrane proteins: occludin, claudins, and junctional adhesion molecules (JAMs) (15). To date, 24 isoforms of claudins and 4 isoforms of

JAMs have been identified. Occludin and claudins are tetraspan proteins while JAMs are single transmembrane domain proteins. The extracellular domains of these tight junction proteins constitute barrier in the paracellular space while their carboxyl-terminal domains interact with tight junction-associated proteins such as ZO-1, ZO-2, and ZO-3. These ZOs have several PDZ domains, which are protein-protein interaction domains responsible for intermolecular association. Through these PDZ domains ZOs directly bind to transmembrane proteins and link them to the actin cytoskeleton (26). Tight junction proteins act as a physiological barrier between separate body compartments. Tight junction proteins, such as claudin-4, also form ion selective pores in the tight junctions and regulate paracellular permeability. Therefore, tight junctions in vas deferens epithelia mediate fluid and solute movement across epithelial monolayers and contribute substantially to the stability of the luminal microenvironment.

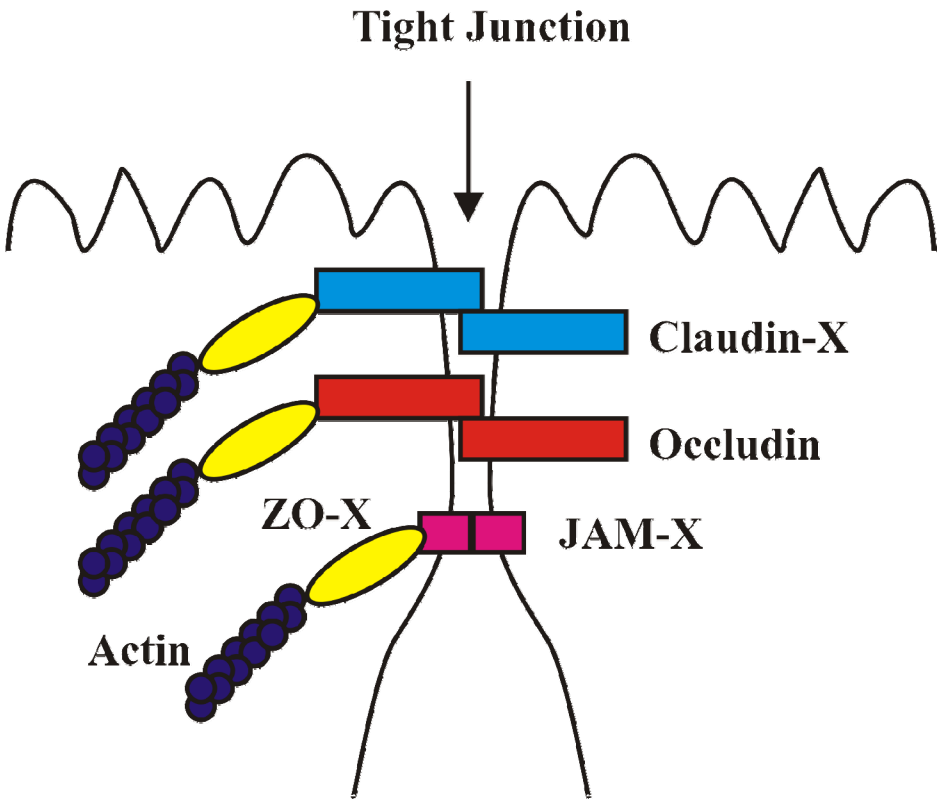

Figure 1.8 Schematic representation of tight junction proteins.

Tight junction proteins occludin, claudin-X, and junctional adhesion molecule-X (JAM-X) link to accessory proteins ZO-X, and thus link to the actin cytoskeleton. Claudin-X indicates claudin

family members 1-24, JAM-X indicates JAM family members 1-4, and ZO-X indicates ZO family members 1-3.

Ion Transport across Vas Deferens Epithelia

Emerging evidence has suggested that the vas deferens is more than a storage and transit tube. The pseudostratified epithelial cells in the vas deferens also function in ion secretion or absorption. Functional and molecular studies performed in cultured lamb and porcine vas deferens epithelial cells suggested that cells lining the vas deferens express CFTR and ENaC as well as SLC4A4, a sodium-bicarbonate cotransporter (7, 12). Moreover, studies focusing on the effects of neurotransmitters and hormones on vas deferens epithelium suggested that ion transport across vas deferens epithelial cells is tightly regulated both acutely and over extended periods (11, 29, 67, 87).

A basic cellular model of vas deferens epithelial cells is proposed as shown in Figure 1.9 (13, 87). In the apical cell surface, there exist CFTR channels as well as chloride-bicarbonate exchangers SLC26A3 and SLC26A6 while the basolateral cell surface includes sodium-potassium-ATPase, sodium-potassium-chloride (NKCC) cotransporter, potassium channels, and the sodium-bicarbonate cotransporter SLC4A4. The expression of ENaC channel can be induced or upregulated by exposure to dexamethasone in primary cultures of vas deferens (7, 12). However, PVD9902 cells do not express the β subunit of ENaC (13). Therefore, ENaC is not shown in the cellular model. The presence of ion pumps, exchangers, cotransporters, and channels in the model of vas deferens epithelial cells has been demonstrated by molecular assays such as RT-PCR and western blot. In electrophysiological experiments, forskolin-stimulated ion transport can be selectively reduced by CFTR inhibitors, DASU-02, glibenclamide and GlyH-101, by sodium-potassium-ATPase inhibitor, ouabain, by NKCC cotransporter inhibitor, bumetanide, by potassium channel inhibitors, clotrimazole and $BaCl_2$, and by the sodium-bicarbonate cotransporter inhibitor, DNDS (87). The effects of these blockers on forskolin-stimulated I_{sc} suggested that these ion pumps, cotransporters, and channels have regulated activities in these cells. Besides forskolin, exposure to norepinephrine, vasopressin, ATP, adenosine, or histamine also induces a substantial increase in I_{sc}, suggesting that these neuro-hormonal agents stimulate vas deferens epithelial ion transport (87).

Ion transport across vas deferens epithelia through the CFTR channel is highlighted in Figure 1.9. We propose that chloride enters the cell at the basolateral membrane via NKCC and that bicarbonate enters the cell at the basolateral membrane via SLC4A4. Chloride and bicarbonate exit the cell across the apical membrane through CFTR. Upon exposure to agents that increase the intracellular cAMP generation such as forskolin, an adenylyl cyclase activator, CFTR channels are activated. Activated CFTR mediates the secretion of chloride and bicarbonate, and accounts for the elevated I_{sc}.

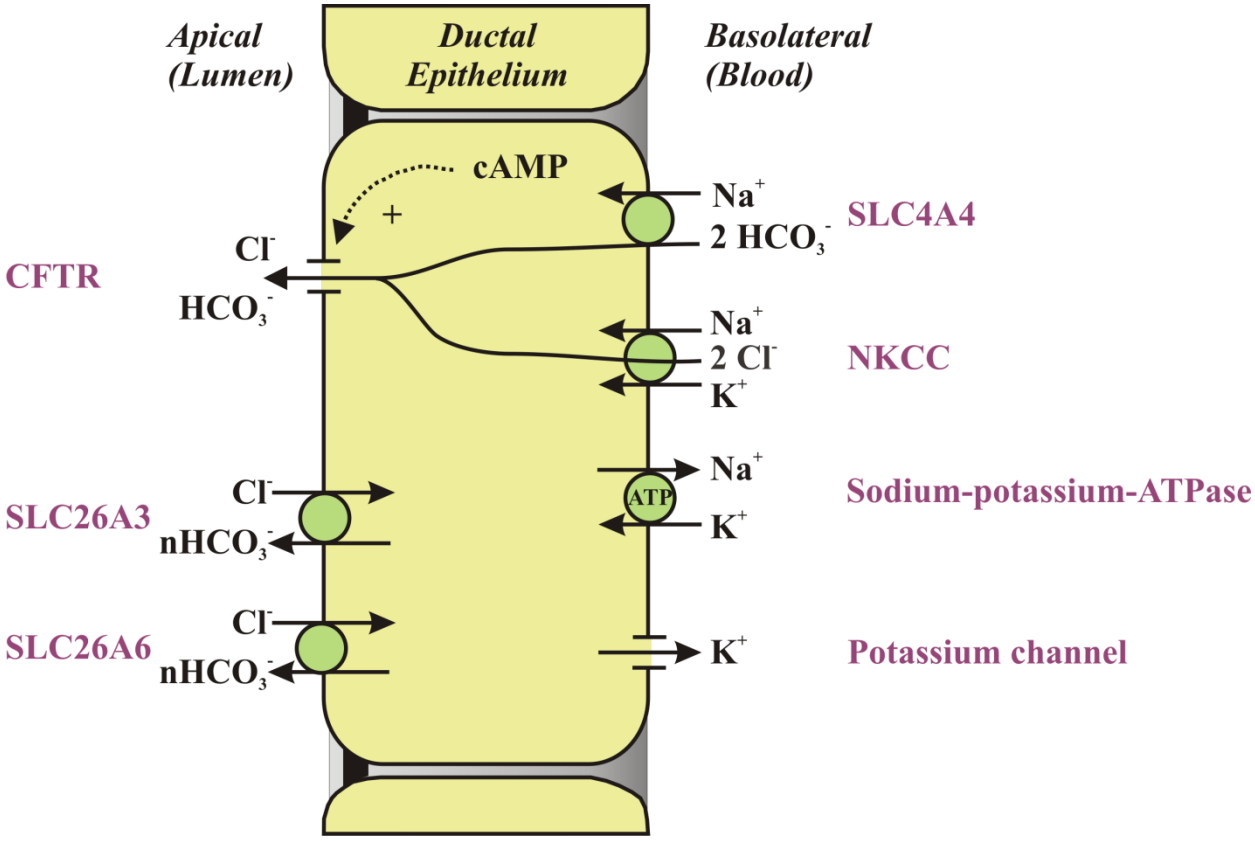

Figure 1.9 A proposed model to account for anion secretion by vas deferens epithelial cells. The vas deferens epithelial cells contain numerous membrane transport proteins including SLC26A3, SLC26A6, and CFTR in the apical cell surface and sodium-potassium-ATPase, NKCC, potassium channels, and SLC4A4 in the basolateral cell surface (13, 87).

Ion transport across vas deferens epithelia modulates the microenvironment to which sperm are exposed, and thus, is of great importance. The epididymis is reported to establish an acid luminal environment for the maturation and the storage of sperm (65). pH measurements in anesthetized

boars showed that systemic adrenergic stimulation can cause a rapid and profound increase in luminal pH (69). As the sperm transit through the vas deferens before and during ejaculation, the sperm are exposed to an alkaline luminal environment, which induces sperm motility and initiates a process that is required to achieve fertilizing capacity. Numerous ion channels and transporters in the vas deferens epithelia provide for regulated transport and account for changes in lumen volume and composition. The secretion of bicarbonate also contributes to the regulation of luminal pH (Figure 1.9). Therefore, the membrane transport proteins in the vas deferens epithelial cells and ion transport stimulated by neurotransmitters and hormones across vas deferens epithelial monolayers have important physiological and pathophysiological implications.

Goals of the Present Study

With the progression in medical care and the expanding life expectancy of cystic fibrosis patients, infertility has become a more pressing problem. Interventions to treat or circumvent abnormalities in reproductive duct architecture or function are sought to increase the opportunity of male cystic fibrosis patients to foster children.

TGF-β1, a multifunctional cytokine, has been associated with the severity of cystic fibrosis lung disease. The goal of the present study was to determine whether TGF-β1 also affects vas deferens, an organ that is commonly affected in male cystic fibrosis patients. Functional and molecular assays were conducted to determine whether TGF-β1 modulates electrophysiological parameters of primary cultures of vas deferens epithelial cells (in Chapter 2) and cultured PVD9902 cells (in Chapter 3).

References

1. **Anderson DH**. Cystic fibrosis of the pancreas and its relation to celiac disease. *Am J Dis Child* 56: 344–399, 1938.

2. **Anzano MA, Roberts AB, Meyers CA, Komoriya A, Lamb LC, Smith JM, and Sporn MB**. Synergistic interaction of two classes of transforming growth factors from murine sarcoma cells. *Cancer Res* 42: 4776-4778, 1982.

3. **Arkwright PD, Laurie S, Super M, Pravica V, Schwarz MJ, Webb AK, and Hutchinson IV**. TGF-beta(1) genotype and accelerated decline in lung function of patients with cystic fibrosis. *Thorax* 55: 459-462, 2000.

4. **Bachelder RE, Yoon SO, Franci C, de Herreros AG, and Mercurio AM**. Glycogen synthase kinase-3 is an endogenous inhibitor of Snail transcription: implications for the epithelial-mesenchymal transition. *J Cell Biol* 168: 29-33, 2005.

5. **Berger HA, Travis SM, and Welsh MJ**. Regulation of the cystic fibrosis transmembrane conductance regulator Cl- channel by specific protein kinases and protein phosphatases. *J Biol Chem* 268: 2037-2047, 1993.

6. **Bergeron A, Soler P, Kambouchner M, Loiseau P, Milleron B, Valeyre D, Hance AJ, and Tazi A**. Cytokine profiles in idiopathic pulmonary fibrosis suggest an important role for TGF-beta and IL-10. *Eur Respir J* 22: 69-76, 2003.

7. **Bertog M, Smith DJ, Bielfeld-Ackermann A, Bassett J, Ferguson DJ, Korbmacher C, and Harris A**. Ovine male genital duct epithelial cells differentiate in vitro and express functional CFTR and ENaC. *Am J Physiol Cell Physiol* 278: C885-894, 2000.

8. **Blobe GC, Schiemann WP, and Lodish HF**. Role of transforming growth factor beta in human disease. *N Engl J Med* 342: 1350-1358, 2000.

9. **Border WA, and Noble NA**. Transforming growth factor beta in tissue fibrosis. *N Engl J Med* 331: 1286-1292, 1994.

10. **Brown PD, Wakefield LM, Levinson AD, and Sporn MB**. Physicochemical activation of recombinant latent transforming growth factor-beta's 1, 2, and 3. *Growth Factors* 3: 35-43, 1990.

11. **Carlin RW, Lee JH, Marcus DC, and Schultz BD**. Adenosine stimulates anion secretion across cultured and native adult human vas deferens epithelia. *Biol Reprod* 68: 1027-1034, 2003.

12. **Carlin RW, Quesnell RR, Zheng L, Mitchell KE, and Schultz BD**. Functional and molecular evidence for Na(+)-HCO cotransporter in porcine vas deferens epithelia. *Am J Physiol Cell Physiol* 283: C1033-1044, 2002.

13. **Carlin RW, Sedlacek RL, Quesnell RR, Pierucci-Alves F, Grieger DM, and Schultz BD**. PVD9902, a porcine vas deferens epithelial cell line that exhibits neurotransmitter-stimulated anion secretion and expresses numerous HCO3(-) transporters. *Am J Physiol Cell Physiol* 290: C1560-1571, 2006.

14. **Chaudhury A, and Howe PH**. The tale of transforming growth factor-beta (TGFbeta) signaling: a soigne enigma. *IUBMB Life* 61: 929-939, 2009.

15. **Chiba H, Osanai M, Murata M, Kojima T, and Sawada N**. Transmembrane proteins of tight junctions. *Biochimica Biophys Acta* 1778: 588-600, 2008.

16. **Choi ME, Ding Y, and Kim SI**. TGF-beta signaling via TAK1 pathway: role in kidney fibrosis. *Semin Nephrol* 32: 244-252, 2012.

17. **Collaco JM, and Cutting GR**. Update on gene modifiers in cystic fibrosis. *Curr Opin Pulm Med* 14: 559-566, 2008.

18. **Crawford SE, Stellmach V, Murphy-Ullrich JE, Ribeiro SM, Lawler J, Hynes RO, Boivin GP, and Bouck N**. Thrombospondin-1 is a major activator of TGF-beta1 in vivo. *Cell* 93: 1159-1170, 1998.

19. **Cui W, Fowlis DJ, Bryson S, Duffie E, Ireland H, Balmain A, and Akhurst RJ**. TGFbeta1 inhibits the formation of benign skin tumors, but enhances progression to invasive spindle carcinomas in transgenic mice. *Cell* 86: 531-542, 1996.

20. **Cuppens H, and Cassiman JJ**. CFTR mutations and polymorphisms in male infertility. *Int J Androl* 27: 251-256, 2004.

21. **Daniel C, Wiede J, Krutzsch HC, Ribeiro SM, Roberts DD, Murphy-Ullrich JE, and Hugo C**. Thrombospondin-1 is a major activator of TGF-beta in fibrotic renal disease in the rat in vivo. *Kidney Int* 65: 459-468, 2004.

22. **Dawson DC, Smith SS, and Mansoura MK**. CFTR: mechanism of anion conduction. *Physiol Rev* 79: S47-75, 1999.

23. **De Bleser PJ, Niki T, Rogiers V, and Geerts A**. Transforming growth factor-beta gene expression in normal and fibrotic rat liver. *J Hepatol* 26: 886-893, 1997.

24. **de Larco JE, and Todaro GJ**. Growth factors from murine sarcoma virus-transformed cells. *Proc Natl Acad Sci U S A* 75: 4001-4005, 1978.

25. **Denning CR, Sommers SC, and Quigley HJ, Jr.** Infertility in male patients with cystic fibrosis. *Pediatrics* 41: 7-17, 1968.

26. **Forster C**. Tight junctions and the modulation of barrier function in disease. *Histochem Cell Biol* 130: 55-70, 2008.

27. **Gilligan PH**. Microbiology of airway disease in patients with cystic fibrosis. *Clin Microbiol Rev* 4: 35-51, 1991.

28. **Greger R**. Role of CFTR in the colon. *Annu Rev Physiol* 62: 467-491, 2000.

29. **Hagedorn TM, Carlin RW, and Schultz BD**. Oxytocin and vasopressin stimulate anion secretion by human and porcine vas deferens epithelia. *Biol Reprod* 77: 416-424, 2007.

30. **Harris WT, Muhlebach MS, Oster RA, Knowles MR, Clancy JP, and Noah TL**. Plasma TGF-beta(1) in pediatric cystic fibrosis: potential biomarker of lung disease and response to therapy. *Pediatr Pulmonol* 46: 688-695, 2011.

31. **Harris WT, Muhlebach MS, Oster RA, Knowles MR, and Noah TL**. Transforming growth factor-beta(1) in bronchoalveolar lavage fluid from children with cystic fibrosis. *Pediatr Pulmonol* 44: 1057-1064, 2009.

32. **Herrmann U, Dockter G, and Lammert F**. Cystic fibrosis-associated liver disease. *Best Pract Res Clin Gastroenterol* 24: 585-592, 2010.

33. **Huang XZ, Wu JF, Cass D, Erle DJ, Corry D, Young SG, Farese RV, Jr., and Sheppard D**. Inactivation of the integrin beta 6 subunit gene reveals a role of epithelial integrins in regulating inflammation in the lung and skin. *J Cell Biol* 133: 921-928, 1996.

34. **Hug MJ, Tamada T, and Bridges RJ**. CFTR and bicarbonate secretion by [correction of to] epithelial cells. *News Physiol Sci* 18: 38-42, 2003.

35. **Hwang TC, and Kirk KL**. The CFTR ion channel: gating, regulation, and anion permeation. *Cold Spring Harbor Perspect Med* 3: a009498, 2013.

36. **Ito N, Kawata S, Tamura S, Shirai Y, Kiso S, Tsushima H, and Matsuzawa Y**. Positive correlation of plasma transforming growth factor-beta 1 levels with tumor vascularity in hepatocellular carcinoma. *Cancer Lett* 89: 45-48, 1995.

37. **Ivanovic V, Todorovic-Rakovic N, Demajo M, Neskovic-Konstantinovic Z, Subota V, Ivanisevic-Milovanovic O, and Nikolic-Vukosavljevic D**. Elevated plasma levels of transforming growth factor-beta 1 (TGF-beta 1) in patients with advanced breast cancer: association with disease progression. *Eur J Cancer* 39: 454-461, 2003.

38. **Katsuno Y, Lamouille S, and Derynck R**. TGF-beta signaling and epithelial-mesenchymal transition in cancer progression. *Curr Opin Oncol* 25: 76-84, 2013.

39. **Kattla JJ, Carew RM, Heljic M, Godson C, and Brazil DP**. Protein kinase B/Akt activity is involved in renal TGF-beta1-driven epithelial-mesenchymal transition in vitro and in vivo. *Am J Physiol Renal Physiol* 295: F215-225, 2008.

40. **Kaur S, Norkina O, Ziemer D, Samuelson LC, and De Lisle RC**. Acidic duodenal pH alters gene expression in the cystic fibrosis mouse pancreas. *Am J Physiol Gastrointest Liver Physiol* 287: G480-490, 2004.

41. **Keski-Oja J, Koli K, and von Melchner H**. TGF-beta activation by traction? *Trends Cell Biol* 14: 657-659, 2004.

42. **Kisseleva T, and Brenner DA**. Mechanisms of fibrogenesis. *Exp Biol Med (Maywood)* 233: 109-122, 2008.

43. **Kloppel G, Detlefsen S, and Feyerabend B**. Fibrosis of the pancreas: the initial tissue damage and the resulting pattern. *Virchows Arch* 445: 1-8, 2004.

44. **Kuruvilla AP, Shah R, Hochwald GM, Liggitt HD, Palladino MA, and Thorbecke GJ**. Protective effect of transforming growth factor beta 1 on experimental autoimmune diseases in mice. *Proc Natl Acad Sci U S A* 88: 2918-2921, 1991.

45. **Landstrom M**. The TAK1-TRAF6 signalling pathway. *Int J Biochem Cell Biol* 42: 585-589, 2010.

46. **Lawrence DA, Pircher R, and Jullien P**. Conversion of a high molecular weight latent beta-TGF from chicken embryo fibroblasts into a low molecular weight active beta-TGF under acidic conditions. *Biochem Biophys Res Commun* 133: 1026-1034, 1985.

47. **Leask A, and Abraham DJ**. TGF-beta signaling and the fibrotic response. *FASEB J* 18: 816-827, 2004.

48. **Letterio JJ, and Roberts AB**. Regulation of immune responses by TGF-beta. *Annu Rev Immunol* 16: 137-161, 1998.

49. **Li MO, Wan YY, Sanjabi S, Robertson AK, and Flavell RA**. Transforming growth factor-beta regulation of immune responses. *Annu Rev Immunol* 24: 99-146, 2006.

50. **Lin Y, Kikuchi S, Obata Y, and Yagyu K**. Serum levels of transforming growth factor beta1 are significantly correlated with venous invasion in patients with gastric cancer. *J Gastroenterol Hepatol* 21: 432-437, 2006.

51. **Lyons RM, Keski-Oja J, and Moses HL**. Proteolytic activation of latent transforming growth factor-beta from fibroblast-conditioned medium. *J Cell Biol* 106: 1659-1665, 1988.

52. **Mak V, Zielenski J, Tsui LC, Durie P, Zini A, Martin S, Longley TB, and Jarvi KA**. Proportion of cystic fibrosis gene mutations not detected by routine testing in men with obstructive azoospermia. *JAMA* 281: 2217-2224, 1999.

53. **Massague J**. TGF-beta signal transduction. *Annu Rev Biochem* 67: 753-791, 1998.

54. **Massague J, Seoane J, and Wotton D**. Smad transcription factors. *Genes Dev* 19: 2783-2810, 2005.

55. **Miller A, Lider O, Roberts AB, Sporn MB, and Weiner HL**. Suppressor T cells generated by oral tolerization to myelin basic protein suppress both in vitro and in vivo immune responses by the release of transforming growth factor beta after antigen-specific triggering. *Proc Natl Acad Sci U S A* 89: 421-425, 1992.

56. **Mokhtarian F, Shi Y, Shirazian D, Morgante L, Miller A, and Grob D**. Defective production of anti-inflammatory cytokine, TGF-beta by T cell lines of patients with active multiple sclerosis. *J Immunol* 152: 6003-6010, 1994.

57. **Munger JS, Huang X, Kawakatsu H, Griffiths MJ, Dalton SL, Wu J, Pittet JF, Kaminski N, Garat C, Matthay MA, Rifkin DB, and Sheppard D**. The integrin alpha v beta 6 binds and activates latent TGF beta 1: a mechanism for regulating pulmonary inflammation and fibrosis. *Cell* 96: 319-328, 1999.

58. **Narasimhan M, and Cohen R**. New and investigational treatments in cystic fibrosis. *Ther Adv Respir Dis* 5: 275-282, 2011.

59. **Nistal M, Santamaria L, and Paniagua R**. The ampulla of the ductus deferens in man: morphological and ultrastructural aspects. *J Anat* 180 (Pt 1): 97-104, 1992.

60. **Nocera M, and Chu TM**. Characterization of latent transforming growth factor-beta from human seminal plasma. *Am J Reprod Immunol* 33: 282-291, 1995.

61. **Ohtsuka K, Gray JD, Stimmler MM, Toro B, and Horwitz DA**. Decreased production of TGF-beta by lymphocytes from patients with systemic lupus erythematosus. *J Immunol* 160: 2539-2545, 1998.

62. **Oppenheim JJ, Feldmann M, and Durum SK**. *Cytokine reference : a compendium of cytokines and other mediators of host defense*. San Diego: Academic Press, 2001.

63. **Ozdamar B, Bose R, Barrios-Rodiles M, Wang HR, Zhang Y, and Wrana JL**. Regulation of the polarity protein Par6 by TGFbeta receptors controls epithelial cell plasticity. *Science* 307: 1603-1609, 2005.

64. **Park HW, and Lee MG**. Transepithelial bicarbonate secretion: lessons from the pancreas. *Cold Spring Harb Perspect Med* 2: 2012.

65. **Pastor-Soler N, Pietrement C, and Breton S**. Role of acid/base transporters in the male reproductive tract and potential consequences of their malfunction. *Physiology (Bethesda)* 20: 417-428, 2005.

66. **Perkett EA, Ornatowski W, Poschet JF, and Deretic V**. Chloroquine normalizes aberrant transforming growth factor beta activity in cystic fibrosis bronchial epithelial cells. *Pediatr Pulmonol* 41: 771-778, 2006.

67. **Phillips ML, and Schultz BD**. Steroids modulate transepithelial resistance and Na(+) absorption across cultured porcine vas deferens epithelia. *Biol Reprod* 66: 1016-1023, 2002.

68. **Piek E, Heldin CH, and Ten Dijke P**. Specificity, diversity, and regulation in TGF-beta superfamily signaling. *FASEB J* 13: 2105-2124, 1999.

69. **Pierucci-Alves F, Duncan CL, Lillich JD, and Schultz BD**. Porcine vas deferens luminal pH is acutely increased by systemic xylazine administration. *Biol Reprod* 82: 132-135, 2010.

70. **Politch JA, Tucker L, Bowman FP, and Anderson DJ**. Concentrations and significance of cytokines and other immunologic factors in semen of healthy fertile men. *Hum Reprod* 22: 2928-2935, 2007.

71. **Poulsen JH, Fischer H, Illek B, and Machen TE**. Bicarbonate conductance and pH regulatory capability of cystic fibrosis transmembrane conductance regulator. *Proc Natl Acad Sci U S A* 91: 5340-5344, 1994.

72. **Quinton PM**. Chloride impermeability in cystic fibrosis. *Nature* 301: 421-422, 1983.

73. **Quinton PM**. Cystic fibrosis: lessons from the sweat gland. *Physiology (Bethesda)* 22: 212-225, 2007.

74. **Quinton PM**. Physiological basis of cystic fibrosis: a historical perspective. *Physiol Rev* 79: S3-S22, 1999.

75. **Racke MK, Cannella B, Albert P, Sporn M, Raine CS, and McFarlin DE**. Evidence of endogenous regulatory function of transforming growth factor-beta 1 in experimental allergic encephalomyelitis. *Int Immunol* 4: 615-620, 1992.

76. **Rathaus V, Werner M, Freud E, Mei-Zahav M, Mussaffi H, and Blau H**. Sonographic findings of the genital tract in boys with cystic fibrosis. *Pediatr Radiol* 36: 162-166, 2006.

77. **Ratjen FA**. Cystic fibrosis: pathogenesis and future treatment strategies. *Respir Care* 54: 595-605, 2009.

78. **Reddy MM, and Quinton PM**. Functional interaction of CFTR and ENaC in sweat glands. *Pflugers Arch* 445: 499-503, 2003.

79. **Riordan JR, Rommens JM, Kerem B, Alon N, Rozmahel R, Grzelczak Z, Zielenski J, Lok S, Plavsic N, Chou JL, and et al.** Identification of the cystic fibrosis gene: cloning and characterization of complementary DNA. *Science* 245: 1066-1073, 1989.

80. **Roberts AB, Anzano MA, Lamb LC, Smith JM, and Sporn MB**. New class of transforming growth factors potentiated by epidermal growth factor: isolation from non-neoplastic tissues. *Proc Natl Acad Sci U S A* 78: 5339-5343, 1981.

81. **Roberts AB, Frolik CA, Anzano MA, and Sporn MB**. Transforming growth factors from neoplastic and nonneoplastic tissues. *Fed Proc* 42: 2621-2626, 1983.

82. **Sagel SD, Kapsner R, Osberg I, Sontag MK, and Accurso FJ**. Airway inflammation in children with cystic fibrosis and healthy children assessed by sputum induction. *Am J Respir Crit Care Med* 164: 1425-1431, 2001.

83. **Sato Y, and Rifkin DB**. Inhibition of endothelial cell movement by pericytes and smooth muscle cells: activation of a latent transforming growth factor-beta 1-like molecule by plasmin during co-culture. *J Cell Biol* 109: 309-315, 1989.

84. **Saxena V, Lienesch DW, Zhou M, Bommireddy R, Azhar M, Doetschman T, and Singh RR**. Dual roles of immunoregulatory cytokine TGF-beta in the pathogenesis of autoimmunity-mediated organ damage. *J Immunol* 180: 1903-1912, 2008.

85. **Schultz BD, Singh AK, Devor DC, and Bridges RJ**. Pharmacology of CFTR chloride channel activity. *Physiol Rev* 79: S109-144, 1999.

86. **Schultz BD, Venglarik CJ, Bridges RJ, and Frizzell RA**. Regulation of CFTR Cl-channel gating by ADP and ATP analogues. *J Gen Physiol* 105: 329-361, 1995.

87. **Sedlacek RL, Carlin RW, Singh AK, and Schultz BD**. Neurotransmitter-stimulated ion transport by cultured porcine vas deferens epithelium. *Am J Physiol Renal Physiol* 281: F557-570, 2001.

88. **Snodgrass SM, Cihil KM, Cornuet PK, Myerburg MM, and Swiatecka-Urban A**. Tgf-beta1 inhibits Cftr biogenesis and prevents functional rescue of DeltaF508-Cftr in primary differentiated human bronchial epithelial cells. *PLoS One* 8: e63167, 2013.

89. **Souchelnytskyi S, ten Dijke P, Miyazono K, and Heldin CH**. Phosphorylation of Ser165 in TGF-beta type I receptor modulates TGF-beta1-induced cellular responses. *EMBO J* 15: 6231-6240, 1996.

90. **Stuhrmann M, and Dork T**. CFTR gene mutations and male infertility. *Andrologia* 32: 71-83, 2000.

91. **Tabcharani JA, Chang XB, Riordan JR, and Hanrahan JW**. Phosphorylation-regulated Cl- channel in CHO cells stably expressing the cystic fibrosis gene. *Nature* 352: 628-631, 1991.

92. **Takizawa H, Tanaka M, Takami K, Ohtoshi T, Ito K, Satoh M, Okada Y, Yamasawa F, Nakahara K, and Umeda A**. Increased expression of transforming growth factor-beta1 in small airway epithelium from tobacco smokers and patients with chronic obstructive pulmonary disease (COPD). *Am J Respir Crit Care Med* 163: 1476-1483, 2001.

93. **Tang B, Bottinger EP, Jakowlew SB, Bagnall KM, Mariano J, Anver MR, Letterio JJ, and Wakefield LM**. Transforming growth factor-beta1 is a new form of tumor suppressor with true haploid insufficiency. *Nat Med* 4: 802-807, 1998.

94. **Taussig LM, Lobeck CC, di Sant'Agnese PA, Ackerman DR, and Kattwinkel J**. Fertility in males with cystic fibrosis. *N Engl J Med* 287: 586-589, 1972.

95. **Thompson NL, Flanders KC, Smith JM, Ellingsworth LR, Roberts AB, and Sporn MB**. Expression of transforming growth factor-beta 1 in specific cells and tissues of adult and neonatal mice. *J Cell Biol* 108: 661-669, 1989.

96. **Tsushima H, Kawata S, Tamura S, Ito N, Shirai Y, Kiso S, Imai Y, Shimomukai H, Nomura Y, Matsuda Y, and Matsuzawa Y**. High levels of transforming growth factor beta 1 in patients with colorectal cancer: association with disease progression. *Gastroenterology* 110: 375-382, 1996.

97. **van der Doef HP, Kokke FT, van der Ent CK, and Houwen RH**. Intestinal obstruction syndromes in cystic fibrosis: meconium ileus, distal intestinal obstruction syndrome, and constipation. *Curr Gastroenterol Rep* 13: 265-270, 2011.

98. **van der Ven K, Messer L, van der Ven H, Jeyendran RS, and Ober C**. Cystic fibrosis mutation screening in healthy men with reduced sperm quality. *Hum Reprod* 11: 513-517, 1996.

99. **Verkman AS, Song Y, and Thiagarajah JR**. Role of airway surface liquid and submucosal glands in cystic fibrosis lung disease. *Am J Physiol Cell Physiol* 284: C2-15, 2003.

100. **Wainwright BJ, Scambler PJ, Schmidtke J, Watson EA, Law HY, Farrall M, Cooke HJ, Eiberg H, and Williamson R**. Localization of cystic fibrosis locus to human chromosome 7cen-q22. *Nature* 318: 384-385, 1985.

101. **Weber AM, and Roy CC**. Bile acid metabolism in children with cystic fibrosis. *Acta Paediatr Scand Suppl* 317: 9-15, 1985.

102. **Wynn TA**. Integrating mechanisms of pulmonary fibrosis. *J Exp Med* 208: 1339-1350, 2011.

103. **Xiong B, Yuan HY, Hu MB, Zhang F, Wei ZZ, Gong LL, and Yang GL**. Transforming growth factor-beta1 in invasion and metastasis in colorectal cancer. *World J Gastroenterol* 8: 674-678, 2002.

104. **Yang H, Lee CJ, Zhang L, Sans MD, and Simeone DM**. Regulation of transforming growth factor beta-induced responses by protein kinase A in pancreatic acinar cells. *Am J Physiol Gastrointest Liver Physiol* 295: G170-G178, 2008.

105. **Yang H, Li G, Wu JJ, Wang L, Uhler M, and Simeone DM**. Protein kinase A modulates transforming growth factor-beta signaling through a direct interaction with Smad4 protein. *J Biol Chem* 288: 8737-8749, 2013.

106. **Yang Z, Mu Z, Dabovic B, Jurukovski V, Yu D, Sung J, Xiong X, and Munger JS**. Absence of integrin-mediated TGFbeta1 activation in vivo recapitulates the phenotype of TGFbeta1-null mice. *J Cell Biol* 176: 787-793, 2007.

107. **Zhang L, Duan CJ, Binkley C, Li G, Uhler MD, Logsdon CD, and Simeone DM**. A transforming growth factor beta-induced Smad3/Smad4 complex directly activates protein kinase A. *Mol Cell Biol* 24: 2169-2180, 2004.

108. **Zhang YE**. Non-Smad pathways in TGF-beta signaling. *Cell Res* 19: 128-139, 2009.

109. **Zielenski J**. Genotype and phenotype in cystic fibrosis. *Respiration* 67: 117-133, 2000.

110. **Zielenski J, Rozmahel R, Bozon D, Kerem B, Grzelczak Z, Riordan JR, Rommens J, and Tsui LC**. Genomic DNA sequence of the cystic fibrosis transmembrane conductance regulator (CFTR) gene. *Genomics* 10: 214-228, 1991.

111. **Zielenski J, and Tsui LC**. Cystic fibrosis: genotypic and phenotypic variations. *Annu Rev Genet* 29: 777-807, 1995.

Chapter 2 - Transforming Growth Factor Beta 1 Induces Tight Junction Disruptions and Loss of Transepithelial Resistance across Porcine Vas Deferens Epithelial Cells

This chapter is reprinted from Biology of Reproduction.

Fernando Pierucci-Alves, Sheng Yi, and Bruce D. Schultz. Transforming Growth Factor Beta 1 Induces Tight Junction Disruptions and Loss of Transepithelial Resistance Across Porcine Vas Deferens Epithelial Cells. Biol Reprod 2012; 86 (2):36,1-8.

The Society for the Study of Reproduction (SSR) granted the right of republication.

This chapter includes my contributions to a portion of the electrophysiological and western blot experiments.

With the observation that TGF-β1 disrupts epithelial integrity, it was hypothesized that TGF-β1 might decrease the abundance of tight junction proteins. Therefore, western blot analysis was performed to detect whether TGF-β1 affects the expression of tight junction proteins. I contributed to the quantitative detection of occludin. The outcomes suggest that there is no detectable change in the abundance of occludin after TGF-β1 treatment (see Figure 2.4).

The potential mechanism(s) by which TGF-β1 affects vas deferens epithelial cells was investigated using a pharmacological approach. I performed the Ussing chamber experiments to determine whether the p38 MAPK (defined in this reprint as MAPK11) inhibitor SKF86002 would abrogate the effect of TGF-β1. The outcomes suggest that p38 MAPK inhibition does not prevent TGF-β1-induced decreases in R_{te} (see Figure 2.6).

Chapter 2 - Transforming Growth Factor Beta 1 Induces Tight Junction Disruptions and Loss of Transepithelial Resistance across Porcine Vas Deferens Epithelial Cells

Short title: Vas deferens epithelial barrier is sensitive to TGF-beta1-induced disruptions

Summary sentence:

Epithelia lining the vas deferens respond to TGF-beta1 exposure with severe losses in transepithelial resistance and tight junction organization.

Authors: Fernando Pierucci-Alves, Sheng Yi, Bruce D. Schultz
Department of Anatomy & Physiology
Kansas State University
Manhattan, KS 66506

Support: National Institutes of Health HD058398 and RR017686
This manuscript represents contribution number 11-280-J from the Kansas Agricultural Experiment Station

Corresponding author: Dr. Fernando Pierucci-Alves
Department of Anatomy and Physiology
1600 Denison Avenue, Coles Hall 228
Manhattan, KS-66506
Phone numbers: 785-532-4526 (office)
Email: falves@vet.k-state.edu

Short title: Vas deferens epithelial barrier is sensitive to TGF-beta1-induced disruptions

Abstract

Epithelial cells lining the male excurrent duct contribute to male fertility by employing a number of physiological mechanisms that generate a luminal microenvironment conducive to spermatozoa maturation and storage. Among these mechanisms, male duct epithelia establish intercellular tight junctions that constitute a barrier to paracellular diffusion of water, solutes, large molecules and cells. Mechanisms regulating the male duct epithelial barrier remain unidentified. Transforming growth factor beta (TGFB) is a regulatory cytokine present in high concentrations in human semen. This study examined whether TGFB has any effects on epithelial function exhibited by primary cultures of porcine vas deferens epithelia (1^{o}PVD). TGFB1-exposure caused a 70-99% decrease in basal transepithelial electrical resistance (R_{te}, a sensitive indicator of barrier integrity), while a significant decrease in anion secretory response to forskolin was detected at the highest levels of TGFB1 exposure employed. SB431542, a selective TGFB receptor I (TGFBRI) inhibitor, prevented decreases in barrier function. Results also demonstrated that TGFB1-exposure modifies the distribution pattern of tight junction proteins occludin and claudin 7. TβRI TGFBR1 is localized at the apical border of the native porcine vas deferens epithelium. Pharmacological inhibition of mitogen-activated protein kinase 11 (also known as p38-MAPK) did not alter the effect of TGFB1 on R_{te} significantly. These data suggest that epithelia lining the vas deferens is subject to disruptions in the physical barrier if active TGFB becomes bio-available in the luminal fluid, which might be expected to compromise fertility.

Introduction

Epithelia lining the male excurrent duct (i.e., efferent ducts, epididymis and vas deferens) contribute to the generation of specific luminal fluid compositions that are required for sperm cell maturation and male fertility, as recently emphasized by studies demonstrating infertility or subfertility in men and animal models carrying certain genetic mutations [1-4]. In addition, transport mechanisms employed by these specialized epithelia to promote sperm cell maturation - regulation of luminal water content [5, 6], ion secretion and absorption [7], pH regulation [8, 9] and protein secretion [10] - would not be successful without an effective physical barrier that restricts permeability [11]. Epithelial cells lining the male excurrent duct establish tight junctions, which function as an anatomical physical barrier to the movement of water, solutes and cells such as defense cell types and spermatozoa [12, 13]. Moreover, the male excurrent duct epithelial barrier is thought to include an immune-protective component that prevents autoimmune responses to sperm cells as they transit, mature or remain stored in the lumen of the excurrent system [13-15].

Transforming growth factor beta (TGFB) can induce pathological signaling in differentiated epithelial cells and lead to fundamental changes in cellular phenotype via epithelial-to-mesenchymal transformation (EMT). This process is at the causal core of life-threatening diseases such as kidney and lung fibrosis [16-18]. Furthermore, TGFB receptor (TGFBR1) is co-localized with epithelial tight junctions, where it is structurally linked to occludin, a tight junction integral protein [19-21]. Importantly, activation of TGFBRs and receptor complex formation lead to rapid tight junction dissociations via a transcription-independent mechanism [19, 20].

The male reproductive tract synthesizes and secretes relatively high amounts of TGFB. While normal human plasma concentrations are reportedly 2-18 ng/ml [22, 23], TGFB concentrations in human semen have been reported at 85-238 ng/ml [24, 25]. TGFB exists as a latent or inactive form and as an active form. Active TGFB1 can reach 2 ng/ml in human semen [24]. TGFB in semen is thought to exert an immune-regulatory effect on the female reproductive tract that contributes to spermatozoa survival and fertilization [26]. Additional participation of this signaling pathway in male fertility has been described with the TGFB1-null male mice kept

alive via anti-inflammatory therapy [27]. These mice exhibit major hypothalamic-pituitary-gonadal dysfunction and are infertile [27].

The origin of TGFB in semen has not been determined with certainty. Importantly, high levels of TGFB immunoreactivity is present in rat epididymal epithelia [28], and coding sequences for TGFB isoforms and receptors are expressed in this tissue [29]. However, it remains unknown whether TGFB can regulate physiological parameters of male excurrent duct epithelia, and mechanisms and/or mediators of this signaling have not been identified in the male excurrent system. This study tested whether primary cultures of porcine vas deferens epithelial cells (1ºPVDs) [30] respond to TGFB1 exposure with any significant changes in epithelial barrier function and/or ion transport. Results from initial experiments led us to conduct additional assays to test for the selectivity of the effect detected and to identify a disruptive effect of TGFB signaling on vas deferens tight junctions.

Materials and Methods

Tissue Acquisition and Epithelial Cell Isolation. Porcine vas deferens were surgically excised immediately postmortem from sexually mature boars at a local swine production facility, placed in ice-cold Hank's buffered salt solution (mM composition: 137 NaCl, 5.4 KCl, 0.4 KH_2PO_4, 0.6 Na_2HPO_4, 5.5 glucose) and transported to the laboratory where isolation of epithelial cells was performed as described in detail previously [30]. Segments of porcine vas deferens and skeletal muscle were harvested onto cryogenic tubes and snap-frozen in liquid nitrogen within seconds of excision and also transported to the laboratory, where they were kept at -80C until further use.

Cell Culture. Isolated vas deferens epithelial cells were seeded on 25 cm^2 tissue culture flasks and grown in Dulbecco's Modified Eagle's Medium (Invitrogen, Carlsbad, CA) with 10% fetal bovine serum (Atlanta Biologicals, Atlanta, GA) and 1% penicillin and streptomycin (Invitrogen), where they became confluent in 2-5 days. Subsequently, cells were lifted with phosphate buffered saline (PBS) containing trypsin and ethylene-diaminetetraacetic acid (Invitrogen), suspended in medium, and seeded on 1.13 cm^2 Snapwell permeable supports (Corning-Costar; Cambridge, MA) where they formed confluent monolayers. Paired monolayers from each boar were fed every other day for at least 10 days post-seeding, and then assigned to experimental groups in a given assay. Exposure to active TGFB1 (R&D Systems, Minneapolis, MN) was achieved by its inclusion in the basal compartment medium, while SB431542 (Sigma, Saint Louis, MO), and protein kinase inhibitor SKF86002 (Sigma) were included in both the basal and apical culture media. Monolayers exposed to both TGFB1 and SKF86002 were first exposed to SKF86002 for 30-60 minutes prior to receiving media that contained TGFB1 in addition to the inhibitor. NMuMG and Cos-7 cells were also seeded on permeable supports and cultured with the same medium formulation and feeding protocol described above. NMuMG cells were cultured as epithelial cell monolayers for 10 days before lysis and protein isolation, while Cos-7 cells were cultured until confluence (2-3 days) and then fixed.

Electrophysiology. Epithelial cell monolayers were mounted in modified Ussing flux chambers (model DCV9, Navicyte; San Diego, CA; model P2300, Physiologic Instruments, San

Diego, CA), bathed symmetrically in Ringer solution (composition in mM: 120 NaCl, 25 $NaHCO_3$, 3.3 KH_2PO_4, 0.83 K_2HPO_4, 1.2 $CaCl_2$, 1.2 $MgCl_2$), maintained at 39^oC and bubbled with 5% CO_2-95% O_2 to provide mixing and pH stability. Monolayers were clamped to 0 mV and short circuit current (I_{sc}) was measured continuously with a voltage-clamp apparatus (model 558C; University of Iowa, Dept. of Bioengineering, Iowa City, IA). Data were acquired digitally at 0.1 to 1 Hz with an Intel-based computer using a MP100A-CE interface and AcqKnowledge software (ver. 3.7.3; BIOPAC Systems, Santa Barbara, CA). Once recordings began, this system applied a 5-seconds bipolar voltage pulse every 100 seconds, and the resulting change in I_{sc} was used to calculate transepithelial electrical resistance (R_{te}) via Ohm's law. After at least 10 minutes of recording in basal conditions, monolayers were exposed to forskolin (EMD Chemicals, Gibbstown, NJ). The assay was terminated once I_{sc}-tracings became stable.

Immunohistochemistry and Confocal Microscopy. Monolayers were fixed in 4% paraformaldahyde for 1 hour, washed in PBS five times, incubated twice in 0.2% Triton X-100 (Sigma) for 5 minutes, and blocked in 5% bovine serum albumin (BSA, Thermo Scientific, Rockfort, IL) and 0.2% Triton X-100 for 1 hour. Native tissues were snap-frozen in liquid nitrogen minutes after dissection, blocked in freezing medium and sectioned (CM3050S Cryostat, Leica Microsystems Inc., Buffalo Grove, IL). Sections were collected onto slides, fixed in 4% paraformaldahyde for 15 minutes, washed in PBS and subject to the same subsequent procedure described above for monolayers, except blocking with BSA was conducted overnight. Primary antibody incubations were conducted overnight at 4^oC with the following specifications: anti-occludin (Invitrogen catalog 331500, 3 µg/ml), anti-claudin 7 (Invitrogen catalog 349100, 3 µg/ml), anti-TGFBR1 (Santa Cruz Biotechnology catalog sc-398G, 10 µg/ml) and anti-phosphorylated MAPK11 (Cell Signaling Technology catalog 9215, 0.3 µg/ml). Secondary immunofluorescent labeling was conducted with Alexa 488 and/or 594 (Invitrogen, 2 µg/ml) for 1 hour. Finally, monolayers or tissue sections received a fluorescent nucleic acid stain (DAPI, Invitrogen) and final washes prior to mounting on slides. Monolayers were positioned so that the permeable plastic support faced the slide and the apical cellular membranes faced the cover slip. Scanning confocal microscopy was performed (LSM 510 META and LSM 700, Carl Zeiss Microimaging Inc, Thornwood, NY). Fluorescent signals were acquired independently by different lasers and incorporated in each image. From monolayers, at least ten different unique

images were acquired and at least one stack of images was derived along the Z-axis (apical-to-basolateral). Analysis of confocal microscopy images and Z-Stack projections were conducted with Zeiss LSM Image Browser (version 4.2.0.121, Carl Zeiss), then exported and compiled with Corel Draw X3 (version 13.0.0.739, Corel Corporation, Ottawa, Ontario, Canada). Individual fluorescent signal intensity was measured using ZEN 2010 (version 6.0, Carl Zeiss).

Western Blot Analyses. Protein lysates were derived from 1^{o}PVDs, NMuMG epithelial cell monolayers, native porcine vas deferens and skeletal muscle tissues via direct homogenization and lysis in a Laemmli sample buffer containing 2% SDS, Tris-HCl (62.5 mM) and proteinase inhibitors. Segments of native porcine vas deferens, which had been stored at -80^{o}C, were thawed and their lumens were flushed with PBS prior to homogenization. Following homogenization, samples were aspirated repeatedly through 25 or 30 gauge needles and centrifuged at 14000 rpm, for 15 min at 4^{o}C. Protein concentration was determined by the micro BCA colorimetric assay (Pierce, Rockford IL) and/or a spectrophotometer (ND 8000, NanoDrop Products, Wilmington, DE). Prior to electrophoresis, β-mercaptoethanol, glycerin and bromophenol-blue were added and samples incubated at 95^{o}C for 5 minutes. Equal protein masses from each sample were resolved on 4-18% Tris-HEPES-SDS gradient gels (Pierce). Blotting onto PVDF membranes (Millipore, Billerica, MA) was conducted at 40V, for 2 hours at 4^{o}C. Membranes were blocked in 5% molecular grade dry milk overnight at 4^{o}C, and subsequently incubated overnight at 4^{o}C with primary antibodies: anti-occludin (Invitrogen catalog 331500, 1 μg/ml), anti-claudin 7 (Invitrogen catalog 349100, 1 μg/ml), anti-TGFBR1 (TβRI) (Santa Cruz Biotechnology catalog sc-398G, 10 μg/ml), and anti-actin (Sigma catalog A2066, 1:1000 dilution). Incubations in peroxidase-conjugated secondary antibodies (Pierce) were conducted for 1 hr at 20 ng/ml. Chemiluminescent signals were obtained with a suitable substrate (Pierce) and acquired digitally (Imagestation 4000R, Eastman Kodak Co., Rochester, NY or FluorChem HD2 imager, Alpha Innotech, San Leandro, CA). Measurements of band signal intensity was conducted with UN-SCAN IT Gel (version 6.1, Silk Scientific Inc., Orem, UT) and AlphaEase FC (version 6.0.0, Alpha Innotech).

Statistical Analysis. Paired *t*-tests and analysis of variance were performed as appropriate. These tests, calculation of means and standard error of the mean were performed

with Excel Microsoft Office, Office Suite 2007 (Microsoft Corporation, Redmond, WA). Graphs were made with SigmaPlot version 10.0 (Systat Software Inc., Point Richmond, CA).

Results

TGFB1 disrupts transepithelial resistance and epithelial transport across porcine vas deferens epithelia

To test whether TGFB can induce changes in epithelial function in 1^{o}PVDs, initial experiments employed paired monolayers that were either kept untreated or exposed to TGFB1 (100 ng/ml) for 24 and 72 hours in conditions that have been reported previously [30]. Typical outcomes acquired with three monolayers of cells derived from a single vas deferens are depicted in Fig. 1A. The magnitude of periodic bipolar pulses is inversely proportional to the monolayer's R_{te}. TGFB1-treated monolayers exhibited substantially reduced R_{te}; R_{te} was least in monolayers subject to the longest exposure. Overall, TGFB1 exposure for 24 hours caused a 90% decrease in R_{te}, while 99% of basal R_{te} was ablated in 1ºPVD monolayers exposed to TGFB1 for 72 hours (Fig. 1B). Longer-term exposure impaired forskolin-induced anion secretion across 1ºPVDs significantly (Fig. 1 A and C). Therefore, these initial outcomes suggested that TGFB1 induces a severe and time-dependent loss of barrier function in vas deferens epithelial cells, and that epithelial anion secretion can also be affected.

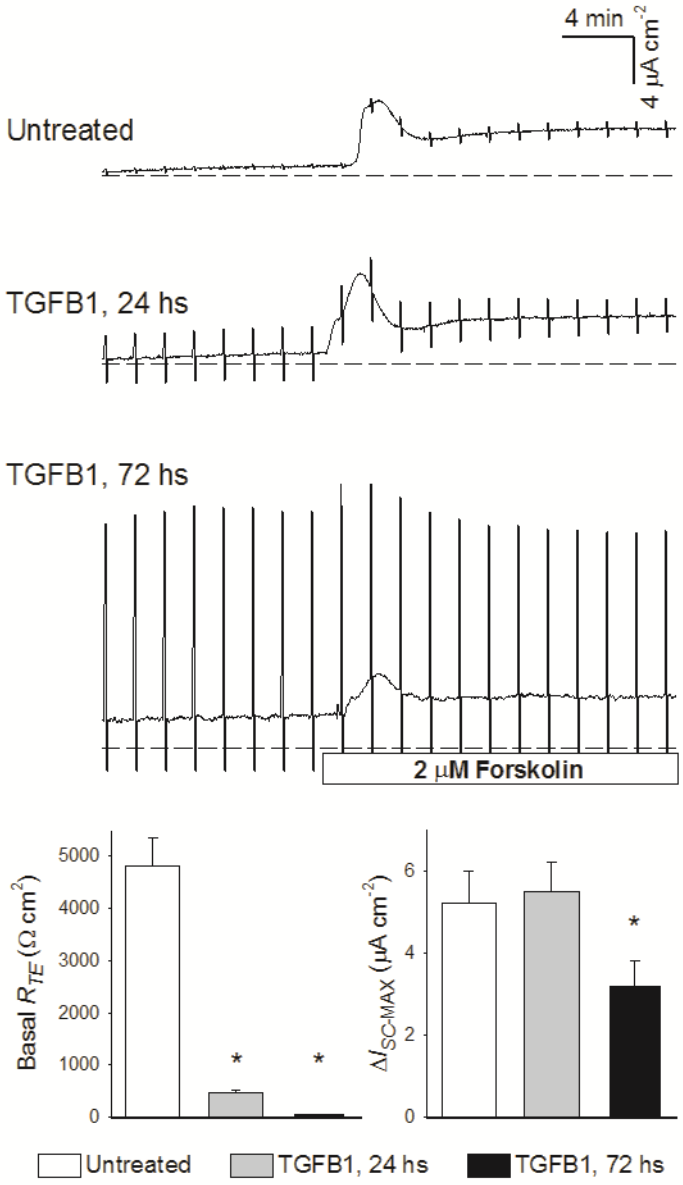

Figure 2.1 Transforming growth factor beta 1 (TGFB1, 100 ng/ml) causes time-dependent R_{te} decreases across primary cultures of porcine vas deferens epithelial cells (1ºPVD).

A) Vertical deflections in these Ussing chamber recordings correspond to pre-set electrical pulses (5 mV) and their magnitude is inversely proportional to R_{te}. Note that very small pulses are present throughout the untreated recording. Pulses shown defined that R_{TE} at basal state was 4800, 400 and 50 Ohms*cm^2 in untreated, 24 and 72 hours, respectively. **B)** Basal R_{te} was significantly reduced after 24 and 72 hours exposure to TGFB1 (100 ng/ml). **C)** The ability to respond to intracellular cAMP-generation (forskolin) with increases in short circuit current (I_{sc}),

indicating net anion secretion or cation absorption) was significantly reduced after 72 hours exposure to TGFB1. * indicates statistically different from untreated (n = 6, P<0.05).

A subsequent set of assays was conducted to test for reproducibility of the TGFB1-effect on R_{te} when exposure is limited to 5 ng/ml for 24 hours. Concurrently, we sought to determine whether this effect was linked to selective TGFBR activation. Consistent with the initial observations, TGFB1-treated 1ºPVDs exhibited a large decrease (95%) in R_{te} (Fig. 2A-B). SB43152, a selective TGFBR1 inhibitor, abrogated the TGFB1 effect on R_{te}. In fact, 1ºPVDs exposed to both TGFB1 and TGFBR1-inhibitor had slightly greater R_{te} on average than untreated 1ºPVDs, although no statistically significant difference was detected between these two groups. Mean forskolin-induced I_{sc} changes were reduced by TGFB exposure although statistically significant differences were not observed (Fig. 2A and 2C). Collectively, results from these experiments provide compelling evidence that selective activation of TGFBRs in vas deferens epithelial cells leads to severe losses of barrier function, although the underlying mechanism is not fully defined.

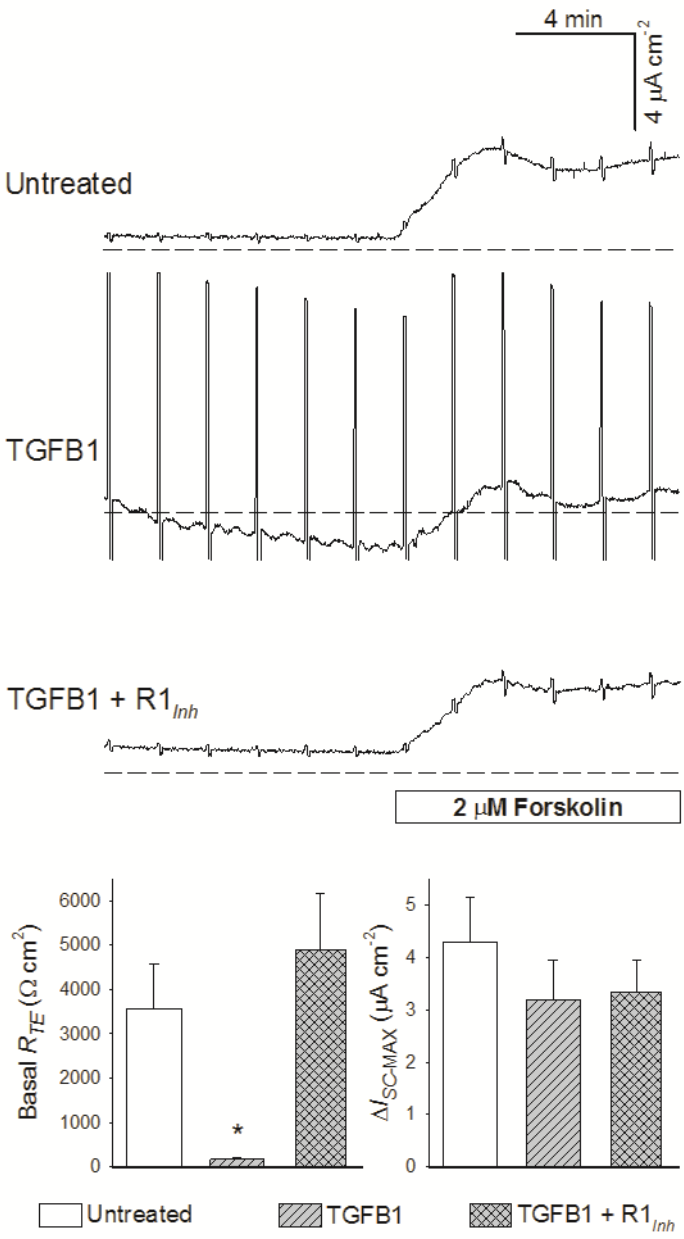

Figure 2.2 A selective TGFB receptor I inhibitor (TGFBR1) $R1_{Inh}$ abolishes the TGFB1 (5 ng/ml, 24 hours) effect on R_{te} across 1ºPVDs.

A) I_{sc} tracings depict the impact of 5 mV pulses on the 3 experimental groups and reveal that R_{te} in 1ºPVD exposed to TGFB1 plus RI_{Inh} SB431542 (10 μM) was similar to that in untreated 1ºPVD. **B)** Summary of observations reveal that monolayers exposed to TGFB1 only had a significant R_{TE} decrease, and monolayers exposed to TGFB1 plus RI_{Inh} exhibited mean basal R_{te} that was greater than untreated, although not significantly different. **C)** Forskolin-induced anion

secretion is not significantly altered across experimental groups. * indicates statistically different from the other 2 groups (n = 5, $P<0.05$).

TGFB1 induces disruptions in tight junction protein immunoreactivity in porcine vas deferens epithelial cells

TGFBR1 localization has been shown to be restricted to tight junctions where it has direct protein-protein interactions with occludin, and binding of TGFB to TGFBRs reportedly leads to the formation of a phosphorylated receptor complex that induces tight junction dissociations [19-21]. Thus, we hypothesized that changes in occludin immunoreactivity might be associated with TGFB1-induced decreases of R_{te} in 1ºPVDs, and tested this via scanning confocal microscopy. Severe disruptions of occludin-immunoreactivity were detected in 1ºPVDs exposed to 100 ng/ml for 72 hours in that the typical reticular pattern was unrecognizable and largely absent (Fig 3A). Only incomplete and irregular occludin strands were detected. At first examination, monolayers exposed to 5 ng/ml for 24 hours appeared to preserve the reticular pattern but abnormalities were clearly present under close examination. Punctate occludin immunoreactivity that was localized away from tight junction strands and largely distributed below the apical region (as seen in Z-stack projection, Fig. 3A) was consistently detected in this experimental group. In addition, a number of occludin strands were apparently dissociated in a manner that seemed to have generated hemi-strands that pulled apart and remained with each of the neighboring cells (Figs 3A and 3B). Based on these results, it was hypothesized that other integral tight junction proteins are similarly affected by TGFB1 exposure. Among the claudins expressed in more distal portions of the male excurrent duct, claudin 7 is one of the most abundant [12]. Therefore, the immunoreactivity pattern of claudin 7 was also tested. Outcomes from these experiments suggest that severe disruptions in the reticular pattern of claudin 7 occur after exposure to TGFB1 exposure (Fig. 3C).

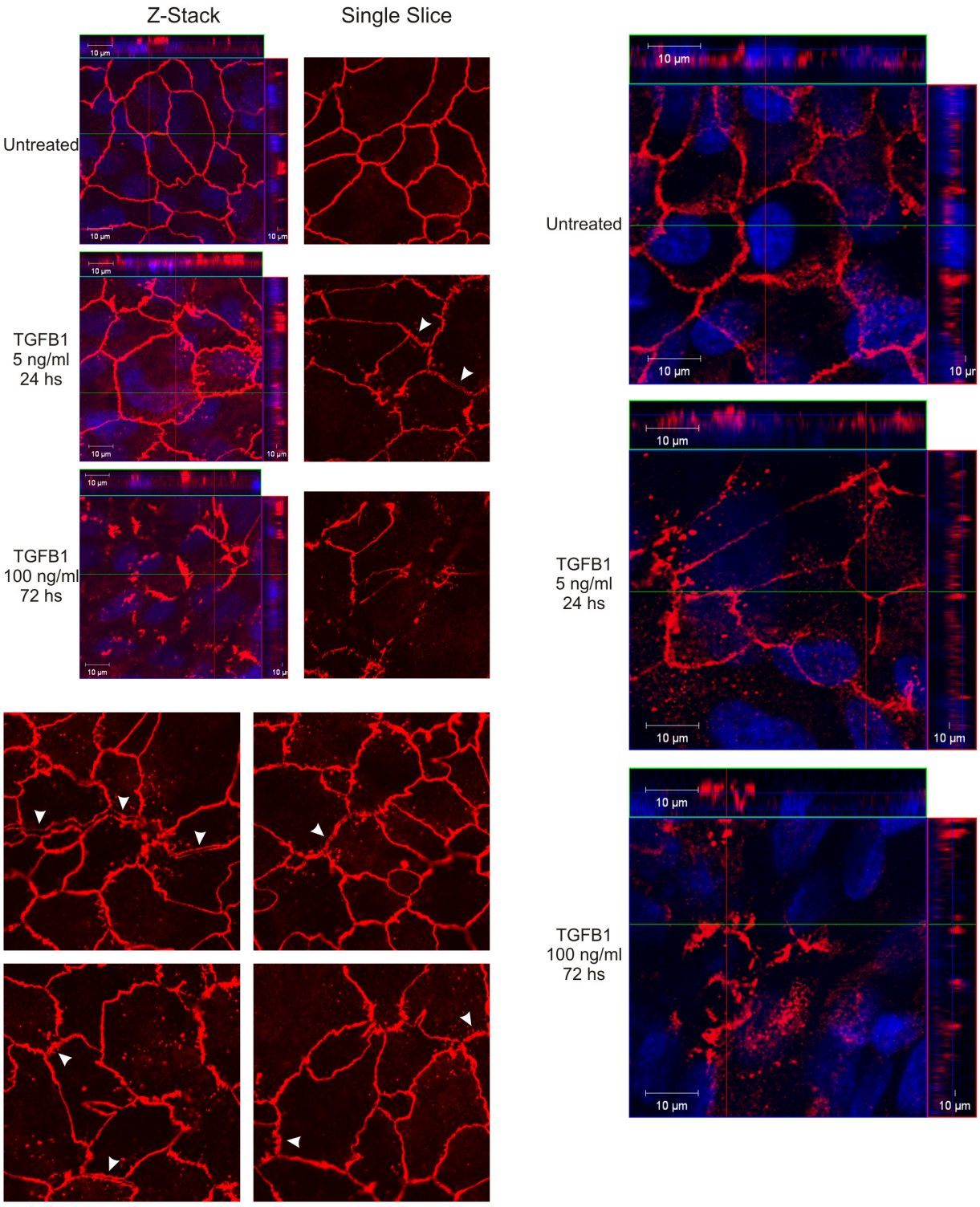

Figure 2.3 TGFB1 exposure induces disruptions in tight junction protein organization in vas deferens epithelia.

A) Untreated 1ºPVD monolayers exhibit a uniform reticular occludin immunoreactivity pattern (red) that is localized apically, above nuclei (blue), as seen in orthogonal projections displayed as banners located at the top and right of each of the left-column images. Severe disruption of the reticular occludin immunoreactivity pattern is present in monolayers exposed to TGFB for 72 hours (100 ng/ml), while exposure for 24 hours (5 ng/ml) induced abnormalities such as punctuate distribution and strand irregularity. Arrow heads indicate locations where occludin strands were apparently dissociated onto two hemi-strands. Single images (second column in panel A) are derived from a plane where occludin immunoreactivity was most abundant. **B)** Additional single Z-slice images derived from 1ºPVD exposed to 5 ng/ml for 24 hours show length-wise tight junction dissociations (arrow heads). **C)** Claudin 7 immunoreactivity (red) is also affected by TGFB1-exposure in a similar pattern as that of occludin. Results shown are representative of 5 paired observations (cells isolated from 5 boars).

The possibility that TGFB1 exposure and signaling induce cellular changes that result in decreases in the abundance of tight junction proteins in 1^{o}PVDs was tested. Results from western blot analyses targeting occludin and claudin 7 and respective densitometry indicate that no detectable changes in abundance of these proteins occur after 72 hours exposure (Fig. 4).

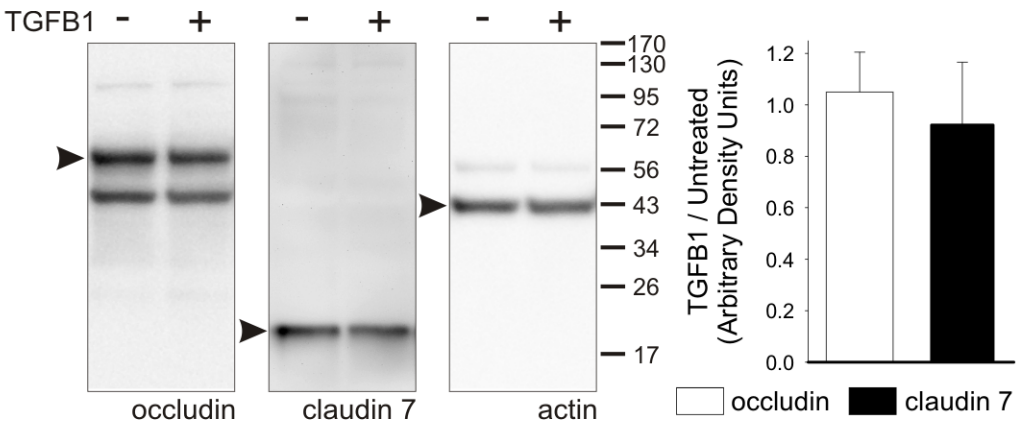

Figure 2.4 TGFB1 exposure (100 ng/ml for 72 hours) does not alter occludin or claudin 7 abundances in whole cell lysates derived from 1°PVD monolayers.

Western blot membranes probed with antibodies targeting occludin (65 kDa), claudin 7 (22 kDa) and actin (42 kDa) revealed bands of expected mobilities (arrows) that had no discernable intensity differences. Digitized images were subject to densitometry and the summarized outcome (bar chart) supports that no changes in the abundances of these proteins occur after TGFB1 exposure. Results shown are representative of 6 paired observations (cells isolated from 6 boars).

Together with the results from the functional assays, these outcomes suggest that, if TGFB1 becomes bioavailable to receptors at vas deferens epithelial cells, it will increase permeability across this epithelium by inducing tight junction dissociations.

TGFBR1 is expressed in apparent high abundance in native vas deferens epithelium

To test for the presence and localization of the TGFBR1 in native vas deferens, western blot and immunohistochemistry coupled to confocal microscopy were conducted. Prominent single bands were evident in lanes loaded with whole vas deferens tissue lysates (Fig. 5). Lanes loaded with 1°PVD cell lysates or lysate derived from the NMuMG cell line also exhibited the equivalent bands but were much fainter (data not shown). A distinct immunochemical signal was also detected on transverse sections of porcine vas deferens. TGFBR1-immunoreactivity was

present in virtually all principal cells of the native epithelium and was localized at the apical border of the epithelium (Fig. 5).

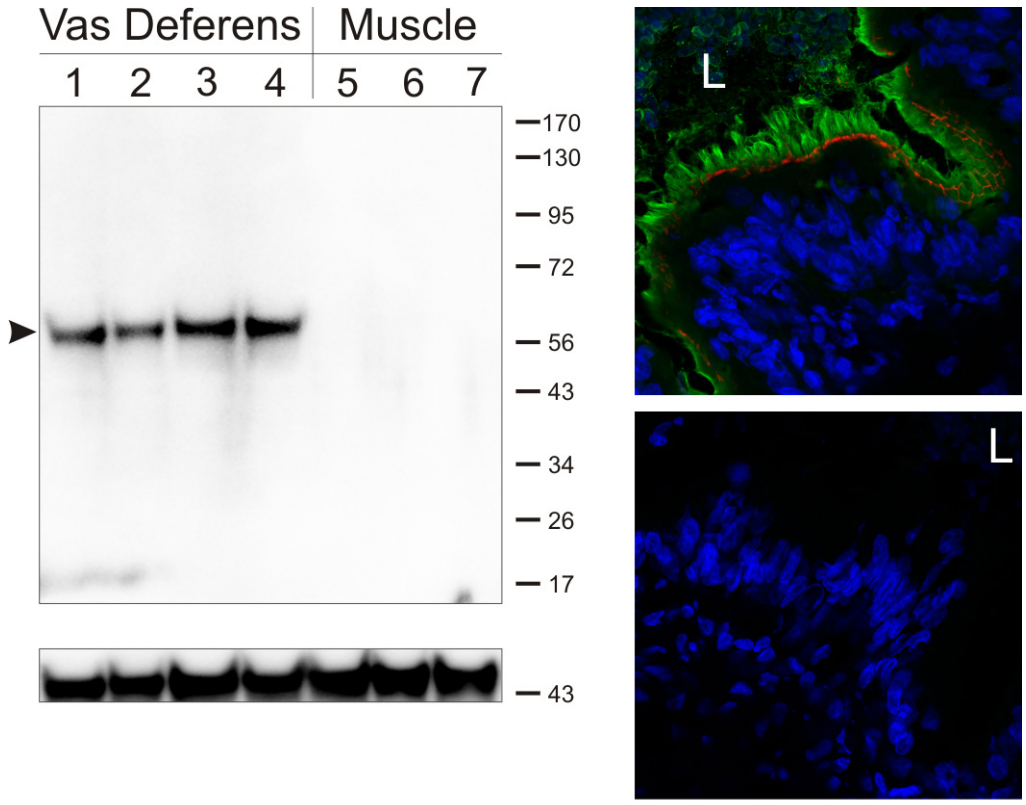

Figure 2.5 TGFBR1 is expressed apically in native vas deferens epithelium.
Western blot analyses (left panels) revealed a single band of expected mobility (predicted 56 kDa porcine protein, arrow) on lanes loaded with vas deferens tissue lysates (lanes 1-4). No bands were detected on lanes loaded with tissue lysates derived from skeletal muscle (lanes 5-7). Actin immunoreactivity was employed as a loading control and is shown on left bottom panel. Protein lysates were derived from different boars (n = 4 vasa deferentia and 3 muscle samples). Results from dual-labeling immunohistochemical analyses (panel on right, top) demonstrate that TGFBR1-immunoreactivity (green) is localized at the apical border of the native epithelium. By employing occludin immunoreactivity (red) as a reference, these results suggest that the TGFBR1 is localized largely at the epithelial brush border. No immunoreactive signals are detected if primary antibodies are subtracted from the preparation (lower panel on right). DAPI-stained nuclei are seen in blue. (n = 3, tissues derived from 3 different boars). L indicates "lumen".

These results suggest that TGFB signaling can occur in the native vas deferens epithelium and potentially lead to the effects observed in cultured vas deferens epithelial cells.

MAPK11 inhibition has no significant effect on TGFB1-induced decreases in transepithelial resistance across vas deferens epithelial cells

Studies addressing TGFB signal transduction in Sertoli cell primary cultures have demonstrated that mitogen-activated protein kinase 11 (MAPK11, also known as p38-MAPK) has a prominent role in mediating this signaling [31]. Thus, we tested whether inhibition of this kinase could prevent TGFB1-induced decreases in R_{te} across 1ºPVDs. Consistent again with initial experiments, TGFB1-exposed 1ºPVDs (100 ng/ml for 72 hours) exhibited a near total loss of R_{te}. Monolayers exposed to a combination of TGFB1 and the MAPK11 inhibitor SKF86002 (10 μM) also exhibited drastic decreases of R_{te} (Fig. 6A). Although SKF86002-treated monolayers had R_{te} means that were approximately twice that of 1ºPVDs exposed to TGFB1 alone, the increment observed with the MAPK11 inhibitor only approached statistical significance ($P<0.08$). A subsequent set of assays was conducted based on similar experimental design, but TGFB1 exposure was restricted to 5 ng/ml for 24 hours. TGFB1-treated 1ºPVDs had 70% less R_{te} when compared to untreated monolayers (Fig. 6B). TGFB1 plus SKF86002-treated monolayers again, on average, had R_{te} that remained greater than that of TGFB1-only, but their differences were not statistically significant ($P<0.06$). To test if 10 μM SKF86002 induced significant MAPK11-inhibition, we conducted an assay in which Cos-7 cells were cultured in the presence or absence of anisomycin (25 μg/ml) and SKF86002 (10 μM). Localization and abundance of phosphorylated MAPK11 (pMAPK11) were then accessed via immunofluorescence detection and scanning confocal microscopy, which employed a primary antibody known to be selective for pMAPK11 [32]. Untreated Cos-7 cells exhibited no discernable pMAPK11 immunoreactivity, while anisomycin-treated presented marked nuclear pMAPK11 immunoreactivity, and anisomycin plus SKF86002-treated cells had significantly less pMAPK11-immunoreactivity than anisomycin-treated (data not shown).

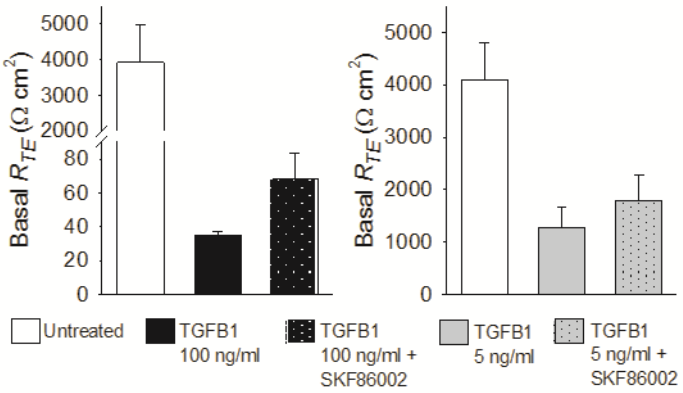

Figure 2.6 Pharmacological inhibition of mitogen-activated protein kinase 11 (MAPK11) does not prevent TGFB1-induced decreases in R_{te} across 1°PVDs.

A) R_{TE} is severely reduced after 72 hours exposure to TGFB1 (100 ng/ml) and SKF86002 (10 μM). **B)** MAPK11 inhibition by SKF86002 (10 μM) also fails to prevent R_{TE}-decreases after 24 hours exposure in which TGFB1 concentration was 5 ng/ml. n = 6 in A, and 11 in B.

Collectively, these outcomes suggest that MAPK11 has a marginal role in the TGFB signaling events leading to decreases in R_{TE} across vas deferens epithelial cells. MAPK11 seems to be expressed in 1°PVDs, to be phosphorylated downstream from TGFBRs activation, but its effect in promoting tight junction disruption is suggestively secondary.

Discussion

The goal of this study was to determine what effects, if any, TGFB exerts on epithelia lining the vas deferens. Outcomes reported here support a scenario in which activation of TβRs expressed in vas deferens epithelia leads to a severe loss in electrical barrier resistivity, while anion secretion can also be affected. Furthermore, losses in barrier function were associated with disruptions in epithelial tight junction protein organization and/or localization. These data are novel and demonstrate that a better understanding of the relationship between TGFB signaling and the physiology of cells lining the male excurrent duct is needed. Moreover, these data and the known fibrogenic effects of TGFB [17, 33] suggest that this signaling pathway may participate in the etiology of human diseases of the male reproductive duct such as epididymal and vas deferens obstructions and congenital bilateral absence of the vas deferens. It is also thought that breaches in the male barrier can promote the synthesis of anti-sperm antibodies, which are arguably responsible for poor spermatozoa motility and male infertility [34].

Our results show that high levels of barrier resistivity exhibited by cultured vas deferens epithelia are virtually eliminated via selective TGFB-receptor activation. R_{te} was decreased over time and by 72 hours it was nearly undetectable. Such severe loss of functional parameters is consistent with TGFB-induced EMT [18, 33]. Although these data reveal a high degree of vulnerability to the effects of this growth factor, it remains to be determined the magnitude of in vivo TGFB signaling in vas deferens epithelia and in epithelial cells lining other segments of the male excurrent duct in either physiological or pathological conditions. It is likely that, in a physiological context, the effective concentration of active TGFB is less than in the conditions employed in these assays. It is possible that, in vivo and under physiological conditions, the concentration of active TGFB is low enough to have minimal effects on barrier resistivity. Under physiological conditions, TGFB signaling is known to induce an inhibitory effect on tissue growth, therefore generating a local tumor-suppressive effect rather than a tumor- or fibrosis-promoting effect [35, 36]. However, epithelial tissues can develop resistance to TGFB's growth-inhibitory effect and switch to a state in which TGFB promotes pathological EMT and tumor formation and/or metastasis [37]. Tumors of primary growth in the vas deferens or epididymis are extremely rare [38, 39] and this is consistent with the possibility that signaling pathways may

exist in these tissues to prevent abnormal tissue growth. Moreover, signaling by TGFB is known to induce an anti-inflammatory effect [40]. Thus, it is possible that this signaling reduces inflammatory responses to spermatozoa present in the excurrent duct luminal environment [26, 33]. Nevertheless, the results presented in this study suggest that the potential exists for induction of pathological processes by activation of the TGFB signaling pathway in vas deferens epithelia.

Immunohistochemical results suggest that TGFB receptor activation leads to disruptions in epithelial barrier organization and the localization of proteins that form tight junctions, which could account for the reduction in R_{te}. While greater concentration and longer duration of exposure revealed profound loss of occludin and claudin 7 from tight junctions, immunoreactivity of these proteins were likewise altered in 1ºPVDs exposed to 5 ng/ml for 24 hours, which was also accompanied by substantial losses in barrier function (70-95%) measured electrically. Abnormalities in occludin immunoreactivity included hemi-strands detected along the apical aspect of neighboring cells. This outcome seems to suggest that a mechanism for dissociation of tight junctions in vas deferens epithelia begins with a length-wise dissociation of the tight junction strand, which 'unzips' the junctional complexes. Corroborating this possibility are reports indicating that TβRI is structurally linked to occludin at tight junctions, and that TGFBRs binding and phosphorylation lead to tight junction dissociations [19-21]. Moreover, the degree of disruption in occludin and claudin 7 organization was proportional to the level of TGFB-exposure, suggesting that increases in local availability of active TGFB in vivo would cause increasing levels of disruption to the vas deferens epithelial barrier. Immunohistochemical results obtained with the claudin 7 antibody revealed more background immunoreactivity and the signal from tight junction strands was less sharp than that obtained with the anti-occludin. This may have contributed to the lack of visualization of the length-wise tight junction strand dissociation that was typically detected with the anti-occludin antibodies.

Outcomes reported here also reveal that TGFBR1 immunoreactivity is markedly present in the apical border of the native porcine vas deferens epithelium. This supports that these epithelia are subject to endogenous signaling if TGFB becomes bio-available at the luminal fluid. No definite evidence is yet available on whether vas deferens epithelial cells synthesize and secrete TGFB, but immunohistochemical data are available to support that epididymal epithelia does [28]. Moreover, local activation of TGFB is a key regulatory mechanism for signaling [41,

42] and, interestingly, epididymal epithelia express proteases that activate TGFB [43, 44]. The luminal environment of the male excurrent duct also presents segmental pH variability which, in segments such as the cauda epididymis, reaches fairly acidic levels. In the healthy duct, one would expect duct luminal pH levels that are more alkaline than those required to activate latent TGFB [45]. However, in pathologies such as cystic fibrosis there may be increased TGFB activation as bicarbonate secretion is thought to be impaired.

MAPK11 mediates changes in barrier function induced by TGFB3 in Sertoli cells [31] and was shown to mediate TGFB-signaling independently in other cell systems [46]. In addition, fundamental barrier function differences exist between Sertoli cell primary cultures and 1ºPVDs: R_{te} levels are in the order of 60 [31] and >4,000 Ohms/cm^2, respectively. Nevertheless, in Sertoli cell primary cultures, MAPK11 inhibition prevented TGFB3-induced R_{te} decreases by 50% [31]. In 1ºPVDs, MAPK11 inhibition reduced the effect of TGFB1 on R_{te} by 18% and R_{te} values were not significantly rescued from a statistical perspective. These outcomes suggest that TGFB1-induced R_{te}-decrease in vas deferens epithelial cells is largely independent of MAPK11. These results, considered together with the apparent tight junction dissociation effect, seems to suggest that a transcription-independent mechanism, as was shown to occur in the NMuMG cell line [19], may account for the extensive barrier function decreases detected in 1^{o}PVD exposed to TGFB1. As demonstrated in NMuMG cells, receptor complex formation at tight junctions and subsequent Par-6 phosphorylation induces binding of the E3 ubiquitin ligase SMURF1. This leads to ubiquination and degradation of RHOA, and tight junction dissociations [19]. It remains an open question whether this mechanism is present in epithelia lining the male excurrent duct.

In summary, this study demonstrates that TGFBR activation in vas deferens epithelia can impair epithelial integrity and function. Specifically, the epithelial barrier to small solute movement becomes virtually absent. This is expected to compromise generation and maintenance of a luminal microenvironment conducive to spermatozoa maturation and male fertility.

Acknowledgments

The authors extend sincere thanks to Henrys Ltd for making tissues available for this study, to the K-State COBRE Confocal Core Facility (RR017686), to Mr. Jimmie Stewart III (Kansas State University) for technical assistance and to Dr. Eric J. Sorscher (University of Alabama at Birmingham) for contributions to this study.

References

1. **Hoglund P, Hihnala S, Kujala M, Tiitinen A, Dunkel L, Holmberg C.** Disruption of the SLC26A3-mediated anion transport is associated with male subfertility. Fertil Steril 2006; 85: 232-235.
2. **Blomqvist SR, Vidarsson H, Soder O, Enerback S.** Epididymal expression of the forkhead transcription factor Foxi1 is required for male fertility. Embo J 2006; 25: 4131-4141.
3. **van der Ven K, Messer L, van der Ven H, Jeyendran RS, Ober C.** Cystic fibrosis mutation screening in healthy men with reduced sperm quality. Hum Reprod 1996; 11: 513-517.
4. **Traystman MD, Schulte NA, MacDonald M, Anderson JR, Sanger WG.** Mutation analysis for cystic fibrosis to determine carrier status in 167 sperm donors from the Nebraska Genetic Semen Bank. Hum Mutat 1994; 4: 271-275.
5. **Hess RA, Bunick D, Lee KH, Bahr J, Taylor JA, Korach KS, Lubahn DB.** A role for oestrogens in the male reproductive system. Nature 1997; 390: 509-512.
6. **Da Silva N, Pietrement C, Brown D, Breton S.** Segmental and cellular expression of aquaporins in the male excurrent duct. Biochim Biophys Acta 2006; 1758: 1025-1033.
7. **Carlin RW, Lee JH, Marcus DC, Schultz BD.** Adenosine stimulates anion secretion across cultured and native adult human vas deferens epithelia. Biol Reprod 2003; 68: 1027-1034.
8. **Shum WW, Da Silva N, McKee M, Smith PJ, Brown D, Breton S.** Transepithelial projections from basal cells are luminal sensors in pseudostratified epithelia. Cell 2008; 135: 1108-1117.
9. **Pierucci-Alves F, Duncan CL, Lillich JD, Schultz BD.** Porcine vas deferens luminal pH is acutely increased by systemic xylazine administration. Biol Reprod 2010; 82: 132-135.
10. **Syntin P, Dacheux F, Druart X, Gatti JL, Okamura N, Dacheux JL.** Characterization and identification of proteins secreted in the various regions of the adult boar epididymis. Biol Reprod 1996; 55: 956-974.
11. **Hinton BT, Howards SS.** Permeability characteristics of the epithelium in the rat caput epididymidis. J Reprod Fertil 1981; 63: 95-99.
12. **Cyr DG, Gregory M, Dube E, Dufresne J, Chan PT, Hermo L.** Orchestration of occludins, claudins, catenins and cadherins as players involved in maintenance of the blood-epididymal barrier in animals and humans. Asian J Androl 2007; 9: 463-475.
13. **Mital P, Hinton BT, Dufour JM.** The blood-testis and blood-epididymis barriers are more than just their tight junctions. Biol Reprod 2011; 84: 851-858.
14. **Knee RA, Hickey DK, Beagley KW, Jones RC.** Transport of IgG across the blood-luminal barrier of the male reproductive tract of the rat and the effect of estradiol

administration on reabsorption of fluid and IgG by the epididymal ducts. Biol Reprod 2005; 73: 688-694.

15. **Itoh M, Chen XH, Takeuchi Y, Miki T.** Morphological demonstration of the immune privilege in the testis using adjuvants: tissue responses of male reproductive organs in mice injected with Bordetella pertussigens. Arch Histol Cytol 1995; 58: 575-579.

16. **Yang J, Zhang X, Li Y, Liu Y.** Downregulation of Smad transcriptional corepressors SnoN and Ski in the fibrotic kidney: an amplification mechanism for TGF-beta1 signaling. J Am Soc Nephrol 2003; 14: 3167-3177.

17. **Liu Y.** Epithelial to mesenchymal transition in renal fibrogenesis: pathologic significance, molecular mechanism, and therapeutic intervention. J Am Soc Nephrol 2004; 15: 1-12.

18. **Alcorn JF, Guala AS, van der Velden J, McElhinney B, Irvin CG, Davis RJ, Janssen-Heininger YM.** Jun N-terminal kinase 1 regulates epithelial-to-mesenchymal transition induced by TGF-beta1. J Cell Sci 2008; 121: 1036-1045.

19. **Ozdamar B, Bose R, Barrios-Rodiles M, Wang HR, Zhang Y, Wrana JL.** Regulation of the polarity protein Par6 by TGFbeta receptors controls epithelial cell plasticity. Science 2005; 307: 1603-1609.

20. **Bose R, Wrana JL.** Regulation of Par6 by extracellular signals. Curr Opin Cell Biol 2006; 18: 206-212.

21. **Barrios-Rodiles M, Brown KR, Ozdamar B, Bose R, Liu Z, Donovan RS, Shinjo F, Liu Y, Dembowy J, Taylor IW, Luga V, Przulj N, Robinson M, Suzuki H, Hayashizaki Y, Jurisica I, Wrana JL.** High-throughput mapping of a dynamic signaling network in mammalian cells. Science 2005; 307: 1621-1625.

22. **Stadnicki A, Machnik G, Klimacka-Nawrot E, Wolanska-Karut A, Labuzek K.** Transforming growth factor-beta1 and its receptors in patients with ulcerative colitis. Int Immunopharmacol 2009; 9: 761-766.

23. **Grainger DJ, Heathcote K, Chiano M, Snieder H, Kemp PR, Metcalfe JC, Carter ND, Spector TD.** Genetic control of the circulating concentration of transforming growth factor type beta1. Hum Mol Genet 1999; 8: 93-97.

24. **Politch JA, Tucker L, Bowman FP, Anderson DJ.** Concentrations and significance of cytokines and other immunologic factors in semen of healthy fertile men. Hum Reprod 2007; 22: 2928-2935.

25. **Nocera M, Chu TM.** Transforming growth factor beta as an immunosuppressive protein in human seminal plasma. Am J Reprod Immunol 1993; 30: 1-8.

26. **Robertson SA, Ingman WV, O'Leary S, Sharkey DJ, Tremellen KP.** Transforming growth factor beta--a mediator of immune deviation in seminal plasma. J Reprod Immunol 2002; 57: 109-128.

27. **Ingman WV, Robertson SA.** Transforming growth factor-beta1 null mutation causes infertility in male mice associated with testosterone deficiency and sexual dysfunction. Endocrinology 2007; 148: 4032-4043.

28. **Desai KV, Flanders KC, Kondaiah P.** Expression of transforming growth factor-beta isoforms in the rat male accessory sex organs and epididymis. Cell Tissue Res 1998; 294: 271-277.

29. **Henderson NA, Cooke GM, Robaire B.** Region-specific expression of androgen and growth factor pathway genes in the rat epididymis and the effects of dual 5alpha-reductase inhibition. J Endocrinol 2006; 190: 779-791.

30. **Sedlacek RL, Carlin RW, Singh AK, Schultz BD.** Neurotransmitter-stimulated ion transport by cultured porcine vas deferens epithelium. Am J Physiol Renal Physiol 2001; 281: F557-570.

31. **Lui WY, Lee WM, Cheng CY.** Transforming growth factor beta3 regulates the dynamics of Sertoli cell tight junctions via the p38 mitogen-activated protein kinase pathway. Biol Reprod 2003; 68: 1597-1612.

32. **Owaki T, Asakawa M, Fukai F, Mizuguchi J, Yoshimoto T.** IL-27 induces Th1 differentiation via p38 MAPK/T-bet- and intercellular adhesion molecule-1/LFA-1/ERK1/2-dependent pathways. J Immunol 2006; 177: 7579-7587.

33. **Thiery JP, Acloque H, Huang RY, Nieto MA.** Epithelial-mesenchymal transitions in development and disease. Cell 2009; 139: 871-890.

34. **Samplaski MK, Agarwal A, Sharma R, Sabanegh E.** New generation of diagnostic tests for infertility: review of specialized semen tests. Int J Urol 2010; 17: 839-847.

35. **Lehmann K, Janda E, Pierreux CE, Rytomaa M, Schulze A, McMahon M, Hill CS, Beug H, Downward J.** Raf induces TGFbeta production while blocking its apoptotic but not invasive responses: a mechanism leading to increased malignancy in epithelial cells. Genes Dev 2000; 14: 2610-2622.

36. **Siegel PM, Massague J.** Cytostatic and apoptotic actions of TGF-beta in homeostasis and cancer. Nat Rev Cancer 2003; 3: 807-821.

37. **Thiery JP.** Epithelial-mesenchymal transitions in tumour progression. Nat Rev Cancer 2002; 2: 442-454.

38. **Kim B, Kawashima A, Ryu JA, Takahashi N, Hartman RP, King BF, Jr.** Imaging of the seminal vesicle and vas deferens. Radiographics 2009; 29: 1105-1121.

39. **Bisceglia M, Dor DB, Carosi I, Vairo M, Pasquinelli G.** Paratesticular mesothelioma. Report of a case with comprehensive review of literature. Adv Anat Pathol 2010; 17: 53-70.

40. **Shull MM, Ormsby I, Kier AB, Pawlowski S, Diebold RJ, Yin M, Allen R, Sidman C, Proetzel G, Calvin D, et al.** Targeted disruption of the mouse transforming growth factor-beta 1 gene results in multifocal inflammatory disease. Nature 1992; 359: 693-699.

41. **Jenkins G.** The role of proteases in transforming growth factor-beta activation. Int J Biochem Cell Biol 2008; 40: 1068-1078.

42. **Rifkin DB.** Latent transforming growth factor-beta (TGF-beta) binding proteins: orchestrators of TGF-beta availability. J Biol Chem 2005; 280: 7409-7412.

43. **Monsees TK, Blocher S, Loddo C, Steger K, Schill WB.** Tissue kallikrein and bradykinin B2 receptors in the reproductive tract of the male rat. Andrologia 2003; 35: 24-31.

44. **Emami N, Diamandis EP.** Potential role of multiple members of the kallikrein-related peptidase family of serine proteases in activating latent TGF beta 1 in semen. Biol Chem 2010; 391: 85-95.

45. **Lyons RM, Keski-Oja J, Moses HL.** Proteolytic activation of latent transforming growth factor-beta from fibroblast-conditioned medium. J Cell Biol 1988; 106: 1659-1665.

46. **Yu L, Hebert MC, Zhang YE.** TGF-beta receptor-activated p38 MAP kinase mediates Smad-independent TGF-beta responses. EMBO J 2002; 21: 3749-3759.

Chapter 3 - Transforming Growth Factor Beta1 Impairs CFTR-Mediated Anion Secretion across Cultured Porcine Vas Deferens Epithelial Monolayer via the p38 MAPK Pathway

Sheng Yi, Fernando Pierucci-Alves, and Bruce D. Schultz

Departments of Anatomy and Physiology
Kansas State University, Manhattan, KS 66506

Corresponding author: Dr. Bruce D. Schultz
Department of Anatomy and Physiology
1600 Denison Avenue, Coles Hall 228
Manhattan, KS-66506
Phone numbers: 785-532-4839 (office), 785-532-4557 (fax).
Email: bschultz@vet.ksu.edu

Running Head: TGF-β1 impairs anion secretion across vas deferens epithelia

This chapter is reprinted from American Journal of Physiology – Cell Physiology.

Abstract

The goal of this study was to determine whether transforming growth factor β1 (TGF-β1) affects epithelial cells lining the vas deferens, an organ that is universally affected in cystic fibrosis male patients. In PVD9902 cells, which are derived from porcine vas deferens epithelium, TGF-β1 exposure significantly reduced short circuit current (I_{sc}) stimulated by forskolin or a cell membrane-permeant cAMP analog, 8-pCPT-cAMP, suggesting that TGF-β1 affects targets of the cAMP signaling pathway. Electrophysiological results indicated that TGF-β1 reduces the magnitude of current inhibited by cystic fibrosis transmembrane conductance regulator (CFTR) channel blockers. Real-time RT-PCR revealed that TGF-β1 down-regulates the abundance of mRNA coding for CFTR, while biotinylation and western blot showed that TGF-β1 reduces both total CFTR and apical cell surface CFTR abundance. These results suggest that TGF-β1 causes a reduction in CFTR expression, which limits CFTR-mediated anion secretion. TGF-β1 associated attenuation of anion secretion was abrogated by SB431542, a TGF-β1 receptor I inhibitor. Signaling pathway studies showed that the effect of TGF-β1 on I_{sc} was reduced by SB203580, an inhibitor of p38 mitogen-activated protein kinase (MAPK). TGF-β1 exposure also increased the amount of phospho-p38 MAPK substantially. In addition, anisomycin, a p38 MAPK activator, mimicked the effect of TGF-β1, which further suggests that TGF-β1 affects PVD9902 cells through a p38 MAPK pathway. These observations suggest that TGF-β1, via TGF-β1 receptor I and p38 MAPK signaling, reduces CFTR expression to impair CFTR-mediated anion secretion, which would likely compound the effects associated with mild CFTR mutations, and ultimately would compromise male fertility.

Key words: TGF-β1, vas deferens epithelial cells, male infertility, CFTR, p38 MAPK

Introduction

Transforming growth factor beta 1 (TGF-β1), the predominant isoform of TGF-β, is a pleiotropic cytokine regulating cell proliferation and apoptosis, differentiation, inflammation, extracellular matrix synthesis, and developmental processes (6). TGF-β1 signals through binding to a cell surface type II serine/threonine kinase receptor, which then recruits and activates the type I receptor. Intracellular signal transduction is most commonly mediated through the canonical Smad pathway, although several non-canonical kinase-mediated pathways (PI3K, Erk, JNK, and p38 MAPK) have been implicated (6, 11). Such components of the activated signaling cascades (whether Smads or protein kinases) translocate into the nucleus and alter gene expression to regulate multiple cellular functions.

Altered expression of TGF-β1 has been involved in fibrotic diseases including cystic fibrosis, a life-shortening disease affecting 1 in every 2,000 – 3,000 newborn Caucasians (7, 9). Cystic fibrosis affects many organ systems including the respiratory, gastrointestinal, musculoskeletal, and reproductive systems. It is associated with variations in the sequence of *CFTR*, the gene coding for the cystic fibrosis transmembrane conductance regulator (CFTR). *CFTR* mutations lead to the reduction or absence of functional CFTR protein in the apical membrane of epithelial cells throughout the body, which results in attenuated anion secretion across epithelial tissues. The clinical severity of cystic fibrosis is determined not only by the type of *CFTR* mutation(s) carried by the patient but also by genetic modifiers (7). Genotyping results suggest that cystic fibrosis patients with a TGF-β1 'high producer' genotype for codon 10 are associated with a more severe lung disease as well as a more rapid deterioration in lung function (1, 12). Additionally, measurement of plasma TGF-β1 levels suggests that higher concentrations of TGF-β1 are correlated with increased severity of lung disease in pediatric cystic fibrosis patients (16). All these observations indicate that elevated levels of circulating TGF-β1 lead to worse cystic fibrosis lung disease.

In cystic fibrosis male patients, vas deferens and epididymis are the most frequently affected tissue and these tissues undergo anatomical disruptions early in life. About 98% of male cystic fibrosis patients are infertile due to congenital bilateral absence of the vas deferens (CBAVD), a condition characterized by duct atresia and post-testicular azoospermia (10, 47). Besides a

population of ~30,000 cystic fibrosis patients in the United States and ~70,000 worldwide, about one in every 25 Caucasians are carriers of disease-associated *CFTR* sequences. Cystic fibrosis carriers will not be diagnosed by the sweat test and do not have apparent cystic fibrosis symptomology, but they are associated with a higher frequency of infertility (27). Genotypic analysis revealed no apparent correlation between CBAVD in European populations and two distinct single nucleotide polymorphisms in the TGF-β1 gene (17). However, no study has focused on whether TGF-β1 affects vas deferens epithelium. It is possible that TGF-β1 attenuates vas deferens epithelial anion secretion in cystic fibrosis carriers who are associated with mild disease or with no typical symptomology, and would promote cystic fibrosis-related pathology.

The objective of the current study was to determine whether TGF-β1 impairs ion transport across cultured vas deferens epithelial monolayers. PVD9902, a cell line that was derived from porcine vas deferens epithelium and recapitulates most ion transport characteristics of freshly isolated porcine vas deferens epithelial tissue, was used (5). Electrophysiological, molecular, and immunological assays were performed to evaluate the changes in PVD9902 cells when exposed to TGF-β1. Experiments were focused to elucidate the potential mechanisms by which TGF-β1 affects vas deferens tissue.

Materials and Methods

Chemicals. Forskolin (*Coleus forskohlii*) was obtained from Calbiochem (La Jolla, CA). GlyH-101 was obtained from Millipore (Billerica, MA). N-[4-methylphenylsulfonyl]-N'-[4-trifluoromethylphenyl] urea (DASU-02) was synthesized in the laboratory. Unless indicated otherwise, chemicals used were purchased from Sigma-Aldrich, Inc. (St. Louis, MO).

Cell culture. PVD9902 cells (5) were seeded onto plastic 25-cm^2 cell culture flasks (Corning, Inc., Corning, NY) and grown in Dulbecco's modified Eagle medium (DMEM, Invitrogen, Carlsbad, CA) supplemented with 10% heat inactivated fetal bovine serum (FBS, Atlanta Biologicals, Atlanta, GA) and 1% penicillin and streptomycin (Invitrogen) in a humidified 5% CO_2 incubator at 37°C. Confluent cells were washed with phosphate buffered saline (PBS), lifted by trypsin-EDTA (0.25%, Invitrogen), seeded onto permeable supports (Snapwell or Transwell, Costar, Corning, Inc.), and cultured for 14 days prior to experimental assay. Media were refreshed every other day and monolayers were exposed to TGF-β1 (5 ng/ml, R&D Systems, Minneapolis, MN) in the basolateral compartments for the last 24 hours prior to assay.

Electrophysiology. PVD9902 monolayers were mounted in modified Ussing-style chambers (model DCV9, Navicyte, San Diego, CA), bathed symmetrically with Ringer solution (composition in mM: 120 NaCl, 25 $NaHCO_3$, 3.3 KH_2PO_4, 0.83 K_2HPO_4, 1.2 $MgCl_2$, and 1.2 $CaCl_2$), maintained at 39°C and bubbled with 5% CO_2-95% O_2. After recording open circuit potential, monolayers were clamped to 0 mV, and a 5-second bipolar pulse was applied every 100 seconds using a voltage clamp (model 558C-5, University of Iowa, Dept. of Bioengineering, Iowa City, IA). Short circuit current (I_{sc}), which represents transepithelial electrogenic ion transport, was monitored and recorded at 1 Hz with an Intel based computer and MP100A-CE interface (v.3.2.6, BIOPAC Systems, Santa Barbara, CA). The change in current in response to the periodic voltage pulse was used to calculate transepithelial electrical resistance using Ohm's law ($R_{te} = \Delta V/\Delta I_{sc}$). Test reagents were added to the apical and/or basolateral side(s) of each chamber as indicated. The magnitude of test reagent-stimulated I_{sc} was determined by ΔI_{sc} between the pre-addition I_{sc} value and the peak value within first 10 minutes after addition.

RNA isolation and real-time RT-PCR. RNA was isolated from PVD9902 monolayers using an RNeasy Mini Kit (Qiagen, Valencia, CA) according to the manufacturer's instructions. RNA quantity was determined spectrophotometrically (ND 8000, NanoDrop Products, Wilmington, DE) while RNA quality was confirmed using microfluidics (Bioanalyzer, Agilent Technologies, Santa Clara, CA). Ten nanograms of RNA were used as template and RT-PCR was performed using the iScript One-Step RT-PCR Kit with SYBR Green (Bio-Rad, Hercules, CA) with specific primer pairs. The sequences of primer pairs were as follows: CFTR (forward) 5'-CCG GGC ACC ATT AAA GAA AAC-3' and (reverse) 5'-GCC ATC AAT TTA CGA ACA CGG C-3' (29); 18s (forward) 5'-GAG GTT CGA AGA CGA TCA GA-3' and (reverse) 5'-TCG CTC CAC CAA CTA AGA AC-3' (49). Relative quantification of mRNA was conducted by a SmartCycler (Cepheid, Sunnyvale, CA) using the ΔΔCt method with 18s as the reference, in which $\Delta Ct=Ct_{(Vehicle)}-Ct_{(Treated)}$, $\Delta\Delta Ct=\Delta Ct_{(Target)}-\Delta Ct_{(Reference)}$; the change in copy number of target RNA relative to reference RNA=$2^{\Delta\Delta Ct}$. The quality of RT-PCR products was validated by a single peak melt curve, which represents single PCR product, and by a single band of expected mobility in a 1.5% agarose DNA gel. The cDNA was visualized by inclusion of ethidium bromide (1 μg/ml) and the product size was determined by a 100-bp DNA ladder (Promega, Madison, WI).

Biotinylation and immunoblotting. PVD9902 monolayers were homogenized and lysed with Laemmli sample buffer (2X) containing 4% SDS, Tris-HCl (125 mM) and protease inhibitors (Roche Diagnostics, Indianapolis, IN). Lysates were passed through 25-gauge needles repeatedly and then centrifuged at 14,000 g for 10 minutes. Supernatant protein concentrations were determined by measuring absorbance at 280 nm (A_{280}). Collected supernatants were then mixed with bromophenol blue (0.01% w/v), glycerin (10%), and DTT (0.1 M) and the mixtures were incubated at 37°C for 2 hours. Equal amounts of protein from each treatment were loaded to 8-16% Tris-HEPES-SDS gradient gels (Pierce, Rockford, IL). Following electrophoresis, proteins were transferred onto Immobilon-P transfer membrane (Millipore). Membranes were blocked with 5% nonfat dry milk (Bio-Rad) in PBS with 0.1% Tween-20 for 2 hours and then probed with primary antibodies: anti-CFTR (Millipore, 05-583), anti-phospho-p38 MAPK (Cell Signaling, 4511, Danvers, MA), and anti-actin (Sigma-Aldrich, A2066) overnight at 4°C, incubated in peroxidase-conjuated secondary antibodies (Pierce) for 1 hour, followed by

development using chemiluminiscent substrates (Super Signal West Pico and Femto, Pierce). Images were obtained digitally (Kodak Image Station 4000 R, Kodak, Rochester, NY) and quantification was performed by measuring band signal intensity (UN-SCAN-IT Gel, Silk Scientific, Inc, Orem, Utah).

For the detection of membrane proteins, filter-grown PVD9902 monolayers were washed and incubated with Ringer solution at 37°C for 30 minutes, and then placed on ice. Biotinylation reagent containing sulfo-NHS-SS-biotin (400 μM, Pierce) in Ringer solution was added to the apical or basolateral compartment for 15 minutes. After biotin incubation, monolayers were rinsed and washed 3 times with Ringer solution containing 50 mM glycine to quench unreacted sulfo-NHS-SS-biotin groups. After removing quenched biotin, PVD9902 monolayers were lysed and homogenized. Supernatants were incubated with immobilized neutravidin-agarose (Pierce) setting in micro-spin columns (Pierce) for 2 hours at room temperature. Non-bound proteins were collected as flow-through samples. Avidin gels were washed 3 times with lysis buffer and incubated with Laemmli buffer containing DTT (50 mM) to elute bound biotinylated proteins. Immunoblotting was completed as indicated previously to detect cell surface labeling.

Lactate dehydrogenase (LDH) assay. The activity of LDH released from damaged cells into the culture medium was measured using the LDH cytotoxicity detection kit (CytoTox-ONE; Promega Corp., Madison, WI). PVD9902 cells were seeded at a density of 1×10^5 cells per well onto sterile 96-well opaque-walled tissue culture plates (Nalge Nunc International Corp., Rochester, NY), cultured for 72 hours, treated with vehicle or TGF-β1 (5 ng/ml) for 24 hours, and incubated with CytoTox-ONE reagent according to the manufacturer's instructions. Lysis solution was added to cells in paired wells to determine maximal LDH release in "lysed" cells. The fluorescence values were recorded to determine LDH activity and to estimate the number of damaged cells.

Data analysis. All numerical results are reported as mean ± SEM. Calculations, t-tests, and graphs were performed with Sigmaplot (v 10.0, SPSS Inc, Richmond, CA) and Excel 2007 (Microsoft Corp, Redmond, WA).

Results

TGF-β1 impairs cAMP-stimulated anion secretion across PVD9902 monolayers.

Paired vehicle- or TGF-β1-treated PVD9902 monolayers were mounted in modified Ussing-style chambers for measurements of R_{te} and I_{sc}. Ussing chamber assays also included in-chamber pharmacological tests and any acute responses were visualized and recorded in real time. Both vehicle and TGF-β1 treated PVD9902 cells formed electrically tight epithelial monolayers. TGF-β1 exposure was associated with lower R_{te} when compared to paired monolayers exposed to vehicle (Table 1) although the difference did not reach statistical significance (P>0.18). Forskolin (2 μM), an adenylyl cyclase activator that increases intracellular cAMP generation, was employed to stimulate cAMP-dependent anion secretion (26, 28). Typically, forskolin exposure elicited a transient peak in I_{sc} followed by a sustained plateau, indicating ongoing anion secretion (Figure 1). In TGF-β1 treated monolayers the response to forskolin followed the same pattern but was reduced to less than half of the typical magnitude. The forskolin-induced increase in I_{sc} was associated with decreased R_{te}, suggesting the activation of channels that contribute to anion secretion. In vehicle treated PVD9902 monolayers, forskolin exposure induced a reduction of 6096 ± 1174 Ω cm^2 in R_{te} while in TGF-β1 treated monolayer, the reduction in R_{te} was significantly less (1799 ± 460 Ω cm^2).

Table 3.1 Basal transepithelial electrical resistance (R_{te}) of PVD9902 cells after different treatments.

Treatment	Basal R_{te}, Ω cm^2
Vehicle	8,184 ± 477
TGF-β1	6,721 ± 803
Vehicle + SB431542	3,923 ± 657
TGF-β1 + SB431542	4,635 ± 783
Vehicle + SB203580	6,731 ± 580
TGF-β1 + SB203580	4,822 ± 683
Anisomycin	4,123 ± 1,026

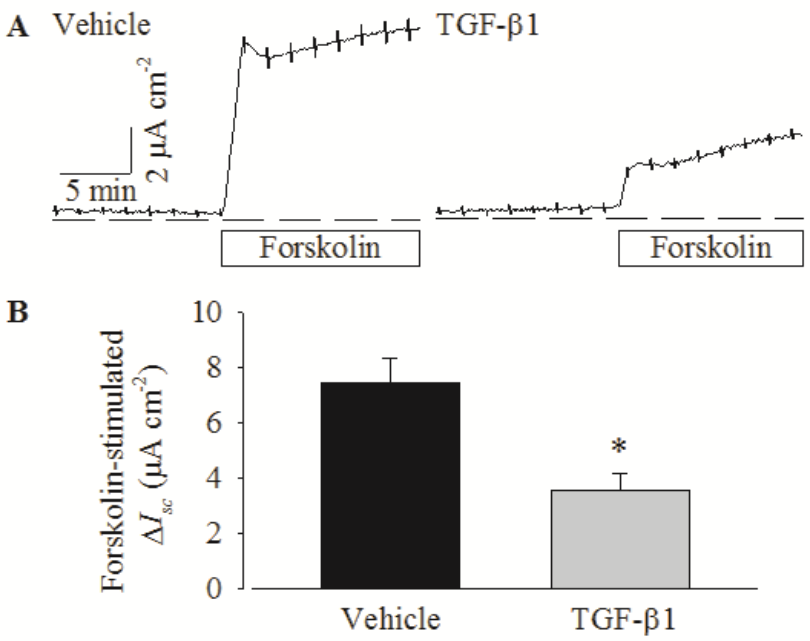

Figure 3.1 TGF-β1 impairs forskolin-stimulated anion secretion across PVD9902 monolayers.

A) Representative Ussing chamber recordings of vehicle or TGF-β1 treated (5 ng/ml, 24 hours) PVD9902 monolayers exposed to forskolin (2 μM). The dashed lines represent the reference point of zero net current, indicating no net ion flux. Bar indicates the duration of symmetrical forskolin exposure. **B)** Summarized results of forskolin-stimulated anion secretion from 7 paired experiments. Asterisk (*) indicates significant difference between vehicle and TGF-β1 treated monolayers ($P<0.05$).

Isobutylmethylxanthine (IBMX, 100 μM), a non-selective cyclic nucleotide phosphodiesterase inhibitor, was added before and with forskolin during some experiments to preclude cAMP breakdown and maximize cytosolic cAMP accumulation. IBMX elicited an immediate increase in I_{sc}, which suggests that the PVD9902 cells have ongoing cyclic nucleotide turnover at rest, and subsequent exposure to forskolin further increased anion secretion (Figure 2). Although PVD9902 monolayers exposed to TGF-β1 responded to both IBMX and forskolin with an increase in I_{sc}, the response to both was significantly muted, suggesting that reduced cytosolic

cAMP concentration in cells exposed to TGF-β1 did not likely account for the differences in outcome. Results from experiments using a membrane-permeant cAMP analog, 8-pCPT-cAMP, to stimulate I_{sc} showed that TGF-β1 also reduces these responses (Figure 3). Taken together, these outcomes suggest that a downstream component(s) of the cAMP signaling pathway or an ion transport protein(s) is negatively impacted by TGF-β1 exposure.

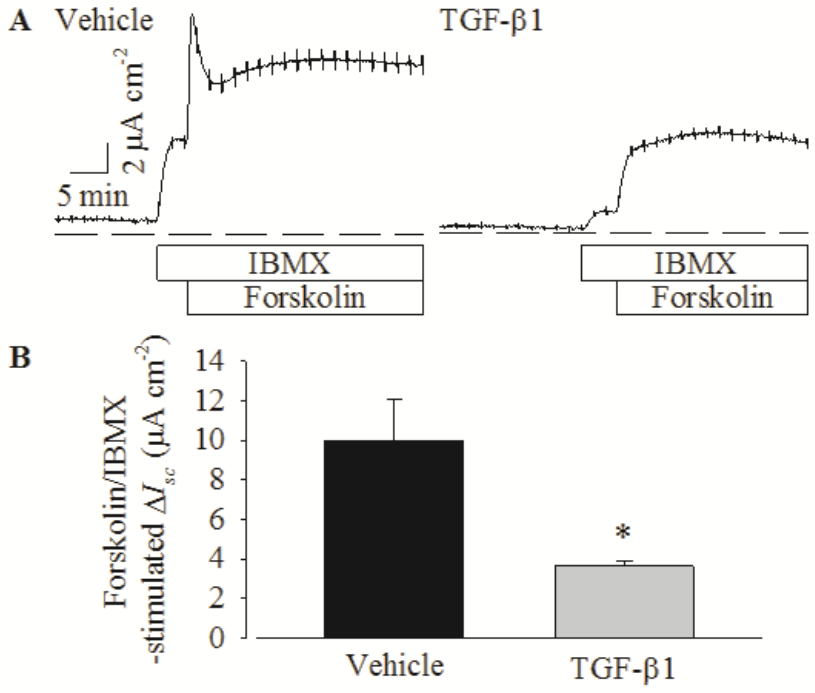

Figure 3.2 TGF-β1 impairs anion secretion across PVD9902 monolayers stimulated by forskolin in the presence of IBMX.

A) Representative current recordings of vehicle or TGF-β1 treated (5 ng/ml, 24 hours) PVD9902 monolayers exposed to IBMX (100 μM) followed by forskolin (2 μM) as indicated by the labeled bars. **B)** Results summarized from 4 paired experiments comparing the responses to the combination of IBMX and forskolin. Asterisk (*) indicates statistical difference from vehicle ($P<0.05$).

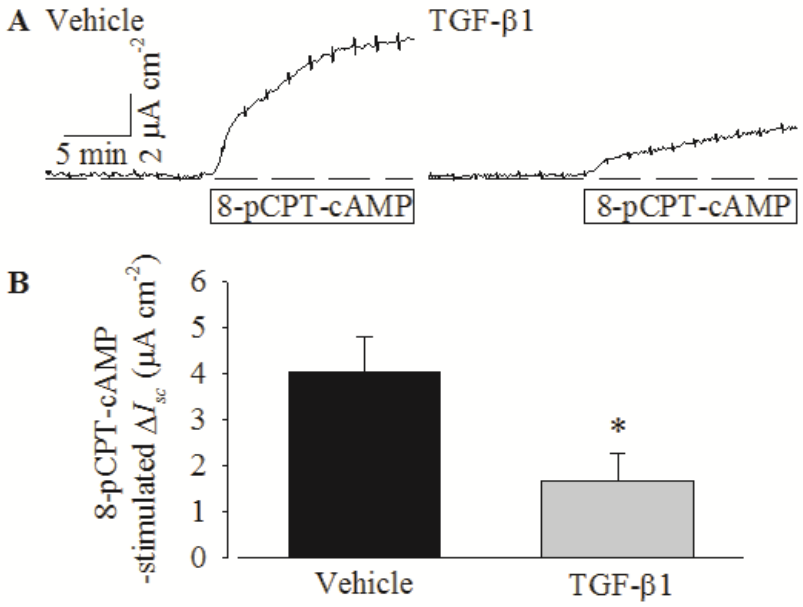

Figure 3.3 TGF-β1 impairs 8-pCPT-cAMP-stimulated anion secretion across PVD9902 monolayers.

A) Ussing chamber traces of vehicle or TGF-β1 treated (5 ng/ml, 24 hours) PVD9902 monolayers in response to 8-pCPT-cAMP (300 μM) are shown. **B)** Summary of responses to 8-pCPT-cAMP from 5 paired experiments. Asterisk (*) indicates statistical significance ($P<0.05$).

To test more directly for TGF-β1-induced changes CFTR-mediated anion secretion, cells were exposed to selective CFTR channel blockers after the sustained response to forskolin had been established. In both vehicle and TGF-β1 treated monolayers, DASU-02 (100 μM) inhibited ~40% of forskolin-stimulated I_{sc} (Figure 4A). However, in vehicle treated PVD9902 monolayers, the absolute value of I_{sc} inhibited by DASU-02 was more than 2 fold of the I_{sc} in TGF-β1 treated PVD9902 monolayers. Another CFTR selective blocker, GlyH-101, was tested, also. Similar to the effect of DASU-02, GlyH-101 (10 μM) inhibited forskolin-stimulated I_{sc} in both vehicle and TGF-β1 treated monolayers. The magnitude of I_{sc} blocked by GlyH-101 in TGF-β1 treated monolayers was much less than in monolayers exposed to vehicle alone (Figure 4B). The attenuated effect of both DASU-02 and GlyH-101 on TGF-β1 treated monolayers, together with

a less profound reduction in R_{te} stimulated by the activation of cAMP-mediated pathway (see Figure 1A), suggest that TGF-β1 exposure reduces CFTR-mediated ion transport.

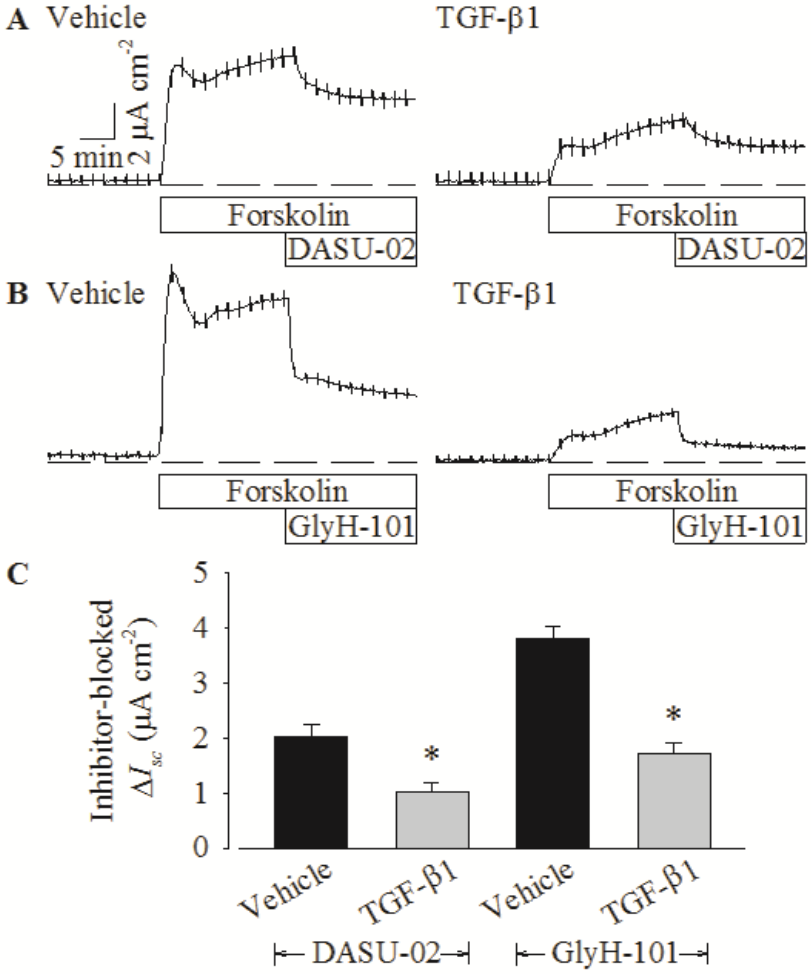

Figure 3.4 TGF-β1 reduces the effect of CFTR inhibitors.

Typical current recordings of vehicle or TGF-β1 treated (5 ng/ml, 24 hours) PVD9902 monolayers exposed sequentially to forskolin (2 μM) followed by **A)** DASU-02 (100 μM) or **B)** GlyH-101 (10 μM). **C)** Summarized results of CFTR inhibitor blocked anion secretion from 5-6 paired experiments. Asterisk (*) indicates statistical difference from vehicle ($P<0.05$).

TGF-β1 down-regulates CFTR mRNA expression.

Real-time RT-PCR was performed using RNA isolated from 5 paired monolayers of different passage numbers to detect the relative abundance of mRNA coding for CFTR. The Ct value for CFTR in vehicle treated PVD9902 cells was 28.9 ± 0.4 while the Ct value of CFTR in TGF-β1 treated cells was 29.8 ± 0.6. For the reference gene 18s, the Ct values in vehicle treated and TGF-β1 treated cells were virtually equal, 12.7 ± 0.3 and 12.8 ± 0.3 for vehicle and TGF-β1 treatments, respectively (Figure 5). Using the ΔΔCt method, the relative abundance of mRNA coding for CFTR in TGF-β1 treated cells was 60.2% ± 8.4% of its abundance in cells exposed to vehicle, indicating that TGF-β1 down-regulates CFTR mRNA expression.

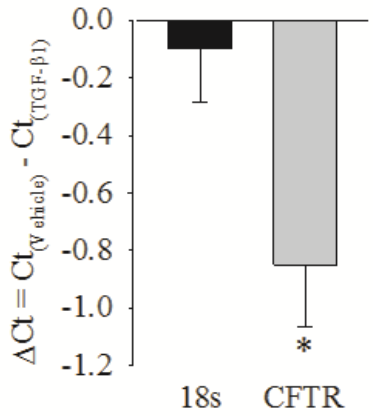

Figure 3.5 TGF-β1 down-regulates CFTR mRNA abundance.
Expression of mRNA coding for CFTR in PVD9902 monolayers exposed to vehicle or TGF-β1 (5 ng/ml, 24 hours) was determined by real-time RT-PCR. Data are summarized from 5 paired experiments and are expressed as the ΔCt between vehicle treated cells and TGF-β1 treated cells for the reference, 18s and for CFTR. Asterisk (*) indicates significant difference ($P<0.05$).

TGF-β1 down-regulates CFTR protein expression.

Given the electrophysiological evidence that TGF-β1 impairs anion secretion through CFTR as well as the RT-PCR outcomes that TGF-β1 down-regulates the copy number of CFTR mRNA, western blot analysis was performed to detect whether TGF-β1 affects the apparent protein

expression of CFTR using an antibody that detects CFTR in primary adult and neonatal porcine vas deferens epithelial cells at the same mobility as in Calu-3 cells (35). Typically, CFTR is observed following electrophoresis in 3 different isoforms, namely A-band, B-band, and C-band, that exhibit distinct mobilities due to the extent of post-translational modification (32). A-band represents nascent CFTR protein lacking glycosylation, B-band represents CFTR with core glycosylation, and C-band represents the mature fully glycosylated form. Both B-band and C-band isoforms were identified by western blot in PVD9902 cells, whereas A-band was not detected (Figure 6A). CFTR protein expression was quantified by densitometry and then normalized to an internal loading control, β-actin. The relative abundance of CFTR following TGF-β1 exposure was then normalized to vehicle monolayers. Summarized immunoblotting results suggest that TGF-β1 exposure led to a significant reduction of the abundance of CFTR protein for both B-band and C-band isoforms (Figure 6A).

Cell surface biotinylation together with western blot analysis were applied to investigate whether TGF-β1 exposure also would decrease apical cell surface CFTR protein expression. PVD9902 monolayers were biotinylated from the apical compartment or from the basolateral compartment. All fractions were subjected to SDS-PAGE followed by western blot analysis. Occludin, a tight junction protein that can be biotinylated from both apical and basolateral compartments, was used to verify unilateral biotin labeling of proteins in either the apical or basolateral membrane in each experiment (data now shown). Results show that CFTR is detected in apical biotinylated cell lysate and flow through but not in basolateral biotinylated cell lysate, which suggests that CFTR exists in the apical cell surface and exists intracellularly, but not in the basolateral cell surface (Figure 6B). Similar to the outcomes in Figure 6A, in the whole cell lysate of TGF-β1 treated PVD9902 cells, the expression of total CFTR was less than its expression in vehicle treated cells. The absolute expression of apical cell surface CFTR in cells exposed to TGF-β1 was also less than its apical expression in cells exposed to vehicle alone. Additionally, the abundance of apical biotinylated CFTR was compared with the abundance of total CFTR in whole cell lysate to evaluate the percentage of apical cell surface CFTR expression. In both vehicle treated cells and TGF-β1 treated cells, apical cell surface CFTR accounts for ~16% of total CFTR, suggesting that TGF-β1 does not affect the relative expression of apical cell surface CFTR (Figure 6B). Taken together, these outcomes suggest that TGF-β1 decreases the total

amount of CFTR protein present in the cells as well as its amount in the apical membrane where it could contribute to anion secretion. Decreased expression could limit CFTR-mediated anion secretion, as was observed.

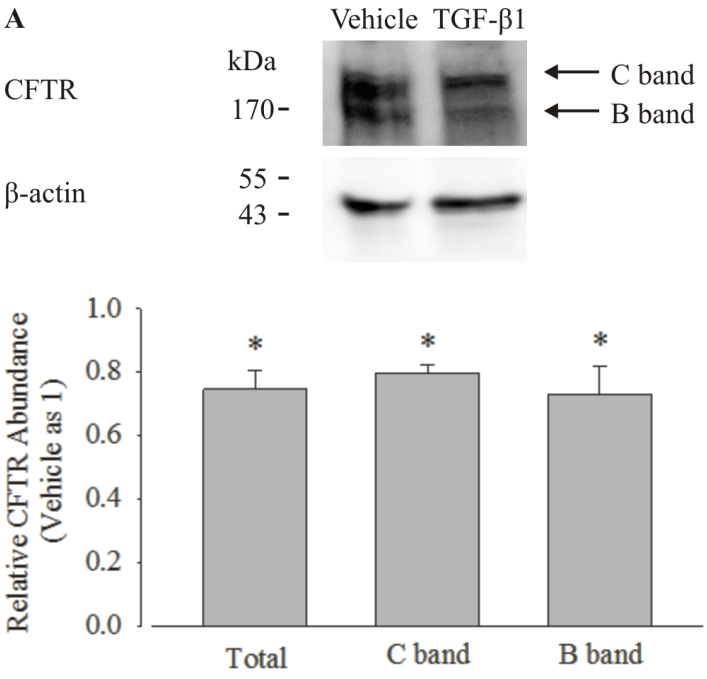
A
Vehicle
TGF-β1
kDa
CFTR
170
C band
B band
β-actin
55
43
Relative CFTR Abundance (Vehicle as 1)
1.0
0.8
0.6
0.4
0.2
0.0
*
*
*
Total
C band
B band

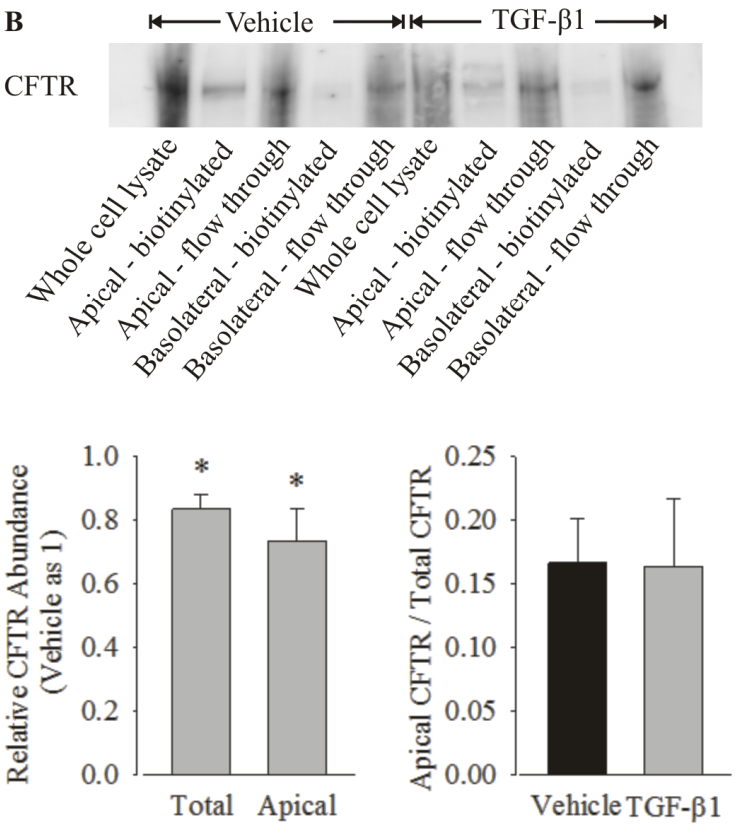
B
Vehicle
TGF-β1
CFTR
Whole cell lysate
Apical - biotinylated
Apical - flow through
Basolateral - biotinylated
Basolateral - flow through
Whole cell lysate
Apical - biotinylated
Apical - flow through
Basolateral - biotinylated
Basolateral - flow through
Relative CFTR Abundance (Vehicle as 1)
1.0
0.8
0.6
0.4
0.2
0.0
*
*
Total
Apical
Apical CFTR / Total CFTR
0.25
0.20
0.15
0.10
0.05
0.00
Vehicle
TGF-β1

Figure 3.6 TGF-β1 reduces CFTR abundance in cell lysates and in the apical cell surface. **A)** CFTR expression was assessed in whole cell lysates from PVD9902 monolayers exposed to vehicle or TGF-β1 (5 ng/ml, 24 hours) by western blots. Densitometric analysis was conducted to quantify signal intensity that could be attributed to total CFTR (C band and B band), fully glycosylated CFTR (C band), and core-glycosylated CFTR (B band). Data are expressed as relative abundance in CFTR normalized to β-actin with respect to vehicle. Data are summarized from 4 independent experiments. **B)** Apical cell surface CFTR expression was determined by biotinylation and western blots from PVD9902 monolayers exposed to vehicle or TGF-β1 (5 ng/ml, 24 hours). Densitometric analysis was conducted to determine protein abundance of total CFTR and apical cell surface CFTR. Summarized relative CFTR abundance is from 6 independent experiments. Asterisks indicate significant reductions when compared to vehicle ($P<0.05$).

Receptor inhibitor abolishes TGF-β1-induced reduction in anion secretion.

TGF-β1 activates transmembrane receptors to elicit cytosolic signaling and ultimately to affect cellular activity. SB431542 (10 μM), a selective TGF-β1 receptor I inhibitor (14, 25), was added into PVD9902 culture media 1 hour prior to TGF-β1 exposure. After 24 hours of TGF-β1 exposure, PVD9902 cells were mounted into modified Ussing chambers to measure forskolin-stimulated anion secretion. In PVD9902 monolayers treated with both TGF-β1 and SB431542, forskolin elicited a sharp increase in I_{sc} that was significantly greater than monolayers exposed to TGF-β1 alone and was not different, statistically, from vehicle alone (Figure 7). The outcome that the reduction of forskolin response by TGF-β1 can be abolished by SB431542 indicates that TGF-β1 receptor signaling pathway is necessary and sufficient to account for TGF-β1-suppressed anion secretion across PVD9902 monolayers.

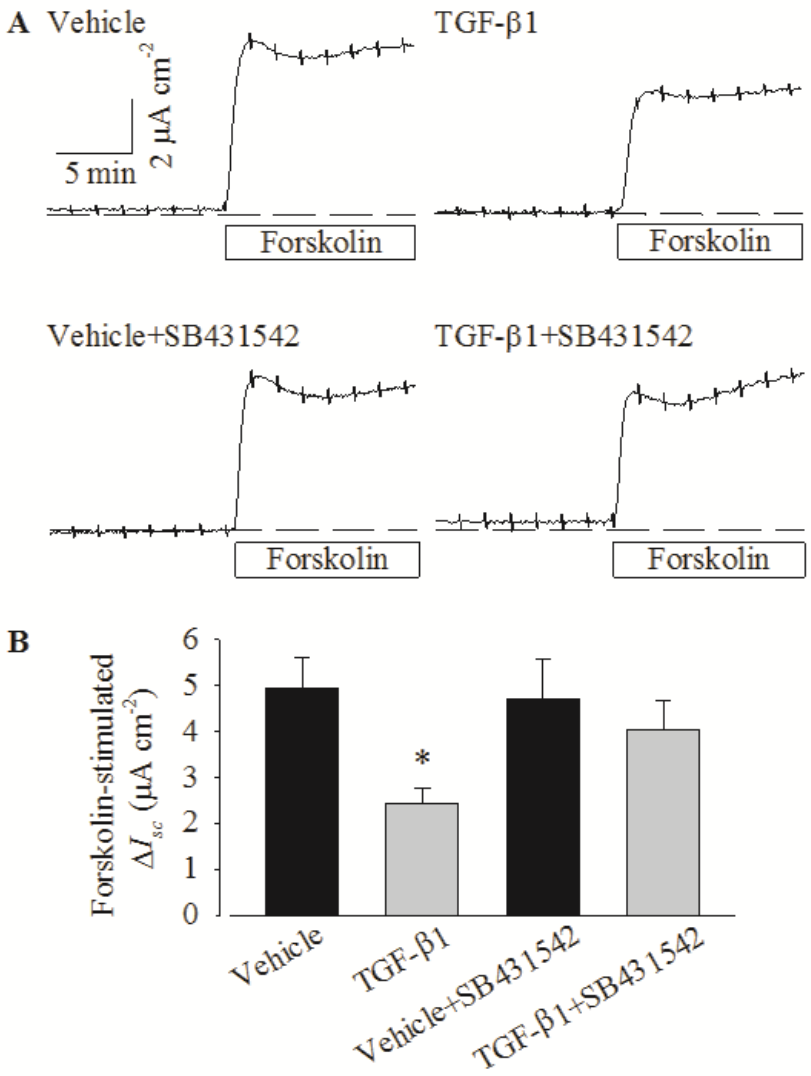

Figure 3.7 A TGF-β receptor I inhibitor, SB431542, abolishes the TGF-β1-associated reduction in the response to forskolin.

A) Typical responses to forskolin (2 μM) in PVD9902 monolayers exposed to vehicle, TGF-β1 (5 ng/ml), SB431542 (10 μM), or TGF-β1 plus SB431542. **B)** Summary of forskolin-stimulated anion secretion from 10-14 experiments. Asterisk (*) indicates statistical difference from vehicle ($P<0.05$).

TGF-β1 activates the p38 MAPK signaling pathway in PVD9902 cells.

Given the observations that TGF-β1 activates its cognate receptor and attenuates CFTR-mediated anion secretion, downstream signaling cascades elicited by TGF-β1 were investigated using a pharmacological approach. PVD9902 cells were exposed to SB203580, a compound that inhibits p38 MAPK catalytic activity (15, 24). PVD9902 monolayers exposed to SB203580 (10 μM) exhibited a rapid response to forskolin that is not significantly different from monolayers exposed to vehicle along. However, monolayers exposed to TGF-β1 plus SB203580 exhibited a significantly higher response to forskolin than monolayers treated with TGF-β1 alone (Figure 8). The observation that SB203580 attenuates the effect of TGF-β1 on forskolin stimulated I_{sc} provides evidence that p38 MAPK is required for the TGF-β1-induced change in ion transport.

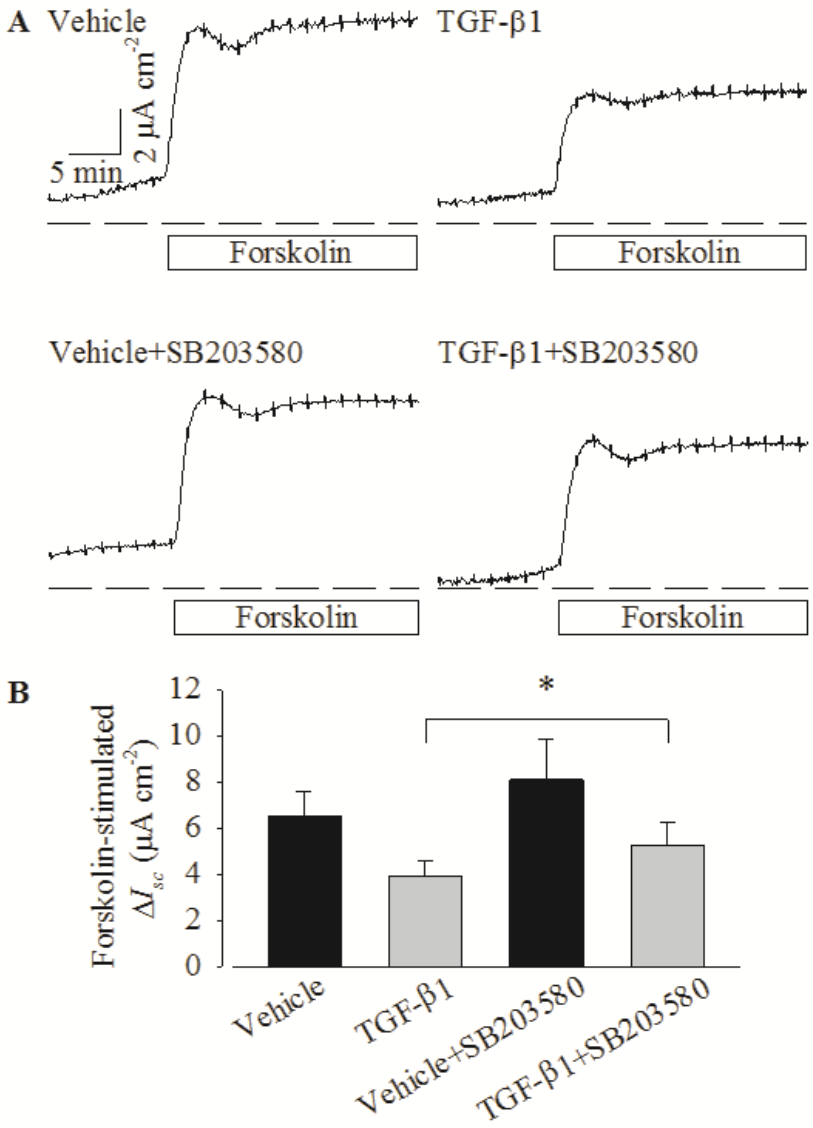

Figure 3.8 A p38 MAPK inhibitor, SB203580, attenuates TGF-β1-impaired forskolin response.

A) Typical responses to forskolin (2 μM) in PVD9902 monolayers exposed to vehicle, TGF-β1 (5 ng/ml), SB203580 (10 μM), or TGF-β1 plus SB203580. **B)** Responses to forskolin are summarized from 4-5 experiments. Asterisks (*) indicate statistical significance ($P<0.05$).

Western blot analysis was performed to detect phospho-p38 MAPK, which is thought to be the active form. Results presented in Figure 9 demonstrate that phospho-p38 MAPK is present in all

samples, regardless of TGF-β1 exposure. However, after normalization to β-actin as a loading control, the intensity of the phospho-p38 MAPK band was ~1.7 fold in samples from cells exposed to TGF-β1 when compared to cells exposed to vehicle. This increase in the relative abundance of phospho-p38 MAPK was prevented by the pre-treatment of SB431542, suggesting that TGF-β1-induced activation of p38 MAPK signaling pathway is through the activation of TGF-β1 receptor. Together with ion transport results showing that p38 MAPK inhibitor attenuates the effect of TGF-β1, these outcomes suggest quite strongly that TGF-β1, through the activation of its receptor, induces phosphorylation of p38 MAPK and, thus, activates the p38 MAPK signaling pathway.

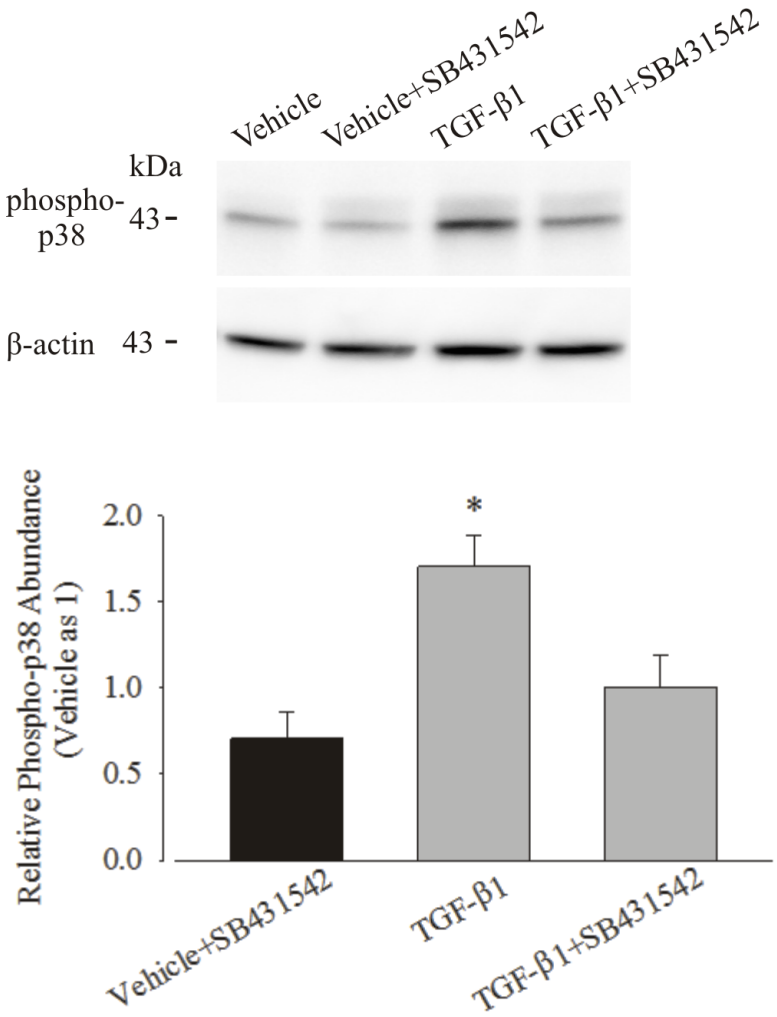

Figure 3.9 TGF-β1 up-regulates the abundance of phospho-p38.

The expression of phospho-p38 MAPK was determined by immunoblots and measured by densitometric analysis using whole cell lysates isolated from PVD9902 monolayers treated with vehicle, SB431542 (10 μM), TGF-β1 (5 ng/ml), or TGF-β1 plus SB431542. The relative abundance of phospho-p38 under each treatment is normalized to β-actin with respect to vehicle. Summarized data are from 6-12 independent experiments. Asterisks indicate significant reductions when compared to vehicle ($P<0.05$).

The role of the p38 MAPK signaling pathway in forskolin-stimulated anion secretion was also tested by anisomycin, an activator of the p38 MAPK pathway (3, 50). PVD9902 cells were exposed to vehicle or anisomycin (2 μg/ml) for 24 hours followed by modified Ussing chamber

experiments. Similar as the effect of TGF-β1, anisomycin exposure led to a significant reduction in forskolin-stimulated anion secretion compared with paired monolayers (Figure 10). Real-time RT-PCR was also performed to identify the effect of anisomycin on CFTR mRNA abundance. The ΔCt value between vehicle and anisomycin treated PVD9902 cells for CFTR was ~-0.4 while the ΔCt value for 18s was ~0.05, with a ΔΔCt value of -0.4 ± 0.2 (Figure 11). These outcomes suggested that anisomycin exposure was associated with a 24.0% ± 7.7% reduction in mRNA coding for CFTR. These observations show that anisomycin mimics the effect of TGF-β1 on forskolin response and on CFTR mRNA abundance, which provide further evidence that the p38 MAPK signaling pathway is involved in the effect of TGF-β1 on PVD9902 monolayers.

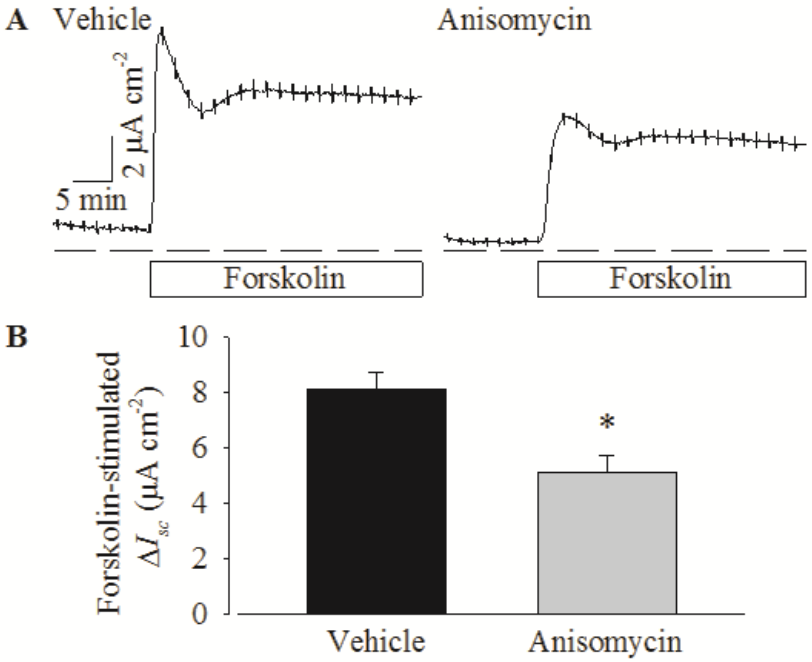

Figure 3.10 A p38 MAPK activator, anisomycin, impairs forskolin-stimulated anion secretion across PVD9902 monolayers.

A) Representative Ussing chamber traces of vehicle or anisomycin treated (2 μg/ml, 24 hours) PVD9902 monolayers exposed to forskolin (2 μM). **B)** Summarized results of forskolin-stimulated anion secretion from 11 paired experiments. Asterisk (*) indicates statistical difference from vehicle ($P < 0.05$).

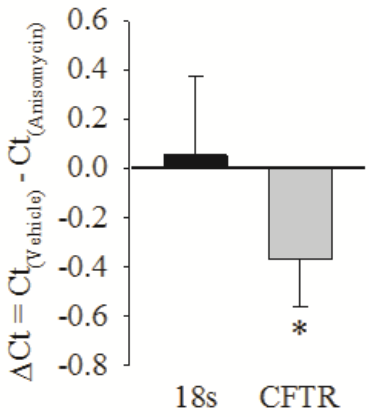

Figure 3.11 Anisomycin down-regulates CFTR mRNA abundance.

CFTR mRNA abundance in PVD9902 monolayers exposed to vehicle or anisomycin (2 μg/ml, 24 hours) was determined by real-time RT-PCR. Data are summarized from 4 paired experiments and are expressed as the ΔCt between vehicle treated cells and anisomycin treated cells for 18s and for CFTR. Asterisk (*) indicates significant difference ($P<0.05$).

TGF-β1 does not affect the viability of PVD9902 cells.

Another mechanism that can explain the reduction of anion secretion induced by TGF-β1 is that TGF-β1 leads to cell death and thus reduces the number of cells present in the monolayer. This mechanism, however, is unlikely based on the R_{te} measured at the outset of Ussing chamber experiments (Table 1). PVD9902 monolayers exposed to TGF-β1 exhibited a high basal R_{te} that was not different, statistically, from vehicle. Additional evidence was gathered by measuring LDH release to determine whether TGF-β1 compromises cell viability. A commercial kit in which florescence is proportional to LDH activity in the cell culture medium was used to measure the release of LDH from cells with damaged membranes. PVD9902 cells were cultured on 96-well plates to measure the leakage of LDH from cytoplasm into culture medium. Cells exposed to TGF-β1 showed an LDH release that was not different from vehicle alone while cells exposed to the lysis solution exhibited a remarkable release (Figure 12). This outcome indicates that TGF-β1 has no measurable effect on cell viability and thus rule out the possibility that reduced anion secretion across PVD9902 monolayers is due to decreased cell numbers.

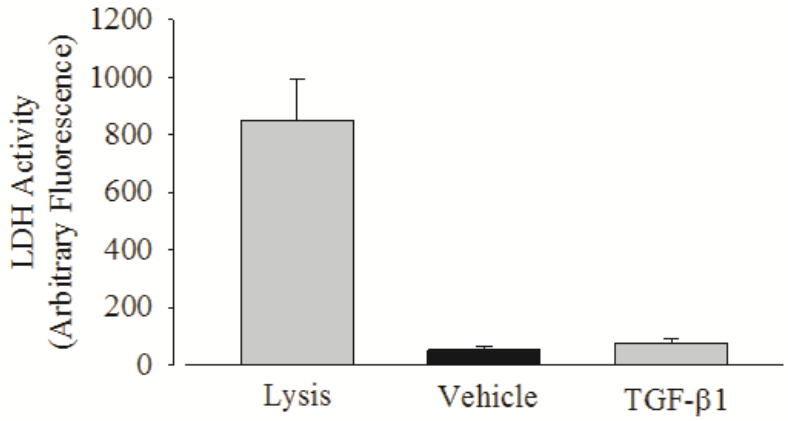

Figure 3.12 TGF-β1 has no detectable effect on lactate dehydrogenase (LDH) release.

PVD9902 cells were grown on 96 well plates for three days and then exposed to vehicle or TGF-β1 (5 ng/ml, 24 hours). Cells in paired wells were lysed to determine maximum LDH activity. LDH activity in the apical medium is proportional to fluorescence at 590 nm. Results are summarized from 6 experiments.

Discussion

This study demonstrated that TGF-β1 exposure reduces the secretory response to a variety of test reagents that initiate signaling through the cAMP-mediated pathway, including forskolin, the combination of forskolin and IBMX, and 8-pCPT-cAMP. Real time RT-PCR, immunoblots, and electrophysiological measurements showed that TGF-β1 reduces the relative copy number of mRNA coding for CFTR, that less CFTR is expressed, that less CFTR is present in the apical cell membrane, and that there is reduced anion secretion attributable to CFTR. Studies focusing on the cellular signal transduction mechanisms suggest that TGF-β1 binds to and activates TGF-β1 receptor I. Receptor activation is associated with an increase in the activity of the p38 MAPK signaling pathway as demonstrated by an increase in the phosphorylated form of the enzyme. Additional support for this scenario was drawn from experiments in which anisomycin mimicked the effect of TGF-β1 on CFTR expression to impaired anion transport across cultured vas deferens epithelial cells. These observations define a scenario by which elevated levels of TGF-β1 could heighten the symptomology of mild cystic fibrosis.

Previous studies suggested that TGF-β1 modulates epithelial ion transport by changing the amount, location or activity of the apical CFTR channel, although none of them has studied the effect of TGF-β1 on vas deferens epithelia (18, 19, 38, 39). TGF-β1 exposure led to a significant reduction in the magnitude of the response to forskolin or a cAMP analog in colonic epithelia, T84 and HT-29 cells, and in kidney epithelia, MDCK cells, by changing the expression and distribution of CFTR (18, 19). A similar role of TGF-β1 to reduce cAMP-driven anion secretion and CFTR expression has been identified in lung and airway epithelial cells (38, 39). The present report demonstrates that TGF-β1 down-regulates the gene expression of CFTR, its protein abundance, and especially the protein abundance of functional CFTR in the cell surface. A single CFTR channel has a conductance of ~10 pS and a channel open probability of ~0.4 when exposed to forskolin (40, 41, 44). If one employs a series of reasonable assumptions that are consistent with a previous report (e.g., PVD9902 cells exposed to forskolin have an apical membrane driving force of ~4 mV, that there are 400 CFTR channels in apical membranes of typical cells, and that there are ~10^6 cells per monolayer), forskolin exposure will induce an increase in I_{sc} of ~6.4 μA, which approximates the magnitude of our observations (Figure 1).

Furthermore, if one assumes apical, basolateral and paracellular resistances of 9,000, 8,000, and 15,000 Ω cm^2 in resting conditions, the calculated R_{te} would be ~8,100 Ω cm^2, which is similar to what is observed for these cell monolayers. Activation of CFTR by forskolin would decrease apical resistance to ~5,900 Ω cm^2 and R_{te} to ~5,500 Ω cm^2. A 25% reduction in the number of channels would be expected to have no effect on basal R_{te}, but would reduce forskolin-stimulated I_{sc} by 25% and would reduce the forskolin-induced change in R_{te} by a lesser amount, which again is consistent with the observations. These simple calculations support certain inferences. First, TGF-β1-attenuated forskolin response is explainable largely by invoking a single change in the cells, a reduced number of CFTR channels in the apical membranes. A change in the signaling cascade leading to channel activation, the CFTR channel activation mechanism, the channel inactivation mechanism, or in maximal channel open probability is not required. However, not all observations are fully explained by this mechanism. Notably, one expects a reduction in channel number to have no effect on basal R_{te}. Further, the full magnitudes of the shifts in R_{te} are not fully explained by the difference in channel expression. Initial sets of experiments were conducted to test for indications either of cell death or of epithelial to mesenchymal transition. In both cases the results were negative. TGF-β1 exposure does not alter the release of LDH, suggesting that TGF-β1 does not affect the viability of PVD9902 cells. Outcomes from western blots showed that TGF-β1 exposure does not alter the expression of E-cadherin, an epithelial cell marker that typically is down-regulated following exposure of epithelial cell types to TGF-β1, suggesting that TGF-β1 did not induce epithelial to mesenchymal transition in PVD9902 cells (data not shown). Clearly, additional experiments are required to address these observations further. Nonetheless, the preponderance of the observed effects can be explained by a TGF-β1 associated reduction in CFTR expression that requires activation of the TGF-β1 receptor I and the p38 MAPK pathway.

TGF-β1 has been associated with reproductive function and male fertility (20). Male TGF-β1 null mutant mice exhibited a reduced level of testosterone as well as a complete inability to mate with females although the weight and histology of male reproductive tissues, including penis, seminal vesicles, and testes, were normal (21). However, the effect of TGF-β1 on vas deferens, especially ion transport across vas deferens epithelia, is unknown. It is of critical importance since the concentration of TGF-β1 in seminal plasma is 85-238 ng/ml (31, 37), which is much

higher than its concentration in plasma or any other bodily fluids (34). These observations, which demonstrate that TGF-β1 modulates ion transport across cultured vas deferens epithelial monolayers, extend our understanding of the physiological and/or pathological roles of TGF-β1 in vas deferens and in male fertility.

Vas deferens epithelia express numerous ion channels and transporters that are required to accomplish vectorial transport of salt and water (4, 5, 43). Among those channels and transporters, CFTR mediates the movement of bicarbonate as well as chloride and contributes to the adjustment of luminal volume and pH (2, 22, 45). Impaired CFTR-mediated anion secretion would diminish water movement, decrease bicarbonate secretion, and change vas deferens luminal pH. An acid environment is required for sperm to mature as they traverse the epididymis. However, an alkaline luminal pH is required to initiate motility and to induce fertilizing capacity of sperm cells (8, 30, 36). The critical role of CFTR in the male reproductive system has been demonstrated by the magnitude of infertility that is associated with CFTR mutations including the high frequency of CBAVD in both severely and mildly affected cystic fibrosis patients. Importantly, men with 'mild' or hemizygous *CFTR* gene mutations that have intact vasa differentia, often exhibit reduced sperm quality and/or male infertility (10, 23, 42, 48). Reduced CFTR function would be expected to result in reduced luminal fluid volume and reduced pH, which ultimately would have a negative impact on sperm maturation, activation, motility and function (33, 46). Our observations that TGF-β1 signaling reduces CFTR expression and limits anion secretion suggests that individuals with an elevated level of TGF-β1 may exhibit aberrant ion transport across epithelia lining the vas deferens. This, by itself, could lead to reduced fertility. Moreover, in CF patients harboring 'mild' or hemizygous *CFTR* mutations, greater TGF-β1 signaling may further compromise fertility.

TGF-β1 modulates ion transport by activating numerous intracellular signaling cascades in different types of epithelial cells. TGF-β1 inhibited fluid transport across ATII monolayers through a PI3K-dependend mechanism (39). Sodium and fluid transport across ATII monolayers were decreased by TGF-β1 through an ERK1/2-dependent mechanism (13). Chloride secretion across T84 monolayers was also impaired through a p38 MAPK pathway (18). In PVD9902 cells, with the observation that TGF-β1 activates TGF-β receptor I, additional experiments were conducted to test for mediators of downstream TGF-β1 signaling. Results from initial

experiments designed with this goal suggested p38 MAPK as a potential mediator. Therefore, subsequent experiments focused on a role for p38 MAPK in the transduction of TGF-β1 signaling in PVD9902 cells. By applying a selective p38 MAPK signaling pathway inhibitor, SB203580, by measuring protein abundance of phosphorylated p38 MAPK, and by using an activator of the p38 MAPK signaling pathway, anisomycin, to mimic the effect of TGF-β1, it was shown that TGF-β1 activates the p38 MAPK signaling pathway in PVD9902 monolayers. Another inhibitor of p38 MAPK, SKF86002, exhibited similar effects as SB203580 (data not shown). PVD9902 cells exposed to the combination of SKF86002 and TGF-β1 exhibited a higher response to forskolin than cells exposed to TGF-β1 only, suggesting the involvement of the p38 MAPK signaling pathway in the effect of TGF-β1.

In conclusion, the results show that PVD9902 cells exposed to TGF-β1 exhibit reduced cAMP-stimulated anion secretion. This effect was associated with the activation of TGF-β receptor I and the activation of the p38 MAPK signaling pathway. Reductions in mRNA coding for CFTR and CFTR protein expression were detected. These observations may have clinical implications because high levels of TGF-β1 in close association with vas deferens epithelial cells might induce aberrant ion transport, change the luminal environment, and reduce male fertility.

Acknowledgements

We thank Ms. Lin-Hua ‘Florence’ Wang and Ms. Qian Wang for their technical assistance.

Grants

This work was supported by the NIH (HD058398) and by the COBRE Epithelial Function in Health and Disease (RR017686).

Disclosures

There is no conflict of interest.

References

1. **Arkwright PD, Laurie S, Super M, Pravica V, Schwarz MJ, Webb AK, and Hutchinson IV.** TGF-beta(1) genotype and accelerated decline in lung function of patients with cystic fibrosis. *Thorax* 55: 459-462, 2000.

2. **Ballard ST, Trout L, Bebok Z, Sorscher EJ, and Crews A.** CFTR involvement in chloride, bicarbonate, and liquid secretion by airway submucosal glands. *Am J Physiol* 277: L694-699, 1999.

3. **Barros LF, Young M, Saklatvala J, and Baldwin SA.** Evidence of two mechanisms for the activation of the glucose transporter GLUT1 by anisomycin: p38(MAP kinase) activation and protein synthesis inhibition in mammalian cells. *J Physiol* 504 (Pt 3): 517-525, 1997.

4. **Carlin RW, Quesnell RR, Zheng L, Mitchell KE, and Schultz BD.** Functional and molecular evidence for Na(+)-HCO cotransporter in porcine vas deferens epithelia. *Am J Physiol Cell Physiol* 283: C1033-1044, 2002.

5. **Carlin RW, Sedlacek RL, Quesnell RR, Pierucci-Alves F, Grieger DM, and Schultz BD.** PVD9902, a porcine vas deferens epithelial cell line that exhibits neurotransmitter-stimulated anion secretion and expresses numerous HCO3(-) transporters. *Am J Physiol Cell Physiol* 290: C1560-1571, 2006.

6. **Chaudhury A and Howe PH.** The tale of transforming growth factor-beta (TGFbeta) signaling: a soigne enigma. *IUBMB life* 61: 929-939, 2009.

7. **Collaco JM and Cutting GR.** Update on gene modifiers in cystic fibrosis. *Curr Opin Pulm Med* 14: 559-566, 2008.

8. **Contri A, Gloria A, Robbe D, Valorz C, Wegher L, and Carluccio A.** Kinematic study on the effect of pH on bull sperm function. *Anim Reprod Sci* 136: 252-259, 2013.

9. **Corvol H, Boelle PY, Brouard J, Knauer N, Chadelat K, Henrion-Caude A, Flamant C, Muselet-Charlier C, Boule M, Fauroux B, Vallet C, Feingold J, Ratjen F, Grasemann H, and Clement A.** Genetic variations in inflammatory mediators influence lung disease progression in cystic fibrosis. *Pediatr Pulmonol* 43: 1224-1232, 2008.

10. **Cuppens H and Cassiman JJ.** CFTR mutations and polymorphisms in male infertility. *Int J Androl* 27: 251-256, 2004.

11. **Derynck R and Zhang YE.** Smad-dependent and Smad-independent pathways in TGF-beta family signalling. *Nature* 425: 577-584, 2003.

12. **Drumm ML, Konstan MW, Schluchter MD, Handler A, Pace R, Zou F, Zariwala M, Fargo D, Xu A, Dunn JM, Darrah RJ, Dorfman R, Sandford AJ, Corey M, Zielenski J, Durie P, Goddard K, Yankaskas JR, Wright FA, and Knowles MR.** Genetic modifiers of lung disease in cystic fibrosis. *N Engl J Med* 353: 1443-1453, 2005.

13. **Frank J, Roux J, Kawakatsu H, Su G, Dagenais A, Berthiaume Y, Howard M, Canessa CM, Fang X, Sheppard D, Matthay MA, and Pittet JF.** Transforming growth factor-beta1 decreases expression of the epithelial sodium channel alphaENaC and

alveolar epithelial vectorial sodium and fluid transport via an ERK1/2-dependent mechanism. *J Biol Chem* 278: 43939-43950, 2003.

14. **Halder SK, Beauchamp RD, and Datta PK.** A specific inhibitor of TGF-beta receptor kinase, SB-431542, as a potent antitumor agent for human cancers. *Neoplasia* 7: 509-521, 2005.

15. **Han J, Lee JD, Bibbs L, and Ulevitch RJ.** A MAP kinase targeted by endotoxin and hyperosmolarity in mammalian cells. *Science* 265: 808-811, 1994.

16. **Harris WT, Muhlebach MS, Oster RA, Knowles MR, Clancy JP, and Noah TL.** Plasma TGF-beta(1) in pediatric cystic fibrosis: potential biomarker of lung disease and response to therapy. *Pediatr Pulmonol* 46: 688-695, 2011.

17. **Havasi V, Rowe SM, Kolettis PN, Dayangac D, Sahin A, Grangeia A, Carvalho F, Barros A, Sousa M, Bassas L, Casals T, and Sorscher EJ.** Association of cystic fibrosis genetic modifiers with congenital bilateral absence of the vas deferens. *Fertil Steril* 94: 2122-2127.

18. **Howe K, Gauldie J, and McKay DM.** TGF-beta effects on epithelial ion transport and barrier: reduced Cl- secretion blocked by a p38 MAPK inhibitor. *Am J Physiol Cell Physiol* 283: C1667-1674, 2002.

19. **Howe KL, Wang A, Hunter MM, Stanton BA, and McKay DM.** TGFbeta down-regulation of the CFTR: a means to limit epithelial chloride secretion. *Exp Cell Res* 298: 473-484, 2004.

20. **Ingman WV and Robertson SA.** The essential roles of TGFB1 in reproduction. *Cytokine Growth Factor Rev* 20: 233-239, 2009.

21. **Ingman WV and Robertson SA.** Transforming growth factor-beta1 null mutation causes infertility in male mice associated with testosterone deficiency and sexual dysfunction. *Endocrinology* 148: 4032-4043, 2007.

22. **Ishiguro H, Yamamoto A, Nakakuki M, Yi L, Ishiguro M, Yamaguchi M, Kondo S, and Mochimaru Y.** Physiology and pathophysiology of bicarbonate secretion by pancreatic duct epithelium. *Nagoya J Med Sci* 74: 1-18, 2012.

23. **Jakubiczka S, Bettecken T, Stumm M, Nickel I, Musebeck J, Krebs P, Fischer C, Kleinstein J, and Wieacker P.** Frequency of CFTR gene mutations in males participating in an ICSI programme. *Hum Reprod* 14: 1833-1834, 1999.

24. **Kumar S, Jiang MS, Adams JL, and Lee JC.** Pyridinylimidazole compound SB 203580 inhibits the activity but not the activation of p38 mitogen-activated protein kinase. *Biochem Biophys Res Commun* 263: 825-831, 1999.

25. **Laping NJ, Grygielko E, Mathur A, Butter S, Bomberger J, Tweed C, Martin W, Fornwald J, Lehr R, Harling J, Gaster L, Callahan JF, and Olson BA.** Inhibition of transforming growth factor (TGF)-beta1-induced extracellular matrix with a novel inhibitor of the TGF-beta type I receptor kinase activity: SB-431542. *Mol Pharmacol* 62: 58-64, 2002.

26. **Laurenza A, Sutkowski EM, and Seamon KB.** Forskolin: a specific stimulator of adenylyl cyclase or a diterpene with multiple sites of action? *Trends Pharmacol Sci* 10: 442-447, 1989.

27. **Lewis-Jones DI, Gazvani MR, and Mountford R.** Cystic fibrosis in infertility: screening before assisted reproduction: opinion. *Hum Reprod* 15: 2415-2417, 2000.

28. **Li C and Naren AP.** Macromolecular complexes of cystic fibrosis transmembrane conductance regulator and its interacting partners. *Pharmacol Ther* 108: 208-223, 2005.

29. **Li H, Ganta S, and Fong P.** Altered ion transport by thyroid epithelia from CFTR(-/-) pigs suggests mechanisms for hypothyroidism in cystic fibrosis. *Exp Physiol* 95: 1132-1144, 2010.

30. **Mannowetz N, Wandernoth PM, and Wennemuth G.** Glucose is a pH-dependent motor for sperm beat frequency during early activation. *PLoS One* 7: e41030, 2012.

31. **Nocera M and Chu TM.** Characterization of latent transforming growth factor-beta from human seminal plasma. *Am J Reprod Immunol* 33: 282-291, 1995.

32. **O'Riordan CR, Lachapelle AL, Marshall J, Higgins EA, and Cheng SH.** Characterization of the oligosaccharide structures associated with the cystic fibrosis transmembrane conductance regulator. *Glycobiology* 10: 1225-1233, 2000.

33. **Okamura N, Tajima Y, Ishikawa H, Yoshii S, Koiso K, and Sugita Y.** Lowered levels of bicarbonate in seminal plasma cause the poor sperm motility in human infertile patients. *Fertil Steril* 45: 265-272, 1986.

34. **Oppenheim JJ, Feldmann M, and Durum SK.** *Cytokine reference : a compendium of cytokines and other mediators of host defense*. San Diego: Academic Press, 2001.

35. **Pierucci-Alves F, Akoyev V, Stewart JC, 3rd, Wang LH, Janardhan KS, and Schultz BD.** Swine models of cystic fibrosis reveal male reproductive tract phenotype at birth. *Biol Reprod* 85: 442-451, 2011.

36. **Pierucci-Alves F, Duncan CL, Lillich JD, and Schultz BD.** Porcine vas deferens luminal pH is acutely increased by systemic xylazine administration. *Biol Reprod* 82: 132-135, 2010.

37. **Politch JA, Tucker L, Bowman FP, and Anderson DJ.** Concentrations and significance of cytokines and other immunologic factors in semen of healthy fertile men. *Hum Reprod* 22: 2928-2935, 2007.

38. **Pruliere-Escabasse V, Fanen P, Dazy AC, Lechapt-Zalcman E, Rideau D, Edelman A, Escudier E, and Coste A.** TGF-beta 1 downregulates CFTR expression and function in nasal polyps of non-CF patients. *Am J Physiol Lung Cell Mol Physiol* 288: L77-83, 2005.

39. **Roux J, Carles M, Koh H, Goolaerts A, Ganter MT, Chesebro BB, Howard M, Houseman BT, Finkbeiner W, Shokat KM, Paquet AC, Matthay MA, and Pittet JF.** Transforming growth factor beta1 inhibits cystic fibrosis transmembrane conductance regulator-dependent cAMP-stimulated alveolar epithelial fluid transport via a phosphatidylinositol 3-kinase-dependent mechanism. *J Biol Chem* 285: 4278-4290, 2010.

40. **Schultz BD, Singh AK, Devor DC, and Bridges RJ.** Pharmacology of CFTR chloride channel activity. *Physiol Rev* 79: S109-144, 1999.

41. **Schultz BD, Takahashi A, Liu C, Frizzell RA, and Howard M.** FLAG epitope positioned in an external loop preserves normal biophysical properties of CFTR. *Am J Physiol* 273: C2080-2089, 1997.

42. **Schulz S, Jakubiczka S, Kropf S, Nickel I, Muschke P, and Kleinstein J.** Increased frequency of cystic fibrosis transmembrane conductance regulator gene mutations in infertile males. *Fertil Steril* 85: 135-138, 2006.

43. **Sedlacek RL, Carlin RW, Singh AK, and Schultz BD.** Neurotransmitter-stimulated ion transport by cultured porcine vas deferens epithelium. *Am J Physiol Renal Physiol* 281: F557-570, 2001.

44. **Singh AK, Schultz BD, van Driessche W, and Bridges RJ.** Transepithelial fluctuation analysis of chloride secretion. *J Cyst Fibros* 3 Suppl 2: 127-132, 2004.

45. **Steward MC, Ishiguro H, and Case RM.** Mechanisms of bicarbonate secretion in the pancreatic duct. *Annu Rev Physiol* 67: 377-409, 2005.

46. **Tajima Y and Okamura N.** The enhancing effects of anion channel blockers on sperm activation by bicarbonate. *Biochimica Et Biophysica Acta* 1034: 326-332, 1990.

47. **Taussig LM, Lobeck CC, di Sant'Agnese PA, Ackerman DR, and Kattwinkel J.** Fertility in males with cystic fibrosis. *N Engl J Med* 287: 586-589, 1972.

48. **van der Ven K, Messer L, van der Ven H, Jeyendran RS, and Ober C.** Cystic fibrosis mutation screening in healthy men with reduced sperm quality. *Hum Reprod* 11: 513-517, 1996.

49. **Wangemann P, Itza EM, Albrecht B, Wu T, Jabba SV, Maganti RJ, Lee JH, Everett LA, Wall SM, Royaux IE, Green ED, and Marcus DC.** Loss of KCNJ10 protein expression abolishes endocochlear potential and causes deafness in Pendred syndrome mouse model. *BMC Med* 2: 30, 2004.

50. **Zhu CB, Carneiro AM, Dostmann WR, Hewlett WA, and Blakely RD.** p38 MAPK activation elevates serotonin transport activity via a trafficking-independent, protein phosphatase 2A-dependent process. *J Biol Chem* 280: 15649-15658, 2005.

Chapter 4 - Summary

The objective of the current study was to determine the effects of TGF-β1 on vas deferens epithelial cells. Primary cultures of freshly isolated vas deferens epithelial cells were used along with an immortalized vas deferens epithelial cell line to test for effects of TGF-β1 on electrophysiological parameters across and protein expression in the epithelium that lines the vas deferens.

In primary porcine vas deferens epithelial cells, monolayers exposed to TGF-β1 (100 ng/ml, 72 hours; 100 ng/ml, 24 hours; and 5 ng/ml, 24 hours) exhibited an impaired tight junction barrier as indicated by a reduction in R_{te} and reorganization of occludin and claudin-7. Attenuated forskolin-stimulated anion secretion was observed also when cells were exposed to the highest concentration of TGF-β1 for the longest period tested. These outcomes suggest that TGF-β1 impairs the barrier integrity of vas deferens epithelium and reduces the activity of one or more components in the ion transport pathway.

PVD9902 cell monolayers exposed to TGF-β1 at a concentration of 5 ng/ml for 24 hours exhibited a significant reduction in response to reagents that initiate signaling through the cAMP-mediated pathway, such as forskolin, forskolin/IBMX, and 8-pCPT-cAMP. Attenuated anion secretion across PVD9902 monolayers was attributable to reduced permeation through CFTR channels, as indicated by a reduced magnitude of current inhibited by CFTR blockers. Real-time RT-PCR and immunoblots showed that TGF-β1 reduces the mRNA and protein abundance of CFTR. These outcomes suggest that TGF-β1 downregulates CFTR expression and limits CFTR-mediated anion secretion. *In vivo*, such an outcome would change luminal composition and pH of vas deferens and would be expected to affect sperm activation, motility, and function.

Both primary porcine vas deferens epithelial cells and PVD9902 cells have been employed to determine the effect of TGF-β1. Primary cells may provide biological responses that are closer to an *in vivo* situation. Moreover, primary cultures derived from different porcine donors may behave differently due to variations between individuals. Therefore, results from primary cultures support inferences to the porcine population. Furthermore, results from our laboratory

suggest that similar phenomena would likely be observed within human tissues (1, 4, 7). However, the access to primary cultures is inconsistent. PVD9902 cells were derived from a single porcine donor and the cells spontaneously immortalized. Therefore, the PVD9902 cell line provides a source of materials that is available consistently. PVD9902 cells recapitulate most observations of primary cultures and thus observations from PVD9902 cells contribute to the characterization of vas deferens epithelia and male reproductive function. In our study, using both primary cell cultures and the PVD9902 cell line, the outcomes demonstrate that TGF-β1 exposure modifies the function of vas deferens epithelia.

There still exist some apparent differences between primary cultures of vas deferens epithelial cells and PVD9902 cells as one assesses the effects of TGF-β1.

First, TGF-β1 induces a robust reduction of basal R_{te} in primary cell cultures, but only a slight reduction in R_{te} across PVD9902 monolayers. Basal R_{te} is determined by paracellular resistance, the sum of tight junction resistance and intracellular space resistance, and transcellular resistance. We speculate that, compared with primary cultures, PVD9902 cells contain less claudin-2, a tight junction protein for which the expression level is reported reciprocal to transepithelial resistance (3) and/or higher number of tight junction strands (2). Typically, PVD9902 cells exhibit a basal R_{te} of >8000 Ω cm^2, which is higher than the basal R_{te} of most primary cell cultures (~4000 Ω cm^2). The high basal transepithelial resistance of PVD9902 may reflect characteristics of the cells at the time of their isolation, *i.e.*, the primary porcine vas deferens epithelial cell cultures from which PVD9902 cells were derived may have exhibited a high innate R_{te}.

The second major difference in outcomes is that TGF-β1 induced a more apparent reduction of forskolin-stimulated anion secretion in PVD9902 cells compared with primary cell cultures. In our proposed cell model (Figure 1.9), chloride and bicarbonate enter vas deferens epithelial cells *via* NKCC and SLC4A4 cotransporters, respectively, across the basolateral membrane and exit cells through CFTR channels in the apical membrane. Our data suggest that TGF-β1 exposure reduces CFTR expression and thus reduces forskolin-stimulated anion secretion. Attenuated forskolin-stimulated anion secretion is not observed in primary cell cultures that are treated with the same concentration and duration of TGF-β1. A possible explanation is that freshly isolated

vas deferens epithelial cells express CFTR in the apical membrane at higher levels such that CFTR is not the factor limiting anion secretion in the presence of maximal cAMP-mediated stimulation. The maximum response to forskolin may be limited by the abundance and/or the activity of basolateral cotransporters that account for anion entry. It is likely that TGF-β1 also reduces CFTR expression in primary cell cultures (unpublished observations from Dr. Vladimir Akoyev and myself). However, we speculate that although the abundance of CFTR is down-regulated, there are still enough CFTR channels in the apical membrane to accommodate all anions that enter cells through the basolateral cotransporters. Our data suggest that only when primary cell cultures are exposed to a high level of TGF-β1 (*e.g.*, 100 ng/ml for 72 hours), CFTR abundance is reduced to an extent that limits anion transport, thereby impairing forskolin-stimulated anion secretion. To test the possibility of this explanation further, western blot experiments can be performed to determine the effect of TGF-β1 on CFTR protein expression in primary cultures and to access the effects of selective CFTR blockers in the absence and presence of the cytokine. We expect that TGF-β1 exposures at different concentrations and durations (*e.g.*, 5 ng/ml for 24 hours; and 100 ng/ml for 72 hours) down-regulate the total CFTR expression and the abundance of CFTR in the apical membrane. Moreover, we expect that CFTR protein abundance is even lower in primary cultures exposed to a high level of TGF-β1 (*e.g.*, 100 ng/ml for 72 hours) compared with primary cultures exposed to a lower level of TGF-β1 (*e.g.*, 5 ng/ml for 24 hours). Therefore, in primary cultures exposed to a lower level of TGF-β1, the remaining CFTR is still sufficient for anion secretion while in primary cultures exposed to a high level of TGF-β1, the further down-regulated CFTR protein is limiting anion secretion upon stimulation.

TGF-β1 exists mainly in a latent form and also in an active form. The concentration of total TGF-β1 in human plasma is ~5 ng/ml (6). The concentration of total TGF-β1 in human semen is much higher, reaching 85-238 ng/ml (5, 9). Furthermore, the concentration of active TGF-β1 in human semen can be as high as ~2 ng/ml (9). The concentrations of TGF-β1 in the luminal and the blood side of vas deferens are unknown. Phosphorylated Smad2/3 can be detected in native vas deferens epithelia, suggesting that activated TGF-β1 is present in the male reproductive tract (unpublished observations from Dr. Fernando Pierucci-Alves). Some of the PVD9902 cultures exposed to the TGF-β receptor blocker showed an elevated basal I_{sc}, suggesting that the

PVD9902 cell culture system may include endogenous TGF-β1 that contributes to the regulation of ion flux across monolayers. These indirect evidences suggest that a modest level of TGF-β1 may be secreted and/or activated by vas deferens epithelial cells in culture to regulate cell function, although the possibility that there is some amount of TGF-β1 in serum in the cell culture media has not been ruled out. Genetic polymorphisms of TGF-β1 likely affect the basal level of TGF-β1 in the lumen and on the blood side of vas deferens. Pathological conditions, such as inflammation may upregulate of TGF-β1 expression or activation and increase TGF-β1 signaling in the vas deferens. Therefore, individuals with lower basal TGF-β1 signaling might be less prone to dysfunction of male reproductive tract while individuals with a TGF-β1 'high producer' phenotype might be predisposed to subfertility and with a second insult such as reduced lumen pH and reduced fluid secretion are likely to exhibit more severe symptoms.

TGF-β1 exposure modulates the barrier function of and/or anion secretion across vas deferens epithelial cells. These TGF-β1-induced changes may modify the ionic composition, pH and volume of fluid in the vas deferens lumen. Under normal conditions without stimulation, sperm in the vas deferens lumen are thought to be exposed to an acidic environment and thus are kept in a quiescent state (8). TGF-β1 exposure disrupts tight junctions between vas deferens epithelial cells, which may lead to mixing of luminal and interstitial fluid, resulting in an increased luminal pH in resting conditions. In the more alkaline environment, some sperm cells could be activated, which would reduce long term viability. When stimulation occurs in conjunction with sexual activity, intracellular cAMP generation of vas deferens epithelial cells is elevated, which activates CFTR and stimulates the vectorial transport of anions and fluid into the lumen. Fluid transport increases the volume of vas deferens luminal fluid while bicarbonate secretion contributes to an alkaline luminal pH. In healthy conditions, rapid alkalization of the luminal fluid would increase sperm motility and favor their fertilizing potential. Again, ducts exposed to TGF-β1 would be expected to have elevated resting pH due to compromised tight junctions and reduced numbers of viable sperms. Additionally, TGF-β1 exposure would downregulate CFTR channel expression and would diminish the ability of these ducts to respond to stimulation with anion and fluid secretion. Epithelial cell exposed to TGF-β1 would be unable to alkalinize the lumen to the extent that occurs in healthy ducts. Thus, under stimulated conditions, sperm cells are likely exposed to a more acidic vas deferens luminal environment, leading to a state of

reduced sperm motility. Male patients with 'mild' *CFTR* mutations or male carriers of single mutant *CFTR* gene express less functional CFTR, which may contribute to attenuated anion secretion at the outset. In these individuals, TGF-β1 exposure would be expected to reduce CFTR expression, further compromise the electrophysiological parameters of vas deferens epithelium, modify the luminal microenvironment in vas deferens, and thus reduce male fertility or induce male infertility.

In summary, these outcomes, using both primary porcine vas deferens cells and cultured PVD9902 cells, suggest that TGF-β1 modulates the electrophysiological parameters of vas deferens epithelia. These observations have clinical implications as vas deferens epithelia would modify dynamically regulate the luminal environment to which sperm are exposed, and thus affect male fertility. Taken together, our results suggest a novel mechanism to account for subfertility and infertility in cystic fibrosis patients harboring 'mild' mutations and in carriers of a mutated CFTR allele. This novel mechanism incorporates the impact of TGF-β1 expression or epithelial function in the context of reduced CFTR expression.

Reference

1. **Carlin RW, Lee JH, Marcus DC, and Schultz BD**. Adenosine stimulates anion secretion across cultured and native adult human vas deferens epithelia. *Biol Reprod* 68: 1027-1034, 2003.
2. **Claude P**. Morphological factors influencing transepithelial permeability: a model for the resistance of the zonula occludens. *J Membr Biol* 39: 219-232, 1978.
3. **Furuse M, Furuse K, Sasaki H, and Tsukita S**. Conversion of zonulae occludentes from tight to leaky strand type by introducing claudin-2 into Madin-Darby canine kidney I cells. *J Cell Biol* 153: 263-272, 2001.
4. **Hagedorn TM, Carlin RW, and Schultz BD**. Oxytocin and vasopressin stimulate anion secretion by human and porcine vas deferens epithelia. *Biol Reprod* 77: 416-424, 2007.
5. **Nocera M, and Chu TM**. Transforming growth factor beta as an immunosuppressive protein in human seminal plasma. *Am J Reprod Immunol* 30: 1-8, 1993.
6. **Oppenheim JJ, Feldmann M, and Durum SK**. *Cytokine reference : a compendium of cytokines and other mediators of host defense*. San Diego: Academic Press, 2001.
7. **Pierucci-Alves F, and Schultz BD**. Bradykinin-stimulated cyclooxygenase activity stimulates vas deferens epithelial anion secretion in vitro in swine and humans. *Biol Reprod* 79: 501-509, 2008.
8. **Pietrement C, Sun-Wada GH, Silva ND, McKee M, Marshansky V, Brown D, Futai M, and Breton S**. Distinct expression patterns of different subunit isoforms of the V-ATPase in the rat epididymis. *Biol Reprod* 74: 185-194, 2006.
9. **Politch JA, Tucker L, Bowman FP, and Anderson DJ**. Concentrations and significance of cytokines and other immunologic factors in semen of healthy fertile men. *Hum Reprod* 22: 2928-2935, 2007.

Appendix A – Permission for reprint

Dear Sheng:

Thank you for your email. Since you are an author on the paper in question, you do not need to secure written permission from SSR. It is SSR policy that authors may reuse their own work provided that the source paper is cited specifically (e.g., Fernando Pierucci-Alves, Sheng Yi, and Bruce D. Schultz. Transforming Growth Factor Beta 1 Induces Tight Junction Disruptions and Loss of Transepithelial Resistance Across Porcine Vas Deferens Epithelial Cells. Biol Reprod 2012; 86 (2):36,1-8.). This information is found in the "Copyright Transfer" section of the Biology of Reproduction Authorship form, "The SSR, in turn, grants to each author the right of republication in any work of which she/he is the author or editor, subject only to giving proper credit to the original journal publication of the article."

Please let us know if you have additional questions.

Kind regards,
Katrina

Please see our website for the Rights of APS authors
http://www.the-aps.org/mm/Publications/Info-For-Authors/Copyright

You may include your article in your dissertation without requesting permission

Carolyn Villemez
APS Production Administrator

Tel: 301-634-7964
Fax: 301-634-7245
Email: cvillemez@the-aps.org
Please check out our Web page
www.the-aps.org